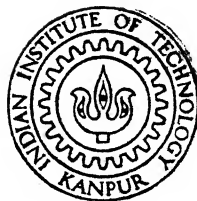


48

MATHEMATICAL MODELLING OF CONTINUOUS CASTING OF STEEL STRIPS

by
ANJAN KUMAR, M. K.



DEPARTMENT OF METALLURGICAL ENGINEERING
INDIAN INSTITUTE OF TECHNOLOGY KANPUR

MAY 1990

ME
1990
M
ANJ
MAT

TH
ME/1990/14
Ansgm

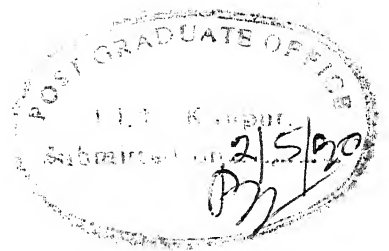
MATHEMATICAL MODELLING OF CONTINUOUS CASTING OF STEEL STRIPS

A Thesis Submitted
in Partial Fulfilment of the Requirements
for the Degree of
MASTER OF TECHNOLOGY

by
ANJAN KUMAR, M. K.

to the
DEPARTMENT OF METALLURGICAL ENGINEERING
INDIAN INSTITUTE OF TECHNOLOGY KANPUR
MAY 1990

CERTIFICATE



This is to certify that the work "Mathematical Modelling of Continuous Casting of Steel Strips" has been carried out by Mr Anjan Kumar M.K. under my supervision and it has not been submitted elsewhere for a degree.

S. P. Mehrotra

Dr. S. P. Mehrotra

Professor

Dept. of Metallurgical Engineering.

Indian Institute of Technology

Kanpur

ACKNOWLEDGEMENTS

I am extremely grateful to my guide Professor S.P. Mehrotra for introducing me to the wonderful world of Mathematical Modelling. I consider meeting him the best thing that happened to me in my career. Without his timely guidance and encouragement throughout the course of this study along with the highly thought provoking discussion he used to have with us about the project, I do not think I would have been able to complete this work.

I would also like to record my thanks to SAIL R & D personnel at Ranchi for their help in familiarising me with the process about which the present work is directed and for the hospitality they provided me during my visits to that place.

Last but never the least, I am thankful to my colleagues in the lab and in particular to Mr R.K. Mallik for providing the best environment for work.

30th April 1990

Kanpur

M K Anjan Kumar

CONTENTS

	Page No.
CERTIFICATE	i
ACKNOWLEDGEMENTS	ii
CONTENTS	iii
ABSTRACT	vi
LIST OF FIGURES	viii
LIST OF TABLES	xi
NOMENCLATURE	xii
 Chapter-1. INTRODUCTION	 1
 Chapter-2. LITERATURE REVIEW	
2.1 Description of various Near-Net-Shape-Casters	5
2.1.1 Stationary Mould Casters	7
2.1.2 Travelling Mould Casters	8
2.1.2.1 Twin Belt Thin Slab Casters	9
2.1.2.2 Moving Belt with 1 or 2 Rollers	10
2.1.3 Spray Deposition Process	11
2.2 Mathematical Modelling of the Physical Phenomenon involved in Near-Net-Shape Casting	12
2.3 Heat Transfer Coefficient Data	18
 Chapter-3. PROCESS DESCRIPTION	
3.1 Description of Caster	21
3.1.1 Tundish	21
3.1.2 Copper Drum/Roller	22
3.1.3 Pressure Roll	23
3.1.4 Water Spray	23
3.1.5 Water Outlet	24
3.1.6 Knife Edge	24
3.1.7 Electric Motor	24
3.2 Description of the Physical Phenomenon	25

Chapter-4.	MACROSCOPIC HEAT BALANCE MODEL	26
4.1	Angular Relationships	27
4.2	Heat Balance at the Melt-Solid Interface	27
4.3	Heat Balance on the Liquid Pool	28
4.4	Quantification of Latent Heat and the Mushy Zone Phenomenon	30
4.5	Computation of Liquid Pool Temperature	31
4.6	Integration of the Heat Balance Equation at the Melt-Solid Interface	35
4.7	Solution of the Model Equation	41
4.8	Results and Discussion	43
Chapter-5.	MICROSCOPIC HEAT BALANCE MODEL BASED ON SYSTEM ENTHALPY	50
5.1	Different modes of Heat Transfer into and out of the System	52
5.2	Macroscopic Heat Energy Balance	52
5.2.1	Heat Energy in	53
5.2.2	Heat Energy Generated	53
5.2.3	Heat Energy out of the System	54
5.2.3.1	Conduction	54
5.2.3.2	Bulk Heat Carried by Strip at Exit	57
5.2.3.3	Bulk Heat Carried by Copper Drum at Exit	60
5.2.3.4	Heat Loss due to Radiation	62
5.2.4	Final Governing Equation	63
5.3	Temperature along the Surfaces of the Drum	64
5.4	Results and Discussion	68
Chapter-6.	CONCLUSION	
6.1	Conclusions Relating to Process Operation	75
6.2	Conclusions Relating to Process Design	77

Chapter-7. SUGGESTIONS FOR FUTURE WORK

7.1	Macroscopic Model	79
7.2	Microscopic Model	80
FIGURES		83
TABLES		111
APPENDIX		117
BIBLIOGRAPHY		121

ABSTRACT

The Near-Net-Shape route of manufacturing flat products has received considerable importance in the recent times due to the economic advantages associated with it. One such process is the single roll/drum horizontal strip caster. In this caster, the liquid metal from tundish is allowed to flow through a nozzle on to the surface of a rotating copper/steel drum which is water cooled from inside. The melt solidifies at the point of contact to form a thin skin which continues to grow to become the strip during the course of motion in the liquid. In the present investigation, an attempt has been made to predict the effect of process parameters on the process performance with the help of two mathematical models which are formulated to simulate the process.

The first formulation is based on the macroscopic heat balance in which the rate of growth of solidification front is expressed as a function of the enthalpy difference of the mass fraction of the liquid undergoing liquid-solid phase transformation. Using this formulation it has been possible to predict the effects of such operating conditions of the caster as the speed of rotation of the drum, cooling rate, melt temperature and the design aspects like the thickness of the drum wall and height of melt fill on the thickness of the strip. The results show that the strip thickness is dependent on these parameters and speed of rotation of the drum is the most important one.

The second model is based on a microscopic heat balance applied in the form of net heat energy entering the system being equal to the net heat leaving the system. Solution of the model equation, gives useful information like the temperatures existing along the surfaces of the drum and in strip for different operating conditions. The results show that the temperature existing on the drum is dependent on the strip thickness being cast and the cooling rate occurring in the casting is strongly dependent on the thickness of drum wall used in the caster.

Simulating the process with the help of these two models, it has been possible to draw some conclusions about the kind of interrelationships that exist between the key variables of the process from the point of view of operation and design.

LIST OF FIGURES

Fig.No.		Page No.
1.1	Process routes for producing flat rolled products	83
2.1	Stationary Mould Casters	84
2.2	Twin Belt Thin Caster	85
2.3	Moving Belt with 1 or 2 Rollers	85
2.4	Single and Twin Roll Caster	86
2.5	Spray Deposition Process	86
2.6	Heat Transfer Coefficient Data	87
3.1	Schematic sketch of the Single Roll (Drum) Horizontal Strip Caster	88
3.2	Schematic sketch of the Tundish	89
3.3	Schematic sketch of the Physical Phenomenon occurring in the Process	90
4.1	Sketch to establish Angular Relationships	90
4.2	Effect of the Speed of Rotation (R.P.M.) on the Strip Thickness at different cooling conditions (Liquid = 1580°C)	91
4.3	Effect of the Speed of Rotation (R.P.M.) on the Strip Thickness at different cooling conditions (Liquid = 1600°C)	92
4.4	Effect of the Cooling conditions at the inner surface of Drum on R.P.M.	93
4.5	Effect of the Thickness of Copper Drum Wall on R.P.M.	94

Fig.No.		Page No.
4.6	Effect of the Thickness of Copper Drum Wall on R.P.M.	95
4.7	Effect of the Superheat of Melt on R.P.M.	96
4.8	Effect of the Superheat of Melt on R.P.M.	97
4.9	Effect of the Superheat of Melt on R.P.M.	98
4.10	Effect of the Metal Head on R.P.M. for casting a particular Strip Thickness	99
4.11	Effect on Liquid Pool Temperature under different Cooling conditions	100
5.1	Schematic sketch of the Microscopic Heat Balance Model based on System Enthalpy	101
5.2	Schematic sketch of the Growth of Solid Skin on Copper Drum	102
5.3	Schematic sketch of the Thermal Composite Layers of Strip at β_2 for evaluating the Bulk Heat	102
5.4	Schematic sketch of the Thermal Composite Layers of the Wall of Copper Drum at β_2 for evaluating the Bulk Heat	102
5.5	Effect of Casting different Strip Thicknesses on the Surface Temperature of Copper Drum	103
5.6	Effect of Cooling condition on the Surface Temperature of Copper Drum	104
5.7	Effect of Drum Wall Thickness on its Surface Temperature	105

5.8	Effect of Casting different Strip Thicknesses on the Cross sectional Temperature of Strip and Drum at exit (β_2)	106
5.9	Effect of cooling condition on the Cross sectional Temperature of Strip and Drum at exit (β_2)	107
5.10	Effect of Drum Wall Thickness on the Cross sectional Temperature of Strip and Drum at exit (β_2)	108
5.11	Recirculation Heat associated with R.P.M.	109
7.1	Schematic sketch of Model based on Unsteady State Heat Transfer	110

LIST OF TABLES

Table

No.	Page No.
1.1 Comparison of the energy required to make carbon steel strip/sheet by three different processes	111
2.1 Worldwide activities in the field of Near-Net-Shape Casting	112
3.1 Specifications of Water Spray Nozzle	113
4.1 Output from the Macroscopic Model Solution (0.2-3.9 R.P.M.)	114
4.2 Output from the Macroscopic Model Solution (2.1-2.2 R.P.M.)	115
4.3 List of Constants used in Simulation	116 --

NOMENCLATURE

Temperatures

T	Variable temperature, $^{\circ}\text{C}$
T_a	Ambient air temperature, $^{\circ}\text{C}$
T_{Cu}	Variable temperature along the thickness of copper drum, $^{\circ}\text{C}$
$T_{\text{Cu1}}, T_{\text{Cu2}}, \dots, T_{\text{Cum}}$	Temperatures at the 'm' different points along the thickness of Cu drum in different composite layers at β_2 (exit), $^{\circ}\text{C}$
T_{Cuin}	Mean input temperature of Cu drum, $^{\circ}\text{C}$
T_F	Freezing temperature of melt, $^{\circ}\text{C}$
T_1	Temperature of melt, $^{\circ}\text{C}$
T_L	Liquidus temperature of alloy, $^{\circ}\text{C}$
T_P	Temperature of melt in pool, $^{\circ}\text{C}$
T_{rad}	Mean of T_F and T_1 for quantifying radiation, $^{\circ}\text{C}$
T_S	Solidus temperature of the alloy, $^{\circ}\text{C}$
$T_{\text{S1}}, T_{\text{S2}}, \dots, T_{\text{Sj}}$	Temperatures at the 'j' different points along the thickness of strip in different composite layers at β_2 (exit), $^{\circ}\text{C}$
$T_{\text{Si1}}, T_{\text{Si2}}, \dots, T_{\text{Sin}}$	Temperature along the inner surface of the in the 1st, 2nd,nth cylindrical element
$T_{\text{So1}}, T_{\text{So2}}, \dots, T_{\text{Son}}$	Temperature along the outer surface of the in the 1st, 2nd,nth cylindrical element
T_w	Temperature of spray water, $^{\circ}\text{C}$

Thermal Quantities

c_{pCu}	Mean heat capacity of solid copper, W/
$c_{\text{pCu}}(T)$	Heat capacity of solid copper at temperature
c_{pl}	Mean heat capacity of liquid, W/kg. $^{\circ}\text{C}$
c_{ps}	Heat capacity of solid, W/kg. $^{\circ}\text{C}$
$c_{\text{ps}}(T)$	Heat capacity of solid at temperature

ϵ_1	Emissivity of liquid
h_{CuW}	Heat transfer coefficient between inner surface of copper drum and spray water, $W/m^2 \cdot ^\circ C$
h_{PF}	Heat transfer coefficient between liquid pool and liquid-solid interface, $W/m^2 \cdot ^\circ C$
$H(T_1)$	Enthalpy of melt at temperature T_1 , W/kg
$H(T_P)$	Enthalpy of liquid in pool, W/kg
$H_S(T_F)$	Enthalpy of solid at temperature T_F , W/kg
k_{Cu}	Thermal conductivity of solid copper, $W/m^2 \cdot ^\circ C$
k_S	Thermal conductivity of solid, $W/m^2 \cdot ^\circ C$
L	Latent heat of fusion of solid, W/kg
Q_{Cuin}	Bulk heat flow input of Cu drum, W
$Q_{Cu1}, Q_{Cu2}, \dots, Q_{Cum}$	Bulk heat carried by 1st, 2nd, ...mth composite layer of copper drum at exit, W
$Q_{d1}, Q_{d2}, \dots, Q_{dn}$	Conductive heat in the 1st, 2nd, ...nth cylindrical element along radial direction, W
$Q_{S1}, Q_{S2}, \dots, Q_{Sj}$	Bulk heat carried by 1st, 2nd, ...jth composite layer of strip at exit, W

Angles

β	Angular variable
β_1	Position of start of solidification, radians
β_2	Position of end of solidification, radians
$\Delta\beta$	Angle subtended by each of the solid cylindrical element at the centre of Cu drum, radians
ω	Angular velocity of Cu drum, radians/sec.

Geometric terms

j	Number of composite cylindrical elements in solid at β_2
m	Number of composite cylindrical elements in copper drum at β_2
n	Number of cylindrical elements on drum and

skin surface

Geometric terms

R_d	Radius of copper drum, m
r, R	Variable radial coordinate, m
t_1, t_2, \dots, t_n	Thickness of skin in 1st, 2nd, ... nth cylindrical element, m
t_i	Initial thickness of skin at β_1 , m
t_f	Thickness of strip, m
t_{Cu}	Thickness of copper drum, m
δ	Distance of separation between drum and tundish, m
z	Width of strip, m

Others

ρ_s	Density of solid metal being cast, kg/m^3
ρ_l	Density of liquid metal, kg/m^3
ρ_{Cu}	Density of solid copper, kg/m^3
σ	Stefan-Boltzman's constant
V_l	Volumetric flow rate of liquid, $\text{m}^3/\text{sec.}$
τ	Variable time, secs.

Chapter 1

INTRODUCTION

The conventional methods of producing metallic strips and sheets require the casting of large ingots or slabs which are subsequently hot rolled and cold rolled to final thickness. Several unit operations like ingot soaking, slabbing, slab grinding, intermediate annealing, pickling, coil grinding, final annealing and final pickling are generally involved. These operations consume time and energy and often require expensive equipments. An alternative to this route, which has shown a lot of potential is the near-net-shape casting (also known as direct strip casting). In this method, the steel strips/thin slabs are cast close to the final strip thickness and thus many of the unit operations of the conventional method are eliminated. The two routes namely, the conventional route and the direct strip casting route are shown pictorially in Fig. 1.1 .

The casting of strips and sheets directly from liquid metal has become an established practice in aluminium and other low melting alloys. Casting high melting point metals like steel has however not yet been commercialised widely in spite of the fact that the first attempts to cast steel strip and sheet date back to over a hundred years. In July 1865, a U.S. patent was issued to Sir Henry Bessemer on a process for 'rolling sheets, plates, bar and other forms from fluid malleable iron or steel by running or pouring the

said fluid material between rolls'. But this process could not succeed at that time because of constraint in the quality of material and the inadequate process control. With the advancement of Technology, most of these problems have been overcome and very recently Nippon Steel, Japan announced the production of stainless steel sheet using such technique.

Table 1.1 shows a comparison of energy consumption between the three carbon steel sheet/strip producing processes : Ingot casting, Conventional continuous casting and Direct strip casting (DSC). The figures represent the energy requirements for producing steel strip from the molten metal stage to the final product. For the direct strip casting process, the figures include the energy required in ladle holding and heating, tundish pre-heating, casting and post casting treatments such as pickling, rolling and annealing. The figures indicate that approximately 68% energy savings is possible by using the direct strip casting method in place of ingot process. Comparison of the conventional continuous casting process and the direct strip casting method indicates a saving of 61% energy savings from the use of the latter.

The direct strip casting units are classified into four categories based on the thickness of strip/slab these are capable of producing :

- (1) The thin slab caster producing 20-40mm thick slabs which could be directly fed into the finishing stands of the hot strip mill.
- (2) The thick strip casters giving 5-15mm thick strips which need some limited hotrolling due to metallurgical reasons.
- (3) Strip casters producing strips less than 10mm thickness which go directly to the cold rolling plant.
- (4) The thin strip caster which would produce directly a final product equivalent either to the as rolled sheet or to the cold rolled sheet : the thickness then goes down to 1/10ths of a mm.

In the light of the numerous advantages that the near-net-shape casters offer, attempts are being made all over the world to develop these processes. Research & Development unit of the Govt. of India owned public sector undertaking 'Steel Authority of India Ltd.' (SAIL) is attempting to indigenously develop one such process (single roll, horizontal design). The task of developing the mathematical model for quantitative analysis of the single roll process to predict the effect of process parameters e.g., speed of rotation of the drum, cooling conditions of the drum, composition of steel, superheat of molten steel etc. on the final product thickness has been entrusted on this department. The present investigation is a part of this major project.

The main aim in the present investigation is to develop simple but realistic enough mathematical models based on the conservation of heat which can be used to predict the effect of various process parameters on the process performance in terms of strip thickness and the rate of production etc. It is envisaged that such an analysis will give insight about the process which may be desirable from the point of view of designing the caster

Chapter 2

LITERATURE REVIEW

This chapter has been divided primarily into two parts. In the first part, a brief description of various near-net-shape casters is presented whereas the second part consists of a critical review of the literature on the mathematical modelling of the physical phenomenon involved.

2.1 DESCRIPTION OF VARIOUS NEAR-NET-SHAPE CASTERS

The design and implementation of near-net-shape casters must meet certain requirements in order to prove more effective to the conventional continuous casters. Some of these requirements are :

- (1) Their productivity must match at least with that of 1-strand continuous caster producing the same width in order to avoid excessive multiplication of casting strands. This means that the casting speed has to be increased in inverse proportion to the ratio of thicknesses.
- (2) Stationary oscillating moulds are unable to cope with such high speeds - the traveling mould that accompanies the product during its withdrawal is the solution.

Belts and rolls are the best designs that could be considered.

- (3) The feeding of molten steel should be gentle to avoid splashes which could lead to poor surface quality. Molten steel pre-treatment, dynamic control of temperature, prevention of reoxidation and renitrogenation by the air are essential to ensure satisfactory quality. Surface and internal quality must be irreproachable, since there is no chance to correct these defects in the as cast condition. The geometry of the product should also be adequate : flatness, longitudinal and transverse profiles and width must be controlled.
- (4) At the exit of mould, the cast product should be easily stripped from the mould surface.
- (5) For thin slab casting, the surface temperature over the entire strand dimension should be high enough to allow subsequent hot rolling when necessary.
- (6) Comprehensive production planning and quality control systems for casting different types of steel with properties equal to or superior to the ones produced through conventional routes.

The various types of near-net-shape casters for steel which are under development or have already been introduced at least at the laboratory/pilot plant stage can be classified into 3 categories:

- (1) Stationary mould casters

- (2) Travelling mould casters
- (3) Spray deposition casters

2.1.1 Stationary Mould Casters

These designs are based on the familiar technology of conventional continuous slab casting but for product thickness from 40-70mm in widths of up to 1.6m and at a speed of 5-6m/min. Figure 2.1 depicts some of the stationary mould designs. Most of these designs incorporate the 'classical' vertical mould with oscillation movement. In order to avoid metal feeding problems, the upper mould section is made wide enough to accommodate a refractory tube. The strand which is still not completely solidified is reduced to its final thickness through one of the following methods :

- an oval casting section with reduction below the mould
- a partially oval ('bellied') section with reduction below the mould
- a flat section gradually reduced over the mould's full length
- a rhombic section gradually reduced in the upper part of the mould
- a 'bellied' section gradually reduced in the upper half of the mould incorporating movable narrow faces to compensate

for the width increase experienced during thickness reduction.

SMS Schloemann-Siemag have reported the use of funnel shaped stationary mould with a specially contoured submerged nozzle to prevent steel reoxidation in their 1985 pilot plant for slab casters. A high casting speed of 6 m/min. and mould oscillation of 400 cycles/min. at stroke lengths of 4-8mm has been tested for producing all types of steels that are conventionally castable. Use of new viscosity, low melting point mould powder is used. MDH and MRW of FRG have announced the development of a slab caster (40 - 70mm thickness, 1.2m wide) with narrow submerged nozzle, vertical curved mould with parallel broad faces to guide the strand vertically in the upper part of the mould and tangentially at the lower mould region and adjustable mould width. The caster can also work under any dry conditions without water spray. Direct hot rolling to 10mm has also been tested. In all these stationary mould processes, a high mould friction is the limiting factor. Therefore casting speeds are limited and so is the throughput rate. This is apart from the hazard of surface defects when casting thin sections with mould powder as the lubricant or without any lubricant at all.

2.1.2 Travelling Mould Casters

Fig. 2.2-2.4 depicts some of the casters in this category. The aim

in these designs is to minimise the interaction between the mould wall and cast product which is a major deficiency in the earlier mentioned process for casting thin sections at high speeds. These casters require no casting powder for lubrication but for heat flow reasons a suitable coating is provided. Some of the prominent casters in this category are explained in the following pages :

2.1.2.1 Twin Belt Thin Slab Caster

A general design differentiating diagram of the different casters in this category is shown in Fig. 2.2. The Hazelett twin belt caster, the concept of which was proposed in 1940 by Hazelett for casting non ferrous metals has been tried with steel. The top and bottom mould surfaces consist of thin endless steel belts supported by large finned pulleys. The belts are driven by nip pulleys, while surface flatness throughout the length of mould is provided by tension pulleys. Several finned backup rolls give further support. The width and thickness of slab is determined by a series of steel edge dam blocks attached to a welded stainless steel strip. The mould cavity is formed by sandwiching the edge dam block between the upper and lower belts. Both the belts are water cooled. High pressure water is directed towards the front end of the caster belt and low pressure water in other regions. To assure consistent heat transfer and to separate the belt from slab at exit, a consumable coating and parting agent is used. The stock from this caster is fed to a slightly lower speed rotating pinch roll which accommodates constant compression during total solidification.

Kawasaki and Hitachi have attempted a vertical configuration of the above process with a V shaped mould and submerged nozzle. Krupp, Sumitomo Metal Industries, U.S.Steel and Bethlehem Steel Corporation are the others who are attempting this process with improvements. Problems in direct hot charging, steel feeding, side sealing and width adjustment during casting have been reported.

2.1.2.2 Moving Belt with 1 or 2 Rollers

The use of rollers is required to eliminate the last mentioned problem of the previous process namely width adjustment and steel feeding. The designs are still not perfected and investigations in this direction are actively being pursued at NSC, NKK, Kawasaki Steel, Kobe Steel, Nippon Metals all from Japan and Bethlehem Steel-USA, IRSID and many research establishments in Europe.

The processes in this category involve feeding liquid metal between the gap of the two rotating rollers or a roller and belt the inside of which are water cooled. Fig. 2.3 schematically shows of some of these processes. British Steels, U.K. has reported the use of a mould car to pour metal onto a horizontally moving belt. In these processes, the speed of rotation of the rollers is crucial since shearing of strip is to be avoided. The problems reported in these designs is the difficulty in controlling the process, which is important since the internal quality very much depends on the process condition and requires the maintenance of constant temperature

across the width.

SINGLE ROLL CASTERS which make use of only 1 roller belong to the typical melt-drag processes. One such process which has been examined in this investigation is described in detail in chapter 3. The different types of casting machines in this category are shown in Fig. 2.4. The single roll casters have been built or announced by Battelle Columbus, MIT, National Steel, Armco, Allied Chemical, Allegheny Ludlum, Voest Alpine and Nippon Metal Industry (NTK). NTK jointly with Krupp Stahl have developed a twin roll caster with unequal diameter stainless steel rollers as the cooling substrate. The reported strip thickness is 1-4mm in widths of 30cm at casting speed of 10-40 m/min. The problems reported in these processes is the dependency of strip thickness on the process conditions and the criticality in the requirement of substrate surface quality. But the process has the advantage of simple machine design and the internal quality of strip is largely independent of process conditions.

2.1.3 Spray Deposition Process

Fig. 2.5 shows the different designs in this category. In these processes the steel issuing from tundish is atomised by a nozzle. The droplets deposit and solidify on a collection surface or substrate which is moving. Depending on the substrate used, billets, slabs, tubes, strip or even coatings can be produced.

The use of several nozzles permits the production of composites and multi layer materials. Using an injector nozzle it is possible to incorporate finely dispersed particles. A variation of this process is the spray rolling process in which the sprayed mass is hot or cold rolled to eliminate porosity and obtain a smooth semi-finished sheet product. The reported problem of this process is the typical surface texture in the cast product. The worldwide activities in the area of near-net-shape casting processes is shown in table 2.1.

2.2 MATHEMATICAL MODELLING OF THE PHYSICAL PHENOMENON INVOLVED IN NEAR-NET-SHAPE CASTING PROCESSES

In the near-net-shape casting processes, the liquid with some amount of superheat comes in contact with a moving substrate which is at low temperature and continuously cooled from spray water. Due to the rapid heat extraction, the liquid solidifies on the substrate to a small thickness which continues to grow to final thickness during the further course of motion of the substrate in the liquid metal. In the following paragraphs a critical review of the literature on the mathematical modelling of the physical phenomenon involved is presented.

The general numerical treatment of the rapid solidification

phenomenon occurring in the rotary type of continuous casters have been researched by Clyne¹² and Takeshita¹⁶. They have analysed the heat transfer problem with phase transformation during the quenching to predict the solid-liquid interface and the temperature change. The analysis couple the heat flow with crystal growth kinetics. The selection of appropriate boundary conditions is also given.

Stanek and Szekeley¹¹ have quantified a drum and ring type of horizontal strip caster using an analytical method. The analytical expressions were obtained on the basis of two heat balances : (i) the growth of shell on the drum and ring was through a dynamic heat balance between the rate at which thermal energy was supplied and withdrawn at the melt-solid interface, and (ii) the rate of heat input by the metal stream must be equal to the sum of the rates of heat removed by the drum and ring. The two equations involving strip thickness and speed of rotation as variables was solved by trial and error. The model equations have been tested for two steel strip thicknesses namely, 3.8mm and 12.5mm. In the former, the growth of skin matched closely with the numerical trend taking a near linear form from start to end, while in the latter, there was slight deviation from the numerical trend but still retained the linear near form.

One of the major shortcomings of this model is its inability to

account for the rapidly solidified component in the growth of skin. The drum and ring stay in heat supply zone for less than $1/4$ th of the time required to complete 1 revolution and during the entire period, both are continuously cooled from spray water. So the temperature at which the drum and the ring enter the heat supply zone is very much less compared to the temperature of liquid, with the result that as soon as this surface comes in contact with liquid, there is rapid quenching transforming it into solid at the start of solidification. The growth of skin into final strip thickness takes place above this rapidly solidified mass.

Pimputkar *etal*² have shown that in case of single roll horizontal caster, the final strip thickness t_f is built from three contributions t_i , t_v and t_p where t_i is the thickness from rapid solidification, the determination of which is through an approximation of heat transfer to that occurring between two semi-infinite media; t_v is the component from liquid which is dragged along by the solidifying strip due to viscous traction; and t_p is the thickness from pressure or head driven liquid flow. The results show that the stand-off distance between the tundish and nozzle, the head height, wheel speed and melt pressure to be strongly affecting the strip thickness while the orientation of orifice and its size, superheat of melt, substrate temperature and material to be weakly affecting the strip thickness.

Very thin strip formation in single roll chill block casters is both heat and momentum controlled¹⁸ and not just momentum controlled¹⁷. The results of such an analysis show that the strip thickness increases with cooling conditions. The problem was treated as a two dimensional transient fluid flow with free boundaries using a SOLA-VOF code computer program and the results showed the presence of some rotational fluid flow in the melt puddle and the length of puddle decreased with increase in substrate velocity. But the puddle length increased with decrease of melt-jet velocity¹⁹. Experimental investigations for thermal contact between melt and substrate showed that the value of heat transfer coefficient was not constant throughout the strip length but a higher value at the start and lower value towards the end prevailed. In addition to an effect from roll material and substrate velocity, the strip thickness increased with increase in contact area but the growth was more at the start and almost constant towards the end²⁰.

For the same single roll chill block melt spinning process, Gutierrez¹³ has solved the momentum and energy equation right upto the meniscus in liquid based on the dominance of capillary fluid dynamics in the process. The equation used for correlating the height of meniscus was from the formulations developed while withdrawing solid bodies from liquid. An explicit finite difference scheme was used to solve the partial differential equations. The predictions from the model are similar to the earlier ones. The existence of a large area of slowly

recirculating flow centred about the middle of the puddle was shown. The temperature gradient across the different sections of the flow were able to explain the microstructural characteristics of the cast strip.

Yu¹⁴ for the same process used the rate of growth of solidification front data to locate the solid-liquid interface. The conservation of mass and momentum were set up for the different regions of the process and the differential equation of the meniscus profile was expressed in terms of the atmospheric pressure and the pressure inside puddle using the thin film theory. The equations were solved iteratively with an assumed value of puddle pressure and confirmed if the height of meniscus at the point of final strip thickness was zero. A fourth order Runge-Kutta method was used for solving the differential equation of the meniscus. The model has been tested for aluminium strip thickness of 0.15-0.70mm and tundish-roll gap of 0.75-1.20mm. The results show the possibility of casting thinner strips at high speed and reduced width of nozzle passage. Not much variation in strip thickness was observed while altering the roll-tundish gap which contradicted the experience with casting slightly higher strip thickness². The main difficulty associated with this model is the generation of rate of growth of solidification front data. The latter is a function of the speed of rotation of substrate material, heat transfer coefficient, superheat of liquid and the thermal conductivity of substrate material.

recirculating flow centred about the middle of the puddle was shown. The temperature gradient across the different sections of the flow were able to explain the microstructural characteristics of the cast strip.

Yu¹⁴ for the same process used the rate of growth of solidification front data to locate the solid-liquid interface. The conservation of mass and momentum were set up for the different regions of the process and the differential equation of the meniscus profile was expressed in terms of the atmospheric pressure and the pressure inside puddle using the thin film theory. The equations were solved iteratively with an assumed value of puddle pressure and confirmed if the height of meniscus at the point of final strip thickness was zero. A fourth order Runge-Kutta method was used for solving the differential equation of the meniscus. The model has been tested for aluminium strip thickness of 0.15-0.70mm and tundish-roll gap of 0.75-1.20mm. The results show the possibility of casting thinner strips at high speed and reduced width of nozzle passage. Not much variation in strip thickness was observed while altering the roll-tundish gap which contradicted the experience with casting slightly higher strip thickness². The main difficulty associated with this model is the generation of rate of growth of solidification front data. The latter is a function of the speed of rotation of substrate material, heat transfer coefficient, superheat of liquid and the thermal conductivity of substrate material.

Berger¹⁵ used a control volume approach for different zones of the process instead of seeking the solution to full governing non-linear partial differential equations. Momentum conservation equations were written for different zones while the solidification zone included an additional energy conservation equation taking into account the pool heat transfer coefficient between liquid and solid and the latent heat. It was assumed that the liquid-solid interface was flat. The contact angle between the solid-liquid interface and the substrate surface, and the strip thickness were the variables in the final equation. A major assumption that the contact angle value for any particular tundish-roll gap which also corresponds to the maximum strip thickness that could be cast was considered valid for strip thicknesses less than this. By, this different strip thicknesses were determined for different operating conditions. The results indicate the maintenance of a certain amount of curvature for the meniscus in the process.

Miyazawa²¹ has modelled a double roll caster for casting strips of 0.01-0.10mm thickness. Both fluid flow phenomenon and the plastic deformation of the solid phase are included for quantification. The two dimensional convective-diffusion energy equation was solved using an implicit finite difference scheme. The results of the model showed that the range by which the operating parameters (roll gap, angular velocity of rolls, feed rate of material) could be varied was narrow and a vortex in liquid was observed just above the point where the two solid

shells join to form the strip. Some amount of solid recirculation at the solid fusion point was observed for high volumetric flow rate of incoming liquids.

The model equations have been extended to cast strips upto 1mm using copper rolls and the supercooling phenomenon of liquid was taken into account²¹. Detailed mathematical analysis is not provided, but the effect of roll rotation speed on the distance from meniscus to the starting point of solidification is shown. With increased initial undercooling, commencement of solidification was delayed. The end point of solidification did not depend on the initial undercooling because the solidification rate increased with increased undercooling.

2.3 HEAT TRANSFER COEFFICIENT DATA

Some results of the experiments conducted for measuring the heat transfer coefficient required in the mathematical modelling of near-net-shape casting processes indicate a dependence of the latter on the type of spray, distance of separation of spray from the surface and the water flux falling on the surface. These are available in the form of graphs which is shown in Fig. 2.6²²⁻²⁴

In view of the non-availability of an appropriate mathematical model for a single roll horizontal strip caster capable of producing strips in the thickness range 3-10mm, an attempt is made in the present investigation to develop some simple mathematical models which can be used to predict the effect of the operating parameters of the process like melt temperature, speed of rotation, contact area etc. on the process performance in terms of strip thickness, temperature distribution in the strip and copper drum etc.

Chapter 3 describes the construction and design of the strip caster that has been mathematically modelled in this investigation.

In chapter 4, a mathematical model based on the macroscopic heat balance is given. The principle involved in the development is expressing the rate of growth of solidification front as a function of enthalpy difference. Using this, two simultaneous equations are arrived at, in which the strip thickness and the speed of rotation of the roller are the only variables. These equations have been solved analytically to examine the effects of speed of rotation of the roller, cooling rate, melt temperature etc. on the strip thickness. The results based on this model are presented at the end of this chapter.

A microscopic heat balance model is developed in chapter 5 which is based on the principle that the net enthalpy input into the system must be equal to the net heat removed from the system. The heat balance is carried out along the system boundaries in microscopic elements. The model can give information like the temperature that exist along the inner and outer surfaces of the roll for different strip thicknesses, for different cooling conditions and for variations in the geometry of the process.

Based on the experience of the simulation of the process using the two mathematical models, some tentative conclusions that can be drawn about the process are given in chapter 6.

Chapter 7 contains some suggestions and the scope of enlarging the present models for further refinements.

PROCESS DESCRIPTION

The single roll strip casting process that has been modelled and simulated in the present investigation is the one being envisaged and fabricated by R & D Centre for Iron and Steel, SAIL, Ranchi. In the first section of this chapter, a brief description of the caster is presented while the physical phenomenon taking place during the casting is described in the last section.

3.1 DESCRIPTION OF CASTER

A schematic sketch of the caster is shown in Fig. 3.1. The set up consists of the following main components :

- | | | | |
|---|--------------------|---|----------------|
| 1 | Tundish | 5 | Water Outlet |
| 2 | Copper Drum/Roller | 6 | Knife edge |
| 3 | Pressure Roll | 7 | Electric Motor |
| 4 | Water Sprays | | |

3.1.1 Tundish

It is made of alumina-graphite refractory and is designed to hold liquid metal upto a capacity of 50 kgs. The refractory wall of tundish facing the copper drum has a concentric profile to the

latter and is positioned as close to it as possible so that no scratches occur on the drum surface. A diagram of the tundish is shown in Fig. 3.2. The internal dimensions of the tundish are 240x150x200mm (length-150mm, breadth-200mm, height-240mm). The tundish has a rectangular nozzle opening at the bottom of the wall facing the drum through which liquid metal flows on to the rotating drum. The liquid pool for solidification is contained in the gap (20mm) between the tundish and the drum. To place the tundish at different positions above the horizontal plane of the drum, different tundishes with slightly different wall contours to match the surface contour of the drum are used.

3.1.2 Copper Drum / Roller

It is made of 99.999% electrolytic grade copper and has an outer diameter of 0.25m. The wall thickness of the drum is 50mm. The ends of the drum are fixed to close fitting flanges at the centre of which a shaft passes. Powered from a DC motor, the drum can rotate between 0.1-11.5 RPM as per requirement. The surface of drum has been finished to mirror quality. The liquid metal strikes the drum surface above the horizontal plane of drum at some point depending on the position of the tundish. Heat is continuously extracted from the internal surface by water sprays which are located inside the drum. A knife edge located on the other side peels off strip from the drum. To measure the temperature of the drum, there is provision to insert thermocouple temperature sensors : one near the outer surface, one at the centre and the

third one towards the inner surface. For a given height of liquid in the tundish, strips of different thicknesses can be produced by varying the speed of rotation of the drum. The copper drum has a width of 400mm.

3.1.3 Pressure Roll

Situated vertically above the copper drum, the primary aim of this component is to uniformise the thickness of strip. Its diameter is 80mm and made from stainless steel. It is capable of vertical movement for adjustments to different strip thicknesses.

3.1.4 Water Spray

The spray water extracts heat from copper drum which in turn extracts heat from the liquid metal thus facilitating solidification. The inlet water is through a horizontal pipe passing along the axis of the drum. On this pipe are mounted 12 nozzles. These are arranged in 3 rows each row having 4 nozzles. These 4 nozzles are positioned at right angles to each other. The diameter of the nozzle at the exit point is 5mm and the solid angle of spray cone ranges between $61^\circ - 64^\circ$. Some additional details of the nozzle are included in table 3.1. The nozzles are stationary at all times. The inlet water pressure normally is in the range of 4-5 kg/cm².

3.1.5 Water Outlet

The temperature of cooling water after heat extraction is expected to be about 60-70°C. After striking the inner surface of the copper drum, the spray water falls to the bottom of the drum, from where it is continuously pumped out.

3.1.6 Knife Edge

The knife edge is fixed to a stand which is to the left of copper drum. By giving appropriate horizontal and vertical movements, the knife edge can be positioned to any location on the upper left of the drum. The primary function of the knife edge is to separate the strip from the drum surface and direct it to the finishing stand.

3.1.7 Electric Motor

The requisite power to rotate the copper drum at a desired R.P.M. is provided by a DC type motor of 3.5 H.P. The motor drives a worm reduction gear box (ratio 1:70) which in turn rotates the shaft of the drum.

3.2 DESCRIPTION OF THE PHYSICAL PHENOMENON

The phenomenon occurring in the process can be explained by referring to Fig. 3.3. Liquid metal at a particular temperature T_1 is held in the tundish where the liquid metal level is always kept constant to a height D by continuously pouring the melt from the top. The melt continuously enters the region between the rotating drum and the tundish wall through the nozzle at the bottom at temperature T_1 . As soon as the melt comes in contact with the drum which is at a substantially lower temperature, a skin of solid metal t_1 is formed at the angular position β_1 . The skin continues to grow during the course of motion in the liquid pool. Water at an input temperature T_w is sprayed on to the inner surface of copper drum which experiences continuous cooling. The wall thickness of copper drum is t_{Cu} . The skin attains the final thickness t_f (which is the thickness of the strip) at the angular position β_2 . The drum rotates with an angular velocity ω . Due to the continuous rotation of the drum, every point on it stays in the heat supply zone between β_1 and β_2 for a certain length of time depending on ω and for the remaining period it stays out of this zone during every complete revolution. Under steady state conditions, because of the alternate heating and continuous cooling of the drum, it always carries with it a certain amount of 'recirculating heat'. The liquid pool and skin are contained in the gap ϕ between the drum surface and tundish wall. At the solid-liquid boundary, the liquid to solid phase transformation reaction takes place releasing the latent heat of fusion L .

Chapter 4

MACROSCOPIC HEAT BALANCE MODEL

In this chapter, a mathematical model based on the overall heat balance quantifying the rate of growth of solidifying front is developed to predict the effect of various process parameters on the process performance.

The following assumptions are made for the development of the model:

- (1) Perfect mixing of molten metal in the pool which is at uniform temperature.
- (2) As soon as the liquid metal comes in contact with the copper drum, an initial thickness t_i is formed.
- (3) There is perfect thermal contact between the solidified shell and copper drum and no slip occurs during motion.
- (4) The thermal conductivity of solid shell and the copper drum are considered independent of temperature.
- (5) The width of strip is sufficiently large to neglect the end effects.

4.1 ANGULAR RELATIONSHIP

The following angular relationships are valid in the model.
(Figures 3.3 and 4.1 are referred to for description.)

$$\rho_2 - \rho_1 = \alpha_1 + \alpha_2 \quad (4.1)$$

$$\beta_2 = \beta_1 + \alpha_1 + \alpha_2 \quad (4.2)$$

$$\sin \alpha_1 = \frac{(D - Y)}{(R_d - t_f)} \quad ; \quad \alpha_1 = \sin^{-1} \frac{(D - Y)}{(R_d - t_f)} \quad (4.3)$$

$$\sin \alpha_1 = \frac{Y}{R_d} \quad ; \quad \alpha_2 = \sin^{-1} \left(\frac{Y}{R_d} \right) \quad (4.4)$$

Substituting equations (4.3) and (4.4) in (4.2)

$$\beta_2 = \beta_1 + \sin^{-1} \left(\frac{D - Y}{R_d - t_f} \right) + \sin^{-1} \left(\frac{Y}{R_d} \right) \quad (4.5)$$

4.2 HEAT BALANCE AT THE MELT-SOLID INTERFACE

The growth of solidified shell on the copper drum surface is established by a dynamic heat balance between the rate at which thermal energy is supplied and withdrawn at the metal solid interface.

$$\begin{aligned}
 & \left[\begin{array}{l} \text{Rate of advancement of} \\ \text{solidification front} \end{array} \right] \times \left[\begin{array}{l} \text{Effective latent heat} \\ \text{per unit volume} \end{array} \right] \\
 &= \left[\begin{array}{l} \text{Rate of heat conduction into} \\ \text{the solidified shell from} \\ \text{the solidification boundary} \end{array} \right] - \left[\begin{array}{l} \text{Heat flux from the} \\ \text{melt to the solid-} \\ \text{ification boundary} \end{array} \right] \quad (4.6)
 \end{aligned}$$

$$\begin{aligned}
 & \left[k_S \frac{\partial T}{\partial R} - h_{PF}(T_P - T_F) \right] \left[R_d + \frac{(t_i + t_f)}{2} \right] (\beta_2 - \beta_1) z \\
 &= \rho_S \left[R_d + \frac{(t_i + t_f)}{2} \right] \omega z \frac{dt}{d\beta} (\beta_2 - \beta_1) [H(T_P) - H_S(T_F)] \quad (4.7)
 \end{aligned}$$

$$k_S \frac{\partial T}{\partial R} - h_{PF}(T_P - T_F) = \rho_S \frac{dt}{d\beta} \omega [H(T_P) - H_S(T_F)] ; t_i < t < t_f \quad (4.8)$$

$$\text{for } R = R_d + t \text{ and } \beta_1 < \beta < \beta_2$$

4.3 HEAT BALANCE ON THE LIQUID POOL

The following are the different thermal energy terms associated with the heat balance in the liquid pool:

Rate of thermal energy introduced into the pool by feeding a melt with volumetric flow rate V and enthalpy $H(T_1) = V \rho_1 H(T_1)$

Enthalpy of the material leaving the pool through the solidified shell and associated entrained liquid $= V \rho_1 H(T_P)$

Rate of heat extracted from the pool by the cooled surface

$$= h_{PF} (T_P - T_F) z \int_{\beta_1}^{\beta_2} (R_d + t) d\beta \quad ; \quad t_i < t < t_f$$

Net Heat Balance on the Pool

$$\left[\begin{array}{c} \text{Enthalpy entering} \\ \text{the pool} \end{array} \right] - \left[\begin{array}{c} \text{Enthalpy leaving} \\ \text{the pool} \end{array} \right] = \left[\begin{array}{c} \text{Heat extracted} \\ \text{from pool by} \\ \text{conduction /} \\ \text{convection} \end{array} \right]$$

Hence,

$$V \rho_1 [H(T_1) - H(T_P)] = h_{PF} (T_P - T_F) z \int_{\beta_1}^{\beta_2} (R_d + t) d\beta \quad (4.9)$$

But,

$$\text{mass flow rate, } V \rho_1 = \left[R_d + \frac{t_f}{2} \right] \omega t_f z \rho_S \quad (4.10)$$

Also,

$$\int_{\beta_1}^{\beta_2} (R_d + t) d\beta = R_d (\beta_2 - \beta_1) + \int_{\beta_1}^{\beta_2} t d\beta \quad ; \quad t_i < t < t_f \quad (4.11)$$

$$\text{Assuming a mean thickness } t = \frac{(t_i + t_f)}{2}$$

$$\int_{\beta_1}^{\beta_2} t d\beta = 0.5 (t_i + t_f) (\beta_2 - \beta_1) \quad (4.12)$$

Combining equations (4.10), (4.11), (4.12) with (4.9) ;

$$(R_d + 0.5t_f) \omega t_f \rho_S [H(T_L) - H(T_P)] = h_{PF} (T_P - T_F) [R_d + 0.5(t_i + t_f)] (\beta_2 - \beta_1) \quad (4.13)$$

4.4 QUANTIFICATION OF LATENT HEAT AND THE MUSHY ZONE PHENOMENON

If an alloy is being cast, then the solidification takes place over a temperature range defined by the liquidus (T_L) and the solidus (T_S) temperatures. So the latent heat of fusion L is released continuously in this temperature interval and not at a particular temperature, the melting point, as is the case with pure metals.

The latent heat released during the solidification of an alloy can be accounted for using one of the following two ways :

- (1) To assume a pseudo freezing temperature T_F which is the mean of T_L and T_S and at which all the latent heat is released instantaneously, thus showing a pure metal like behaviour.
- (2) To assume a pseudo freezing temperature T_F , in which a fraction of latent heat is released in the interval T_L to T_F and the remaining at T_F .

In the present model, the second of the said two ways is used for

quantifying the latent heat. In the following lines, the quantification of latent heat as temperature drop occurs from T_L to T_F is shown :

Latent heat (L_{LT}) released while temperature drops from T_L to T is

$$L_{LT} = \frac{(T_L - T)}{(T_L - T_S)} \times L \quad (T_F < T < T_L) \quad (4.14)$$

Latent heat (L_{TF}) released while temperature drops from T to T_F is

$$L_{TF} = \frac{(T - T_F)}{(T_L - T_S)} \times L \quad (T_F < T < T_L) \quad (4.15)$$

The remaining latent heat (L_F) released instantaneously at T_F is,

$$L_F = \frac{(T_F - T_S)}{(T_L - T_S)} \times L \quad (4.16)$$

4.5 COMPUTATION OF LIQUID POOL TEMPERATURE

As already stated, steel is assumed to melt at a fixed temperature T_F which lies between the true liquidus and the solidus temperature i.e. ($T_S < T_F < T_L$). Due to the consideration of the release of latent heat of solidification, one would get two different expressions for the liquid pool temperature depending on

whether,

- (1) the Pool Temperature $T_P > T_L$ and
- (2) the Pool Temperature $T_F < T_P < T_L$

Case I Pool Temperature Greater than Liquidus

Here, during the temperature change of liquid from T_1 to T_P , no latent heat is evolved. Therefore the enthalpy change is given by:

$$H(T_1) - H(T_P) = c_{pl} (T_1 - T_P) \quad (4.17)$$

Where c_{pl} is the heat capacity of liquid,

Substituting equation (4.17) in (4.13),

$$(R_d + 0.5t_f) \omega t_f \rho_S c_{pl} (T_1 - T_P) = h_{PF} (T_P - T_F) [R_d + 0.5(t_i + t_f)] (\beta_2 - \beta_1) \quad (4.18)$$

or

$$\frac{T_1 - T_P}{T_P - T_F} = \frac{h_{PF} [R_d + 0.5(t_i + t_f)] (\beta_2 - \beta_1)}{(R_d + 0.5t_f) \omega t_f \rho_S c_{pl}} \quad (4.19)$$

Rewriting this equation in a slightly different form,

$$\frac{T_1 - T_F}{T_P - T_F} - 1 = \frac{h_{PF} [R_d + 0.5(t_i + t_f)] (\beta_2 - \beta_1)}{(R_d + 0.5t_f) \omega t_f \rho_S c_{pl}} \quad (4.20)$$

or

$$\frac{T_1 - T_F}{T_P - T_F} = \frac{h_{PF}[R_d + 0.5(t_i + t_f)](\beta_2 - \beta_1) + (R_d + 0.5t_f)\omega t_f \rho_S c_{pl}}{(R_d + 0.5t_f)\omega t_f \rho_S c_{pl}} \quad (4.21)$$

Rearranging terms,

$$T_P = T_F + \frac{(R_d + 0.5t_f)\omega t_f \rho_S c_{pl} (T_1 - T_F)}{h_{PF}[R_d + 0.5(t_i + t_f)](\beta_2 - \beta_1) + (R_d + 0.5t_f)\omega t_f \rho_S c_{pl}} \quad (4.22)$$

For an alloy of known composition, the thermophysical properties (c_{pS} , ρ_S) and T_F are fixed. Thus, for a given set of operating conditions T_1 , R_d and β_1 , β_2 are also fixed. Hence equation (4.22) has only two unknowns ω and t_f , i.e.,

$$T_P = f_1(\omega, t_f)$$

Case II Pool Temperature less than Liquidus

Since T_P is less than T_L , latent heat of fusion is released in the pool. The enthalpy change from T_1 to T_P is :

$$H(T_1) - H(T_P) = c_{pl}(T_1 - T_P) + \frac{(T_L - T_P)}{(T_L - T_S)} \cdot L \quad (4.23)$$

Substituting equation (4.23) in (4.13),

$$\begin{aligned}
 & (R_d + 0.5t_f) \omega t_f \rho_S \left[c_{p1} (T_1 - T_P) + \frac{L (T_1 - T_P)}{(T_L - T_S)} \right] \\
 & = h_{PF} (T_P - T_F) [R_d + 0.5(t_i + t_f)] (\beta_2 - \beta_1)
 \end{aligned} \tag{4.24}$$

or

$$\begin{aligned}
 & c_{p1} T_1 - c_{p1} T_P + \frac{L T_L}{(T_L - T_S)} - \frac{L T_P}{(T_L - T_S)} \\
 & = \frac{h_{PF} [R_d + 0.5(t_i + t_f)] (\beta_2 - \beta_1) (T_P - T_F)}{(R_d + 0.5t_f) \omega t_f \rho_S}
 \end{aligned} \tag{4.25}$$

or

$$\begin{aligned}
 & \left[c_{p1} T_1 + \frac{L T_L}{(T_L - T_S)} \right] - \left[c_{p1} + \frac{L}{(T_L - T_S)} \right] T_P \\
 & = \frac{h_{PF} [R_d + 0.5(t_i + t_f)] (\beta_2 - \beta_1) (T_P - T_F)}{(R_d + 0.5t_f) \omega t_f \rho_S}
 \end{aligned} \tag{4.26}$$

or

$$\begin{aligned}
 & \left[\frac{h_{PF} [R_d + 0.5(t_i + t_f)] (\beta_2 - \beta_1)}{(R_d + 0.5t_f) \omega t_f \rho_S} + \left[c_{p1} + \frac{L}{(T_L - T_S)} \right] \right] T_P \\
 & = \frac{h_{PF} [R_d + 0.5(t_i + t_f)] (\beta_2 - \beta_1) T_F}{(R_d + 0.5t_f) \omega t_f \rho_S} + \left[c_{p1} T_1 + \frac{L T_L}{(T_L - T_S)} \right]
 \end{aligned} \tag{4.27}$$

or

$$T_P = \frac{h_{PF} [R_d + 0.5(t_i + t_f)] (\beta_2 - \beta_1) T_F + (R_d + 0.5t_f) \omega t_f \rho_S \cdot F_c}{(R_d + 0.5t_f) \omega t_f \rho_S \cdot F_c + h_{PF} [R_d + 0.5(t_i + t_f)] (\beta_2 - \beta_1)} \quad (4.28)$$

$$\text{where } F_c = \left[c_{pl} T_1 + \frac{L T_L}{(T_L - T_S)} \right] \quad (4.29)$$

Again,

$$T_P = f_2(\omega, t_f)$$

4.6 INTEGRATION OF THE HEAT BALANCE EQUATION AT THE MELT-SOLID INTERFACE

Equation (4.8) can be rewritten as,

$$\frac{dt}{d\beta} = \frac{k_S \frac{\partial T}{\partial R} - h_{PF} (T_P - T_F)}{\rho_S \omega [H(T_1) - H_S(T_F)]} \quad (4.30)$$

The flux $k_S \frac{\partial T}{\partial R}$ when treated in cylindrical coordinates, gives a series summation (of divergent) type of expression for the integration of t . Since no approximation can be done for the series, this approach could not be used. The details of the treatment is given in Appendix-1.

Since the radius of copper drum R_d is very large compared to the drum wall thickness (t_{Cu}) and the strip thickness (t), the heat flux $k_S \frac{\partial T}{\partial R}$ can be approximated to that across a composite wall of thickness $t_{Cu} + t$. One face of this composite wall is the interface at temperature T_F and the other face is the inner wall of copper drum which is sprayed with water at temperature T_W .

Hence,

$$k_S \frac{\partial T}{\partial R} = \frac{(T_F - T_W)}{\frac{t}{k_S} + \frac{t_{Cu}}{k_{Cu}} + \frac{1}{h_{CuW}}} \quad (4.31)$$

$$= \frac{k_S (T_F - T_W)}{t + \left[\frac{k_S t_{Cu}}{k_{Cu}} + \frac{k_S}{h_{CuW}} \right]} \quad (4.32)$$

Substituting equation (4.32) in (4.30)

$$\frac{dt}{d\beta} = \frac{\frac{k_S (T_F - T_W)}{t + \left[\frac{k_S t_{Cu}}{k_{Cu}} + \frac{k_S}{h_{CuW}} \right]} - h_{PF} (T_P - T_F)}{\rho_S \omega [H(T_P) - H_S(T_F)]} \quad (4.33)$$

or

$$\frac{dt}{d\beta} = \frac{k_S (T_F - T_W)}{\rho_S \omega [H(T_P) - H_S(T_F)] \left[t + \left(\frac{k_S t_{Cu}}{k_{Cu}} + \frac{k_S}{h_{CuW}} \right) \right]} - \frac{h_{PF} (T_P - T_F)}{\rho_S \omega [H(T_P) - H_S(T_F)]} \quad (4.34)$$

$$\text{Let } \frac{k_S (T_F - T_W)}{\rho_S \omega [H(T_P) - H_S(T_F)]} = a_1, \quad \frac{h_{PF} (T_P - T_F)}{\rho_S \omega [H(T_P) - H_S(T_F)]} = a_2,$$

$$\left(\frac{k_S t_{Cu}}{k_{Cu}} + \frac{k_S}{h_{CuW}} \right) = a_3 \quad (4.35)$$

Putting the above values in equation (4.34),

$$\frac{dt}{d\beta} = \frac{a_1}{t + a_3} - a_2 \quad (4.36)$$

or

$$\frac{dt}{d\beta} = \frac{(a_1 - a_2 a_3) - a_2 t}{t + a_3} \quad (4.37)$$

or

$$\frac{(t + a_3) dt}{[-a_2 t + (a_1 - a_2 a_3)]} = d\beta \quad (4.38)$$

or

$$- \frac{(t + a_3)}{a_2 \left[t + \left[a_3 - \frac{a_1}{a_2} \right] \right]} dt = d\beta \quad (4.39)$$

or

$$- \frac{1}{a_2} \left[1 + \frac{a_1}{a_2 \left\{ t + \left[a_3 - \frac{a_1}{a_2} \right] \right\}} \right] dt = d\beta \quad (4.40)$$

Integrating equation (4.40),

$$\int_{t_i}^{t_f} - \frac{1}{a_2} \left[1 + \frac{a_1}{a_2 \left\{ t + \left[a_3 - \frac{a_1}{a_2} \right] \right\}} \right] dt = \int_{\beta_1}^{\beta_2} d\beta \quad (4.41)$$

or

$$- \frac{1}{a_2} (t_f - t_i) - \frac{a_1}{a_2^2} \int_{t_i}^{t_f} \frac{dt}{\left\{ t + \left[a_3 - \frac{a_1}{a_2} \right] \right\}} = \beta_2 - \beta_1 \quad (4.42)$$

or

$$-\frac{1}{a_2} (t_f - t_i) - \frac{a_1}{a_2} \ln \left[\frac{\left\{ t_f + \left[a_3 - \frac{a_1}{a_2} \right] \right\}}{\left\{ t_i + \left[a_3 - \frac{a_1}{a_2} \right] \right\}} \right] = \beta_2 - \beta_1 \quad (4.43)$$

or

$$(t_f - t_i) + \frac{a_1}{2} \ln \left[\frac{\left\{ t_f + \left[a_3 - \frac{a_1}{a_2} \right] \right\}}{\left\{ t_i + \left[a_3 - \frac{a_1}{a_2} \right] \right\}} \right] + a_2 (\beta_2 - \beta_1) = 0 \quad (4.44)$$

Substituting a_1 , a_2 and a_3 ,

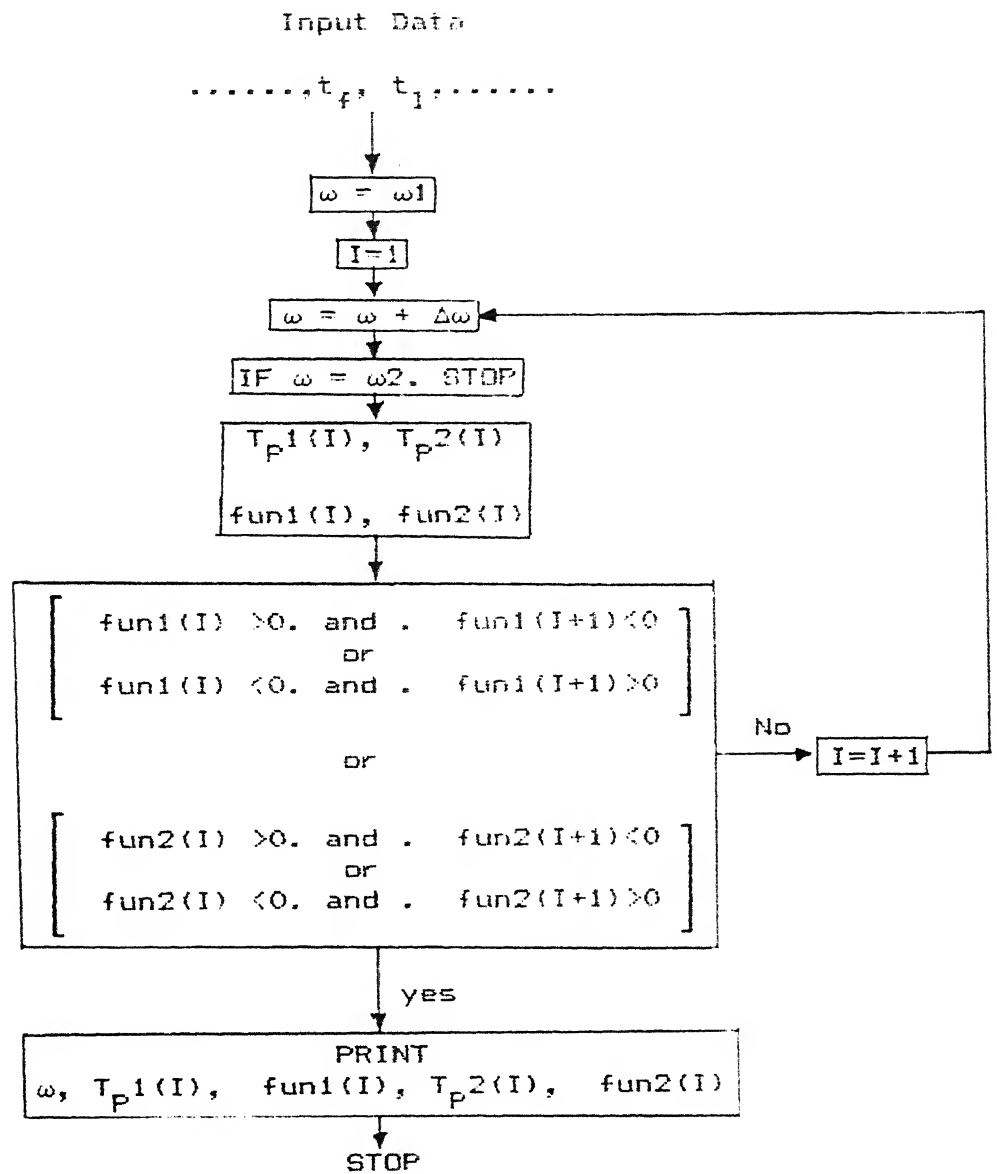
$$(t_f - t_i) + \frac{k_S (T_F - T_W)}{h_{PF} (T_P - T_F)} \ln \left[\frac{\left\{ t_f + \left[\frac{k_S t_{Cu}}{k_{Cu}} + \frac{k_S}{h_{CuW}} - \frac{k_S (T_F - T_W)}{h_{PF} (T_P - T_F)} \right] \right\}}{\left\{ t_i + \left[\frac{k_S t_{Cu}}{k_{Cu}} + \frac{k_S}{h_{CuW}} - \frac{k_S (T_F - T_W)}{h_{PF} (T_P - T_F)} \right] \right\}} \right] + \frac{h_{PF} (T_P - T_F) (\beta_2 - \beta_1)}{\rho_S \omega [H(T_P) - H_S(T_F)]} = 0 \quad (4.45)$$

In the above equation also,

$$f_3(t_f, \omega, T_P) = 0 \quad (4.46)$$

$$\text{or } T_P = f_4(t_f, \omega) \quad (4.47)$$

Block diagram for computer implementation of Macroscopic Model



4.9 SOLUTION OF THE MODEL EQUATION

Thus the governing equations of the model are given by equations 4.22/4.28 and 4.45. In these 2 sets of equations, (4.22) and (4.45) or (4.28) and (4.45), the choice of which depends on the pool temperature, t_f and ω are the only variables. These two final equations of the model cannot be classified under any standard equations for which solution techniques are available. But it is known that for casting a particular strip thickness from a melt of known temperature under a particular cooling condition in the caster, there exists only one ω (R.P.M.). So the solution technique essentially comprises of picking this value. The procedure starts with a lower value of ω (typically 0.1 R.P.M.) being chosen as the casting condition and the value of pool temperature T_p is calculated for the given strip thickness, using the first set of equations (4.22 and 4.28). The two different pool temperatures correspond to whether it is above the liquidus or below the liquidus. Only one of them actually exists in the process. The existence of any one of this pool temperature is confirmed by finding out the corresponding functional value from equation 4.45 which should be equal to zero if for the strip thickness t_f , the assumed angular velocity ω is correct. The functional value taking zero is possible only when the value of ω can be precisely defined by increasing the approximation of the decimal places to a very large value. Since this is practically not possible, the functional value is tested for sign change when an increment in ω is made. If such a change occurs (from +ve to

-ve or -ve to +ve) then it is interpreted that the actual value of R.P.M. for the casting lies between these two values of ω 's. The increment in ω at this juncture is further refined (reduced) and the functional value for sign change is tested again between these two variables of ω . The procedure is repeated for finding out the R.P.M. upto an accuracy of 2 decimals and the final value is taken to be the mean of these two R.P.M.'s.

One typical computation for estimating R.P.M. for casting stainless steel strip of 3mm thickness on copper drum of wall thickness 50mm from a melt at 1580°C is shown in table 4.1. Starting with a very low value of R.P.M. (0.2 R.P.M.), the liquid pool temperature given by equation (4.22/4.28)*, and the functional value given by equation 4.45 are calculated. The R.P.M. values are incremented successively by 0.1. It may be noted that for an R.P.M. value between 2.1 and 2.2 the sign change of the functional value occurs from positive to negative, indicating that the true value of R.P.M. lies between 2.1 and 2.2. For finer tuning of the true R.P.M., the functional value is evaluated between 2.1 and 2.2, in increments of 0.01, as shown in table 4.2. It can be seen that the sign change for functional value occurs between 2.120 and 2.130. The mean of these two numbers is taken as

* If the pool temperature is below the liquidus temperature, then equation 4.22 is used, otherwise equation 4.28 is to be used. In the sample calculation shown in table 4.1 and 4.2, the pool

the true R.P.M. required to produce the strip of 3mm under the conditions specified.

4.8 RESULTS AND DISCUSSION

The model has been tested for casting stainless steel strips in the thickness range of 3-10mm. Table 4.3 gives the geometric constants of the process and the thermal and physical property values used for simulation. Since at the time of carrying out this investigation, no actual value of heat transfer coefficient between the copper drum surface and water spray of the process was available, the model equations have been tested over a wide range of values of the above coefficient. The heat transfer coefficient value corresponding to the heat transfer between the liquid metal pool and the solid-liquid interface has been estimated using the following correlation¹¹:

$$h_{PF} = (0.0156552 - t_f) / 3.08148E-07$$
, where t_f is the strip thickness in metres and h_{PF} is the pool heat transfer coefficient in $W/m^2 \text{ } ^\circ C$.

In the following paragraphs, the result and discussion of the simulation studies are given.

EFFECT OF R.P.M. : The speed of rotation of the drum is the most important parameter that would be affecting the thickness of strip for any particular operating condition of the caster. Figure 4.2 shows the different strip thicknesses that can be obtained by varying the R.P.M. of the drum of a wall thickness of 50mm, when the melt in the tundish is at a particular temperature of 1580°C . The different curves are for different cooling conditions between the drum surface and the water sprays. It is evident from this figure, that (i) for casting thinner strips, higher R.P.M. is required, and (ii) even a small fluctuation in the R.P.M. would have much greater effect on the strip thickness while casting thicker strips than while casting thinner strips. Similar trends are observed for different cooling conditions, referring to different heat transfer coefficients. Figure 4.3 shows a similar behaviour, when the melt temperature in reservoir is 1600°C .

The reason for increased strip thickness at lower R.P.M. is attributed to the larger residence time that the solidifying strip has in the liquid metal pool allowing it to grow thicker. Higher R.P.M. allows lesser residence time producing thinner strips. Thus there is an inverse relationship between the R.P.M. and the strip thickness.

EFFECT OF COOLING CONDITIONS AT THE INNER SURFACE OF DRUM : The variation in cooling conditions at the inner surface of the drum has a significant effect on the output of the process. Cooling conditions are quantitatively characterised in terms of the

25

of heat transfer coefficient between the inner surface of drum wall and spray water, on R.P.M. for producing four different strip thicknesses (3,4,5 & 10mm). It can be seen that for casting a strip of a specified thickness, a higher R.P.M. is required if the cooling conditions at the inner drum surface correspond to a higher heat transfer coefficient condition. The effect of the variation of this heat transfer coefficient is much reduced, in the case of thick strips (near 10mm) but is quite pronounced in the case of thinner strips. Higher heat transfer coefficient permits the passage of high heat flux producing faster growth of solidification front, and thus requiring lesser residence time to produce the same strip thickness. Under low heat transfer coefficient condition, the variation in R.P.M. required for producing strips of different thicknesses is narrowed down, calling for a precise control on the speed of rotation of the drum.

EFFECT OF COPPER DRUM WALL THICKNESS : The wall thickness of the copper drum is expected to have a significant effect on the rate of heat withdrawal from the cooling strip. It is, therefore, likely to have an effect on the final strip thickness at a particular set of operating condition in terms of R.P.M. and heat transfer coefficient between the inner wall of drum and spray water. Figure 4.5 shows the effect of three different wall thicknesses, namely, 10,25 and 50mm for strips of two different thicknesses namely 3 and 4mm strips from a melt at 1580°C . Figure 4.6 is a similar diagram but for casting strips of 5 and 10mm thickness. It is evident from these figures that for casting any

strip thickness, a lower drum wall thickness allows higher R.P.M. and thus increased casting rate. This could be due to two reasons : (i) a lower drum wall thickness would introduce less thermal resistance in the path of heat extraction and allows higher heat flux and (ii) a drum of lower wall thickness is likely to carry less recirculating heat bringing about faster cooling rate in the solidifying strip. These two factors would give faster growth of solidification front requiring lesser residence time for producing a strip of particular thickness. But the limitation in selecting the correct drum wall thickness possibly lies in the correct cooling rate required in the casting. If the latter is too high, which arises if the wall thickness is less (and R.P.M. is high), the model still predicts the possibility of casting different strip thicknesses but the amorphous structure that may result due to rapid quenching may not be of acceptable quality. So to select the correct drum wall thickness for a caster, these factors will have to be considered. Further, too thin a drum may undergo distortions due to steep thermal gradients.

EFFECT OF MELT SUPERHEAT : The temperature of molten metal in the reservoir (tundish) is indicative of the heat content of the melt. Therefore, for liquid metal with different superheats, the R.P.M.s required to produce the same strip thickness are also likely to be different. This is clearly seen in Figs. 4.7, 4.8 & 4.9 which correspond to casting three different strip thicknesses namely 3, 4, and 5mm respectively from four different steel temperatures (1580, 1590, 1600, 1610°C). At low heat transfer coefficient, the

from melts of different superheats is negligible, while for the high values of heat transfer coefficient, the R.P.M. is to be somewhat reduced for melts with higher superheats. This variation is due to the difference in the heat content of the melt maintained at different temperatures.

EFFECT OF METAL HEAD IN THE RESERVOIR : When the height to which the melt is filled in reservoir is varied, it essentially varies the distance of angular separation between β_1 and β_2 on the pool side. Figure 4.10 shows the effect of angular separation on the R.P.M. for casting 3mm strips from a melt of 1580°C . Curves 1, 2, 3 and 4 are for 20° , 25° , 30° and 35° of angular separation respectively. It can be seen that at any particular cooling condition, an increased angular separation (i.e., higher height of melt fill) allows the use of higher R.P.M. and thus higher casting rate. This could be because of the increase in contact area brought about by the increased angular distance of separation which allows higher heat extraction rate thus requiring lesser residence time for the growth of solidification front to any particular strip thickness.

EFFECT ON POOL TEMPERATURE UNDER DIFFERENT COOLING CONDITIONS : The liquid pool temperature that prevails in the caster during the casting operation depends on the strip thickness being cast, R.P.M., cooling conditions etc. The variation in pool temperature that occurs while casting different strip thicknesses from a melt at 1600°C is shown in figure 4.11. The general observed trend is

that while casting thin strips, the pool temperature is high and for thick strips it is low. The deviation from this observation is while casting very thick strips. Here the pool temperature is slightly higher than it is to a strip thinner to it. A possible explanation for this behaviour can be found if the R.P.M. which accompanies such a casting operation is taken into account. While casting thin strips, the R.P.M. required is high (which facilitates good mixing of liquid in pool) and residence time is low. This causes high pool temperature to prevail. While casting high strip thickness, the R.P.M. is low and hence more residence time. This brings down the pool temperature. But while casting very thick strips, the R.P.M. required is extremely low (less than 1 R.P.M.) and hence high residence time in heat supply zone. Due to the lengthy time for which the drum stays in liquid, an increased diffusive heat transfer from the liquid in nozzle is possible.

LIMITATION OF THE MODEL

One of the main limitations of this model is that complete information like the temperatures prevailing along the outer and inner surface of the copper drum and the effect of recirculating heat within the drum cannot be predicted. Also, the generation of the data for the heat transfer coefficient between the liquid pool and the solid-liquid interface is rather difficult. To overcome

these problems, a second mathematical model has been developed which is presented in chapter 5.

Chapter 5

MICROSCOPIC HEAT BALANCE BASED ON SYSTEM ENTHALPY

In this chapter, a mathematical model based on the net energy balance in the liquid and solid regions involving analysis at microscopic level and the accounting for recirculating heat on copper drum has been developed. The model can give useful information regarding the temperature distribution on the strip at the point of its attaining final thickness, as well as the temperatures prevailing on the outer and the inner surfaces of the copper drum.

Following are the assumptions made for the development of this model :

- (1) At angular position β_1 , where the liquid metal strikes the drum, an initial thickness t_i forms and it grows to final thickness t_f of strip at β_2 during the course of motion from β_1 to β_2 .
- (2) The growth of solid skin between β_1 and β_2 is linear and takes place in a stepwise manner. For quantification, the skin between β_1 and β_2 is divided into 'n' number of cylindrical elements, depending on the value of R_d and $(\beta_2 - \beta_1)$. The liquid solid interface passes through the centre of the upper edge of cylindrical elements which is exposed to the liquid pool.
- (3) Due to the high thermal conductivity of copper and the

relatively thick strips that are being cast (the low R.P.M. that makes such a casting possible), a steady state heat flow from liquid-solid interface to copper drum to spray water is established as soon as the drum enters the heat supply zone at β_1 .

- (4) Constant thermal conductivity values are assumed for Cu drum and solid skin and the values taken are at certain constant temperatures which represent some kind of average of temperatures prevailing in the process.
- (5) A definite freezing temperature exists for the liquid being cast. For an alloy like steel this constant freezing temperature is defined in terms of the liquidus and solidus temperatures.
- (6) There is perfect thermal contact between the solid skin and the copper drum and there is no air film between the two. If, however, the precise value of air film thickness and its thermal conductivity are known, this assumption, can in fact be relaxed by incorporating an additional thermal resistance term corresponding to heat transfer through this air film.
- (7) For the range of liquid temperature in the reservoir which is possible through different superheats of the melt, the initial thickness of skin t_i at β_1 , remains constant.
- (8) The temperature of liquid-solid interface of skin is T_F , which is the freezing temperature.
- (9) There is no temperature variation in z direction.

5.1 DIFFERENT MODES OF HEAT TRANSFER INTO AND OUT OF THE SYSTEM

The system being analysed for heat balance has the boundary ABCDEFGA. This is shown in figure 5.1. Following are the different modes of heat transfer :

- (1) The liquid arriving through the nozzle passage has temperature T_1 and at enthalpy $H(T_1)$ which is found from thermodynamics : $H(T_1) = c_{p1} \cdot T_1$
- (2) Heat extraction in the radial direction within skin and Cu drum is through conduction.
- (3) Due to the motion of skin and Cu drum bulk heat transfer takes place in them in angular direction.
- (4) Heat loss due to radiation occurs from the skin surface which is exposed to atmosphere.

5.2 MACROSCOPIC HEAT ENERGY BALANCE

The general heat energy balance equation can be written in words as :

$$\begin{aligned} & \left[\begin{array}{c} \text{Heat Energy} \\ \text{in} \end{array} \right] + \left[\begin{array}{c} \text{Heat Energy} \\ \text{generated} \end{array} \right] - \left[\begin{array}{c} \text{Heat Energy} \\ \text{out} \end{array} \right] - \left[\begin{array}{c} \text{Heat Energy} \\ \text{consumed} \end{array} \right] \\ & = \left[\begin{array}{c} \text{Heat Energy} \\ \text{accumulated} \end{array} \right] \quad \dots\dots\dots (5.1) \end{aligned}$$

Since the process is in steady state in the present case the above reduces to,

$$\begin{matrix} \left[\text{Heat Energy} \right] & + & \left[\text{Heat Energy} \right] & = & \left[\text{Heat Energy} \right] & \text{..... (5.2)} \\ \text{in} & & \text{generated} & & \text{out} & \\ \text{I} & & \text{II} & & \text{III} & \end{matrix}$$

5.2.1 Heat Energy In

(1) From incoming liquid

$$Q_{liq} = t_f \left[R_d + \frac{t_f}{2} \right] \omega z \rho_S H(T_1) \text{ (5.3)}$$

(2) From copper drum

$$Q_{Cuin} = t_{Cu} \left[R_d - \frac{t_{Cu}}{2} \right] \omega z \rho_S [c_{pCu}(T_{Cuin})] \cdot T_{Cuin} \text{ .. (5.4)}$$

In the absence of T_{Cuin} data, Q_{Cuin} is expressed as a percentage of outgoing bulk heat (Q_{Cu}) of copper drum at β_2 .

5.2.2 Heat Energy Generated

The heat generated is due to the liquid --> solid transformation :

$$t_f \left[R_d + \frac{t_f}{2} \right] \omega z \rho_S L \text{ (5.5)}$$

5.2.3 Heat Energy out of the System

Heat energy going out from the system are :

- (1) Conduction
- (2) Bulk flow
- (3) Radiation

5.2.3.1 Conduction

This is the heat being carried out by conduction through the solid skin (t , $t_i < t < t_f$) and copper drum wall thickness (t_{Cu}). One end of the solid skin is the liquid-solid interface which is at temperature T_F , and the other end is in contact with copper drum. The inner surface of copper drum is sprayed from water at temperature T_W . The resistance to heat flow between the solid skin / liquid metal interface and the inner surface of the copper drum / water interface is basically dependent, besides other things (fluid flow conditions at the two interfaces), on the thickness of the solid skin and the copper drum wall thickness. The linear stepwise growth of solid skin t_i from β_1 to t_f at β_2 takes place in 'n' number of steps as shown in Fig. 5.2. In the following paragraph, the procedure to quantify these individual skin thicknesses at each position of β is described :

The linear growth of skin can be given by,

$$t = m'\beta + c \quad ; \quad (t_i < t < t_f), \quad (\beta_1 < \beta < \beta_2) \quad (5.6)$$

$$\text{At } \beta = \beta_1, t = t_i \quad \text{therefore, } t_i = m'\beta_1 + c \quad (5.7)$$

$$\text{At } \beta = \beta_2, t = t_f \quad \text{therefore, } t_f = m'\beta_2 + c \quad (5.8)$$

$$\Rightarrow m' = \frac{(t_f - t_i)}{(\beta_2 - \beta_1)} \quad (5.9)$$

and

$$c = t_i - \left[\frac{t_f - t_i}{\beta_2 - \beta_1} \right] \beta_1 \quad (5.10)$$

Substituting equations (5.9) and (5.10) in (5.6),

$$t = t_i + \left[\frac{t_f - t_i}{\beta_2 - \beta_1} \right] (\beta - \beta_1) \quad (5.11)$$

Angle subtended by every cylindrical element at the centre of copper drum = $\frac{\beta_2 - \beta_1}{n}$ radians

$$\text{i.e., } \Delta\beta = \frac{\beta_2 - \beta_1}{n} \quad (5.12)$$

Thickness of the 1st cylindrical element :

$$t_1 = t_i + \left[\frac{t_f - t_i}{\beta_2 - \beta_1} \right] \left(\beta_1 + 1 \cdot \left[\frac{\beta_2 - \beta_1}{2n} \right] - \beta_1 \right) \quad (5.13)$$

$$t_1 = t_i + \left[\frac{1 \cdot (t_f - t_i)}{2n} \right] \quad (5.14)$$

Thickness of the 2nd element,

Net conductive heat leaving the system, Q_d :

$$Q_d = \Delta\beta \cdot z \cdot (T_F - T_W) \cdot \left[\left\{ \frac{1}{(R_d - t_{Cu}) h_{CuW}} + \frac{\ln \left[\frac{R_d}{R_d - t_{Cu}} \right]}{k_{Cu}} + \frac{\ln \left[\frac{R_d + t_1}{R_d} \right]}{k_S} \right\}^{-1} + \left\{ \frac{1}{(R_d - t_{Cu}) h_{CuW}} + \frac{\ln \left[\frac{R_d}{R_d - t_{Cu}} \right]}{k_{Cu}} + \frac{\ln \left[\frac{R_d + t_2}{R_d} \right]}{k_S} \right\}^{-1} + \dots \text{upto } n \right] \quad (5.22)$$

Since $t_1, t_2, t_3 \dots t_n$ are functions of t_i & t_f only, Q_d will also be a function of t_i & t_f .

5.2.3.2 Bulk Heat Carried By the Strip at β_2

Due to the continuous rotation of the strip away from the system, the solid strip carries with it some amount of heat through bulk motion. For quantification of this bulk heat, the strip thickness (t_f) at β_2 , is divided into 'j' number of composite perfect thermal contact layers, as shown in figure 5.3.

$$\text{Thickness of each layer} = \frac{t_f}{j} \quad (5.23)$$

$T_{S1}, T_{S2}, T_{S3} \dots T_{Sj}$ are the temperatures which exist at the centre of the composite layers 1, 2, 3, ... j, respectively. It is assumed that the temperature within a particular layer, under

consideration is the same throughout, i.e., there is no temperature gradient within a layer. Considering the heat balance at the plane passing through the centre of the 1st composite layer :

Heat Transfer by Conduction,

$$\left[\begin{array}{c} \text{Heat entering the} \\ \text{layer from} \\ \text{Conduction} \end{array} \right] = \left[\begin{array}{c} \text{Heat going out of the} \\ \text{layer through} \\ \text{Conduction} \end{array} \right]$$

$$\frac{(T_F - T_{S1})}{\frac{\ln \left[\frac{R_d + t_f}{R_d + \frac{(2j-1)t_f}{2j}} \right]}{k_S}} = \frac{(T_{S1} - T_W)}{\left[\frac{\ln \left[\frac{R_d + \frac{(2j-1)t_f}{2j}}{R_d} \right]}{k_S} + \frac{\ln \left[\frac{R_d}{R_d - t_{Cu}} \right]}{k_{Cu}} + \frac{1}{(R_d - t_{Cu}) h_{CuW}} \right]} \quad (5.24)$$

Rearranging the terms,

$$T_{S1} = \frac{\left[\frac{\left(\frac{R_d + t_f}{R_d + \frac{(2j-1)t_f}{2j}} \right)}{k_S} \right] T_W + \left[\frac{\ln \left[\frac{R_d + \frac{(2j-1)t_f}{2j}}{R_d} \right]}{k_S} + \frac{\ln \left[\frac{R_d}{R_d - t_{Cu}} \right]}{k_{Cu}} + \frac{1}{(R_d - t_{Cu}) h_{CuW}} \right]}{\left[\frac{\ln \left[\frac{R_d + t_f}{R_d} \right]}{k_S} + \frac{\ln \left[\frac{R_d}{R_d - t_{Cu}} \right]}{k_{Cu}} + \frac{1}{(R_d - t_{Cu}) h} \right]} \quad (5.2)$$

Heat Transfer in 1st composite layer by bulk flow :

$$\left. \begin{array}{l} \text{Bulk heat carried by} \\ \text{1st composite layer} \\ \text{of solid, } Q_{S1} \end{array} \right\} = \left[\left(R_d + \frac{(2j-1)t_f}{2j} \right) \omega \right] \left(\frac{t_f}{j} \right) z \cdot \rho_S \cdot [c_{pl}(T_{S1})] \cdot T_{S1} \quad (5.26)$$

Similar heat balance equations can be written for other strip layers, for the 2nd composite layer of strip,

$$T_{S2} = \frac{\left[\frac{\left(\frac{R_d + t_f}{(2j-3)t_f} \right)}{\left(R_d + \frac{t_f}{2j} \right)} \right] T_W + \left[\frac{\ln \left(\frac{R_d + \frac{(2j-3)t_f}{2j}}{R_d} \right)}{k_S} + \frac{\ln \left(\frac{R_d}{R_d - t_{Cu}} \right)}{k_{Cu}} + \frac{1}{(R_d - t_{Cu}) h_{CuW}} \right] T}{\left[\frac{\ln \left(\frac{R_d + t_f}{R_d} \right)}{k_S} + \frac{\ln \left(\frac{R_d}{R_d - t_{Cu}} \right)}{k_{Cu}} + \frac{1}{(R_d - t_{Cu}) h_{CuW}} \right]} \quad (5.27)$$

and

$$Q_{S2} = \left[\left(R_d + \frac{(2j-3)t_f}{2j} \right) \omega \right] \left(\frac{t_f}{j} \right) z \cdot \rho_S \cdot [c_{pl}(T_{S2})] \cdot T_{S2} \quad (5.28)$$

Similar expressions for T_{S3} , Q_{S3} , T_{S4} , Q_{S4} , ..., T_{Sj} , Q_{Sj} can be written. It is to be noted that T_{S1} , T_{S2} , T_{S3} , ..., T_{Sj} and Q_{S1} , Q_{S2} , ..., Q_{Sj} , are functions of final strip thickness t_f .

Net bulk heat carried by strip at β_2 ,

$$Q_S = Q_{S1} + Q_{S2} + Q_{S3} + \dots + Q_{Sj} \quad (5.29)$$

5.2.3.3 Bulk Heat Carried by Copper Drum at β_2

The Copper drum leaving the system boundary carries with it some amount of heat due to bulk motion. To quantify the same, the Cu drum is divided at β_2 into 'm' number of composite perfect thermal contact layers.

$$\text{Thickness of each layer} = \frac{t_{Cu}}{m} \quad (5.30)$$

Figure 5.4 is referred to for the explanation of the following.

T_{Cu1} , T_{Cu2} , T_{Cu3} T_{Cum} are the temperatures which exist at the centre of each the composite layers 1,2,3,....m, respectively in the copper drum at β_2 . It is assumed that this temperature exists in that entire layer.

Applying heat balance at the centre of the 1st composite layer,

$$\frac{(T_F - T_W)}{\left[\frac{\ln \left(\frac{R_d + t_f}{R_d} \right)}{k_S} + \frac{\ln \left(\frac{R_d}{R_d + \frac{1 \cdot t_{Cu}}{2m}} \right)}{k_{Cu}} \right]} = \frac{(T_{Cu1} - T_W)}{\left[\frac{\ln \left(\frac{R_d - \frac{1 \cdot t_{Cu}}{2m}}{R_d - t_{Cu}} \right)}{k_{Cu}} + \frac{1}{(R_d - t_{Cu}) h_{CuW}} \right]} \quad (5.31)$$

or

$$T_{Cu1} = \frac{\left[\frac{\ln \left(\frac{R_d + t_f}{R_d} \right)}{k_S} + \frac{\ln \left(\frac{R_d}{R_d - \frac{1 \cdot t_{Cu}}{2 \cdot m}} \right)}{k_{Cu}} \right] T_W + \left[\frac{\ln \left(\frac{R_d - \frac{1 \cdot t_{Cu}}{2 \cdot m}}{R_d - t_{Cu}} \right)}{k_{Cu}} + \frac{1}{(R_d - t_{Cu}) h_{Cu}} \right]}{\left[\frac{\ln \left(\frac{R_d + t_f}{R_d} \right)}{k_S} + \frac{\ln \left(\frac{R_d}{R_d - t_{Cu}} \right)}{k_{Cu}} + \frac{1}{(R_d - t_{Cu}) h_{CuW}} \right]} \quad (5.32)$$

$$\left. \begin{array}{l} \text{Bulk heat carried by} \\ \text{1st composite layer} \\ \text{of Copper drum, } Q_{Cu1} \end{array} \right\} = \left[\left(R_d - \frac{1 \cdot t_{Cu}}{2 \cdot m} \right) \omega \right] \left(\frac{t_{Cu}}{m} \right)^2 \cdot \rho_{Cu} \cdot [c_{pCu} (T_{Cu1})] \quad (5.33)$$

Similar heat balance equations can also be written for the other composite layers of the copper drum.

For example, for 2nd layer,

$$T_{Cu2} = \frac{\left[\frac{\ln \left(\frac{R_d + t_f}{R_d} \right)}{k_S} + \frac{\ln \left(\frac{R_d}{R_d - \frac{3 \cdot t_{Cu}}{2 \cdot m}} \right)}{k_{Cu}} \right] T_W + \left[\frac{\ln \left(\frac{R_d - \frac{3 \cdot t_{Cu}}{2 \cdot m}}{R_d - t_{Cu}} \right)}{k_{Cu}} + \frac{1}{(R_d - t_{Cu}) h_{Cu}} \right]}{\left[\frac{\ln \left(\frac{R_d + t_f}{R_d} \right)}{k_S} + \frac{\ln \left(\frac{R_d}{R_d - t_{Cu}} \right)}{k_{Cu}} + \frac{1}{(R_d - t_{Cu}) h_{CuW}} \right]}$$

Similarly, Q_{Cu2}

$$Q_{Cu2} = \left[\left(R_d - \frac{3 \cdot t_{Cu}}{2m} \right) \omega \right] \left[\frac{t_{Cu}}{m} \right] z \cdot \rho_{Cu} \cdot [c_{pCu}(T_{Cu1})] \quad (5.35)$$

The expressions for T_{Cu3} , Q_{Cu3} , T_{Cu4} , Q_{Cu4} , T_{Cum} , Q_{Cum} can be written in a similar way. Here again T_{Cu1} , T_{Cu2} , T_{Cum} and Q_{Cu1} , Q_{Cu2} , Q_{Cum} are function of t_f only.

The net bulk heat carried by the Cu drum, Q_{Cu}

$$Q_{Cu} = Q_{Cu1} + Q_{Cu2} + Q_{Cu3} + \dots + Q_{Cum} \quad (5.36)$$

5.2.4 Heat Loss From The Liquid Metal Surface Due To Radiation

Heat loss due to radiation is given by,

$$Q_{rad} = (\delta - t_f) \cdot z \cdot \sigma \cdot \epsilon_1 \cdot [T_{rad}^4 - T_a^4] \quad (5.37)$$

where δ is the gap between tundish and drum, T_{rad} is the mean of temperatures T_1 and T_F , T_a the ambient temperature, σ is Stefan-Boltzmann's constant and ϵ_1 is the emissivity of liquid.

Net Heat Energy out of the system boundary,

$$= Q_d + Q_s + Q_{Cu} + Q_{rad}$$

5.3 FINAL GOVERNING EQUATION

Substituting the various Heat energy terms in equation (5.2),

$$0.2 \cdot \left\{ \left(R_d + \frac{t_f}{2} \right) \cdot t_f \cdot \rho_S \cdot H(T_1) + \left(R_d - \frac{t_{Cu}}{2} \right) \cdot t_{Cu} \cdot \rho_{Cu} \cdot c_{pCu} (T_{Cuin}) \cdot T_{Cuin} \right.$$

$$\left. \left(R_d + \frac{t_f}{2} \right) \cdot t_f \cdot \rho_S \cdot L \right\} = z \cdot \left[\Delta\beta \cdot (T_F - T_W) \cdot \left\{ \frac{1}{\left(R_d - t_{Cu} \right) h_{CuW}} + \frac{\ln \left[\frac{R_d}{R_d - t_{Cu}} \right]}{k_{Cu}} + \frac{\ln \left[\frac{R_d + t_1}{R_d} \right]}{k_S} \right. \right.$$

$$\left. \dots \right\} + \left[\frac{t_f}{j} \right] \omega \cdot \rho_S \cdot \left[\left[R_d + \frac{(2j-1)t_f}{2j} \right] c_{pS} (T_{S1}) \cdot T_{S1} + \dots \right]$$

$$\left[\frac{t_{Cu}}{m} \right] \omega \cdot \rho_{Cu} \left[\left[R_d - \frac{1 \cdot t_{Cu}}{2m} \right] c_{pCu} (T_{Cu1}) + \dots \right] + (\delta - t_f) \cdot \sigma \cdot \epsilon_1 \cdot [T_{rad}^4 - T_a^4]$$

(5.39)

Rearranging,

$$\Delta\beta \cdot (T_F - T_W) \cdot \left[\left\{ \frac{1}{\frac{(R_d - t_{Cu}) h_{CuW}}{k_{Cu}} + \frac{\ln \left[\frac{R_d}{R_d - t_{Cu}} \right]}{k_{Cu}} + \frac{\ln \left[\frac{R_d + t_1}{R_d} \right]}{k_S}} \right\}^{-1} + \dots \right] + (\delta - t_f) \cdot \sigma \cdot \epsilon_1 \cdot [T_{rad}^4 - T_a^4]$$

$\omega =$

$$\left[(R_d + \frac{t_f}{2}) \cdot t_f \cdot \rho_S \cdot H(T_1) + (R_d - \frac{t_{Cu}}{2}) \cdot t_{Cu} \cdot \rho_{Cu} \cdot c_{pCu} (T_{Cuin}) \cdot T_{Cuin} + (R_d + \frac{t_f}{2}) \cdot t_f \cdot \rho_S \cdot L \right] - \left(\frac{t_f}{J} \right) \cdot \rho_S \cdot \left[\left(R_d + \frac{(2j-1)t_f}{2j} \right) c_{pS} (T_{S1}) \cdot T_{S1} + \dots \right] + \left(\frac{t_{Cu}}{m} \right) \cdot \rho_{Cu} \cdot \left[\left(R_d - \frac{1 \cdot t_{Cu}}{2m} \right) [c_{pCu} (T_{Cu1})] + \dots \right] \quad (5.40)$$

In the above final expression ω is a function of t_i, t_f . Thus for any desired strip thickness, and specified geometry of the caster, the angular velocity ω (hence the r.p.m.) can be determined for the incoming melt.

5.4 TEMPERATURE ALONG THE SURFACES OF THE DRUM

The temperature that exists along the outer and inner surfaces of the drum is dependent on the (i) angular position (ii) strip

thickness being cast (iii) cooling conditions (heat transfer coefficient h_{CuW}) and (iv) the thickness of drum. The procedure to find out these temperatures is explained below :

Applying the heat flux balance in the 1st element at the outer surface of the drum due to conduction,

$$\frac{(T_F - T_{So1}) \cdot \Delta\beta \cdot z}{\ln \left[\frac{R_d + t_1}{R_d} \right] \cdot k_S} = \frac{(T_{So1} - T_W) \cdot \Delta\beta \cdot z}{\ln \left[\frac{R_d}{R_d - t_{Cu}} \right] \cdot k_{Cu} + \frac{1}{(R_d - t_{Cu}) h_{CuW}}} \quad (5.41)$$

Here T_{So1} is the drum outer surface temperature corresponding to the 1st element.

Simplifying the above equation,

$$(T_F - T_{So1}) \left[\frac{\ln \left[\frac{R_d}{R_d - t_{Cu}} \right]}{k_{Cu}} + \frac{1}{(R_d - t_{Cu}) h_{CuW}} \right] = (T_{So1} - T_W) \left[\frac{\ln \left[\frac{R_d + t_1}{R_d} \right]}{k_S} \right] \quad (5.42)$$

Rearranging the terms,

$$T_{So1} = \frac{\left[\frac{\ln \left[\frac{R_d}{R_d - t_{Cu}} \right]}{k_{Cu}} + \frac{1}{(R_d - t_{Cu}) h_{CuW}} \right] T_F + \left[\frac{\ln \left[\frac{R_d + t_1}{R_d} \right]}{k_S} \right] T_W}{\frac{\ln \left[\frac{R_d + t_1}{R_d} \right]}{k_S} + \frac{\ln \left[\frac{R_d}{R_d - t_{Cu}} \right]}{k_{Cu}} + \frac{1}{(R_d - t_{Cu}) h_{CuW}}} \quad (5.43)$$

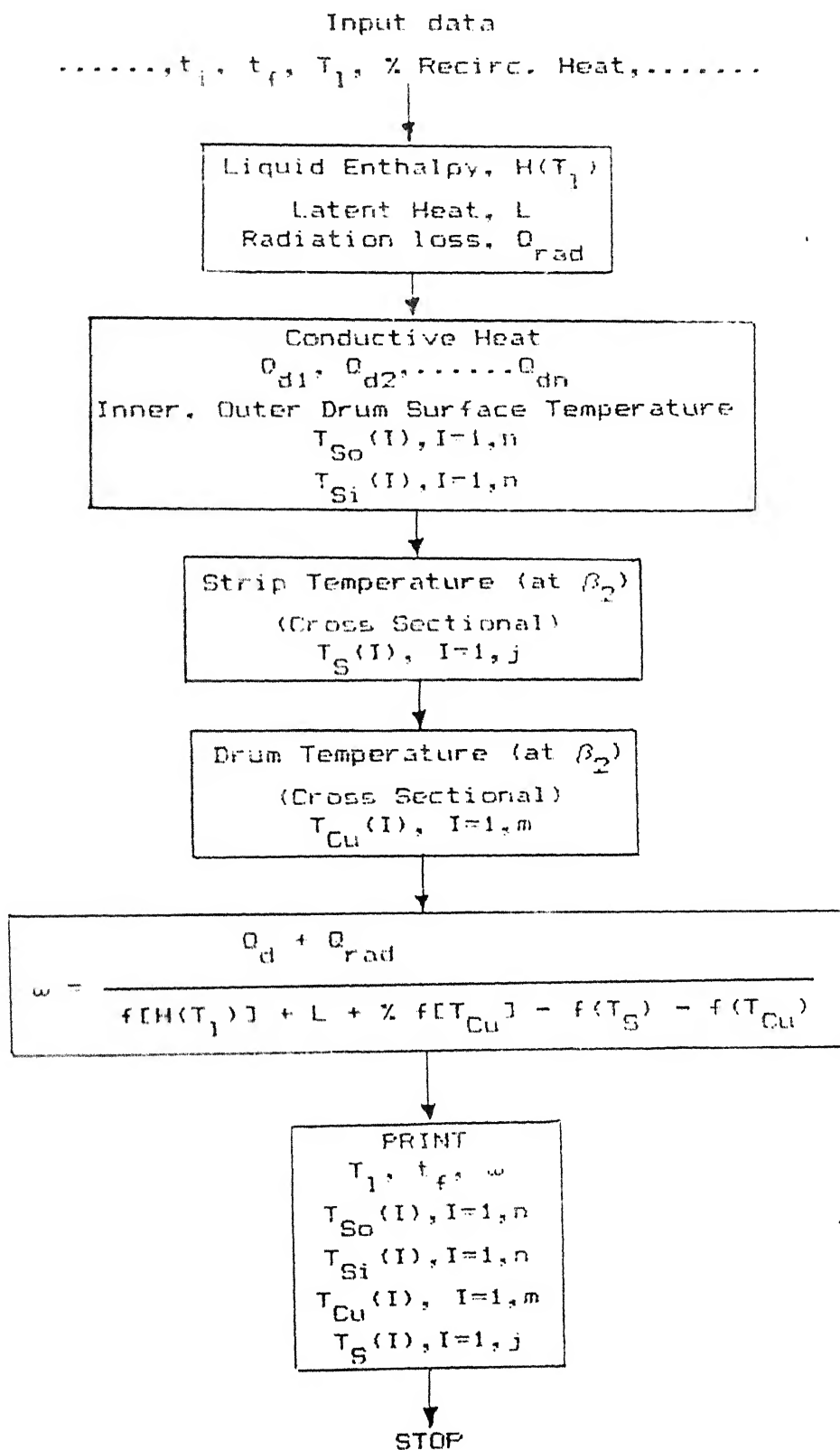
Similarly the temperature along the outer surface of the drum in the 2nd, 3rd,, nth element can be calculated by replacing t_1 in equation (5.43) with t_2, t_3, \dots, t_n respectively.

The expression for temperature along the inner drum wall surface is similarly derived as in the above case by applying conductive heat flux balance at the inner drum wall surface. The temperature along the inner surface at the 1st element T_{Si1} can be shown to be equal to

$$T_{Si1} = \frac{\left[\frac{1}{(R_d - t_{Cu}) h_{CuW}} \right] T_F + \left[\frac{\ln \left[\frac{R_d + t_1}{R_d} \right]}{k_S} + \frac{\ln \left[\frac{R_d}{R_d - t_{Cu}} \right]}{k_{Cu}} \right] T_W}{\frac{\ln \left[\frac{R_d + t_1}{R_d} \right]}{k_S} + \frac{\ln \left[\frac{R_d}{R_d - t_{Cu}} \right]}{k_{Cu}} + \frac{1}{(R_d - t_{Cu}) h_{CuW}}} \quad (5.44)$$

The temperature along the other inner surface points corresponding to 2nd, 3rd, ...nth element can be found by replacing t_1 in the above expression for t_2, t_3, \dots, t_n respectively.

Block diagram for Computer implementation Microscopic Model



5.3 RESULTS AND DISCUSSION

The operating parameters, thermal and physical constants used for the simulation of the caster using this model are the same as the ones used in the earlier model. In this section, the results of the simulation study along with the discussion are presented.

TEMPERATURE ALONG THE SURFACES OF THE DRUM : The temperature that exists along the inner and outer surfaces of the drum wall are different during any operating condition. Figure 5.5 shows the temperature that exists along the outer and inner surfaces of the drum while casting strips of 3, 5 and 10mm from a melt of 1580°C . Figure 5.6 is a similar plot for the temperature that exists while casting 3mm strip under three different cooling conditions and Fig. 5.7 is for casting 3mm strips on three different drum wall thicknesses. The temperature on the drum surfaces (inner as well as outer) continuously decreases during the course of motion from β_1 to β_2 . This is primarily due to the difference in thickness of the solid skin which separates the surface of drum from the liquid pool. At β_1 , the solid skin formation begins, hence only a thin layer of solidified layer is present, while at β_2 the solid shell is fully grown. Solid metal shell being a poorer conductor of heat, gives rise to higher temperature at β_1 as compared to that at β_2 .

TEMPERATURE ALONG THE CROSS SECTION OF STRIP AND DRUM WALL AT EXIT : The temperature that exists along the cross section of the strip and drum wall at the exit of the system boundary can be used as a

measure of the amount of bulk heat leaving the system. The model predicts the temperature profiles at these cross sections at β_2 at various operating conditions. Figure 5.8 shows the temperature profile during the casting of strips of 3, 5 and 10mm from a melt of 1580°C . Figure 5.9 is a similar plot for casting 3mm strip under three different cooling conditions, and Fig. 5.10 is for casting 3mm strips on three different drum wall thicknesses. It is evident from these figures that the thermal gradients within the strip and the drum wall, respectively are quite different. In all these three figures, the curves have two distinct regions. The one with steeper slope and closer to the solid-liquid interface represents the temperature profile in the solidified metal strip at the exit point β_2 , whereas the one with lesser slope and farther away from the liquid-solid interface represents the temperature distribution in the cross section of the drum wall at β_2 . The reason for this behaviour is attributed to the difference in thermal conductivities of the two materials namely the steel strip and the copper drum. Copper has high thermal conductivity while stainless steel has very low value (24 times less than the former).

EFFECT OF STRIP THICKNESSES ON TEMPERATURE PROFILES IN DRUM :

The amount of heat going out of the system through conduction and bulk flow is different while casting strips of different thicknesses. Referring to Fig. 5.5, it can be seen that while casting thin strips, the temperature drop on the surfaces of drum from β_1 to β_2 is not substantially high while for thicker strips, the variation in temperature is large and continuously goes down

towards β_2 . The reason here is again the difference in skin layer thickness during the growth between β_1 and β_2 for different strip thicknesses. For thin strips the thermal resistance between the surface of the drum and the liquid pool is less, and hence higher temperature along the surfaces of the drum is observed, while in the case of thicker strips, because of increased thermal resistance, low temperature profiles are seen. Referring to Fig 5.8 for cross sectional temperature profiles on the drum as well as the strip at the exit point, again it is to be noted that the thermal gradients are going to be different for strips of different thicknesses. The temperature drop between the outer and the inner surfaces of the drum is higher for thin strips and it is lower for thick strips. From these observations it may be concluded that the cooling rate accompanying thin strip formation is higher than that for thicker strip.

EFFECT OF COOLING CONDITION ON TEMPERATURE PROFILES : The temperature that exists along the surfaces of the drum and along the cross section of the strip and drum wall for a particular set of casting parameters is dependent on the value of heat transfer coefficient, h_{CuW} . Referring to Fig. 5.6, it can be observed that higher heat transfer coefficient values bring down the the temperatures on the two surfaces of the drum. An increase of 5000 $W/m^2 \cdot ^\circ C$ in heat transfer coefficient value reduces the outer surface temperature of drum by about $40^\circ C$ and inner surface temperature by $80-100^\circ C$. The effect on cross sectional temperature is similar. A higher heat transfer coefficient introduces steep temperature drop in solidified metal strip as well as the copper

drum. An important observation that can be made from Fig. 5.8 and 5.9 is that in case of thin strips, at the strip-drum wall boundary, the thermal gradient is almost vertical indicating the presence of a contact thermal resistance. So while casting thin strips it is possible that surface adhesion dynamics of the strip to the drum is important.

EFFECT OF DRUM WALL THICKNESS ON TEMPERATURE : The thickness of drum wall has a direct effect on the conductive heat transfer. Hence it is expected to affect the temperature both within the drum and the cast strip. This may be seen in Figs. 5.7 and 5.10 which represents the temperature profiles in the drum surfaces and the metal strip, respectively for drums of three different wall thicknesses. The difference in temperatures between the outer and inner drum surface is larger for thicker walls. The outer surface temperature of the drum wall comes down by more than 100°C when the wall thickness is reduced by 15 or 25mm. This indicates the better penetration of the cooling effect from spray water in case of thin walls than from thick walls. Another observation is the increasing inner wall temperature with decreasing wall thickness. This is important since the heat transfer characteristics between the spray water and drum wall would be substantially affected by this.

The temperature profile at the cross-section of the cast strip at the exit point (fig. 5.10) shows a high thermal gradient in the casting. It also exhibits an increasing contact resistance at the drum-casting interface with increasing drum wall thickness.

75

EFFECT OF RECIRCULATING HEAT ON THE CASTING RATE : As already described in chapter-3, the copper drum, when it enters the heat supply zone is at a fairly high temperature (much above the room temperature). Thus at the entry point, the drum already has within it a certain heat content which we refer to as the 'recirculating heat'. The quantity of this recirculating heat within the drum wall of the caster is likely to substantially affect the the output of the caster. This heat may also give some idea of the thermal shock the drum experiences in each revolution. Since the experimental data about the temperature that would exist in the drum just before it enters the heat supply zone is not known and which is essential for estimating the amount of recirculating heat, it was decided to predict the effect on the other casting conditions for various values of recirculating heat. The amount of recirculating heat is dependent on the strip thickness being cast. The existence of high values of recirculating heat in the drum would necessitate increased cooling rates for casting a particular strip thickness, because the amount of heat that is to be extracted from unit mass of liquid at a known temperature for casting a particular strip thickness is constant. One way to achieve this is to alter the speed of rotation of the drum which essentially controls the cooling rate by varying the residence time. Figure 5.11 shows the effect of variation in the recirculating heat (for casting a particular strip thickness) on the change in R.P.M. that must correspondingly accompany to keep the cooling rate constant. The plots are shown for casting strips

of three thicknesses, namely 3mm, 4mm and 5mm. It can be seen that while casting any strip thickness, a decrease in the amount of recirculating heat is associated with a higher R.P.M. This effect is substantially pronounced in case of thinner strips in which an approximately inverse exponential variation exists between the speed of rotation and the % recirculating heat. The R.P.M. becomes increasingly asymptotic below a certain minimum level of % recirculating heat for thinner strips. Thus for casting strip of a particular thickness, by decreasing the % of recirculating heat through enhanced cooling of the drum, it is possible to operate the caster at higher casting speeds yielding higher production rate.

LIMITATIONS OF THE MODEL

This model which is based on fully developed steady state, one dimensional heat flow from the inner surface of the solid skin to spray water through the wall of drum suggests somewhat higher temperatures on the two surfaces of the copper drum as compared to those quoted in literature²⁵ for the similar process. The main reason for this discrepancy seems to be the invalidity of some of the assumptions made in our formulation. For instance, it is apparent that the process is atleast a two dimensional process and hence any mathematical model based on one dimensional heat flow would give only approximate results. Further, the assumption of steady state is only approximate. More realistic results would be expected if the model is formulated in terms of unsteady state

energy balance equation.

75

Chapter 6

CONCLUSION

The main conclusions that result from this investigation can be classified as :

- (1) related to Process Operation
- (2) related to Process Design

6.1 CONCLUSIONS RELATED TO PROCESS OPERATION

1. For the casting of any strip thickness, the speed of rotation of the drum is extremely important. By controlling the speed of rotation, the residence time for any element of the copper drum surface in heat supply zone between β_1 and β_2 can be controlled.
2. The amount of solid skin thickness from the initial value at β_1 to the final strip thickness at β_2 for any particular heat extraction and melt temperature is governed by the speed of rotation of the drum. Higher the speed, lesser would the time available for the growth of strip giving rise to thinner strips.
3. While producing thicker strips, a more precise control on the speed of rotation (which is low R.P.M.) of the drum is required. Any fluctuation in it can cause non-uniformity in strip thickness.

4. The superheat accompanying the melt has to match with the r.p.m. of the drum for producing any particular strip thickness. In general, lesser the superheat, higher would be the r.p.m. that can be used for any strip thickness and thus an inverse relation between the two. At low heat transfer coefficient values ($h_{CuW} = 1000-3000 \text{ W/m}^2 \cdot ^\circ\text{C}$), the variation in r.p.m. is not substantial. Hence the casting rate remains more or less the value for different superheats.
5. In any particular process setup, the heat transfer coefficient value between the drum surface and spray water cannot be much varied. But if certain relationship exists between the Reynolds number of spray water and the heat transfer coefficient, then it can be varied by exercising control over the former. Use of a higher heat transfer coefficient makes it possible to allow for higher speeds for casting strip of any particular thickness.
6. By controlling the cooling conditions inside the drum through the regulation of water spray, it is possible to control the recirculating heat. Lesser the recirculating heat, higher would be the R.P.M. that can be adjusted for producing the same strip thickness. This control is arising from the fact that such a situation is likely to form higher initial thickness requiring less further growth. The limitation in choosing the right combination of recirculating heat and the R.P.M. is the microstructure required in the strip. The latter should not deviate towards the amorphous structure which does not cater to the end use.
7. The height of liquid pool which corresponds to the height to

which melt is filled in reservoir, controls the angular separation between β_1 and β_2 . For any particular tundish geometry, the height of melt fill has to be kept constant which would otherwise produce non-uniformity in strip the thickness. By using different constant heights of melt fill and the correspondingly matching r.p.m., it is possible to produce the same strip thickness.

6.2 CONCLUSIONS RELATED TO PROCESS DESIGN

1. The linear distance separation between β_1 and β_2 can be increased by taking drum of bigger diameter which would give rise to more contact area through which heat can be extracted requiring less residence time for producing the same strip thickness and correspondingly higher r.p.m. The casting rate can be substantially increased by this.
2. By lowering the recirculating heat it would be possible to operate the process at higher r.p.m. This can be achieved by better cooling conditions made possible through incorporating more number of spray nozzles to sweep the entire inner surface. The limiting condition for choosing the right cooling condition are :
 - (i) the prevention of melt choking at β_1 , if the value of δ , the gap between tundish and drum is less.
 - (ii) the cooling rate to be maintained in the process to cast the required microstructure.
 - (iii) the property of the substrate material to withstand

the repeated thermal shock experienced in the process.

3. The thickness of drum wall is important because using thinner walls, better penetration of cooling effect from water flux can be obtained. But thinner walls are likely to carry less recirculating heat causing more initial thickness of skin at β_1 , producing amorphous structure. The cooling rate of skin is less for higher wall thickness and more for thinner walls. By controlling the spray condition, the cooling rate can be controlled and the structure related problem overcome. So a proper combination of the above factors have to be considered.

SUGGESTIONS FOR FUTURE WORK

The models presented in this investigation are able to predict the nature of variation that occurs between the parameters of the continuous casting process when one of them is altered. It can also qualitatively predict the effect on the output of the caster when some design alterations are carried out in it. In this chapter, some suggestions are given for extending these models to obtain additional details and better accuracy about the casting operation from the perspective of the operating parameters.

7.1 MACROSCOPIC MODEL

- 1) The effect of using different roll materials on the output of the process can be studied by using the corresponding thermal data of the material.
- 2) For casting strips of different metals and alloys, the operating parameters of the caster will be different. These values can be evaluated for the casting of steels of different compositions, aluminium, copper, tin and other metals and alloys.
- 3) One area which has not been attempted in this model is the casting of very thin strips say of 0.5mm and 2.0mm. From the available qualitative relationship, the R.P.M. required for

the casting appears to be quite high which means that the residence time for the growth of solidification front is less. Secondly, an observation was made in the microscopic model about the importance of including surface adhesion dynamics for such thicknesses. Therefore the increase in the temperature of the drum during its motion in the heat supply zone may not be substantial and assuming an average temperature for the drum should give fairly good results. Hence, to couple the lower surface of solid skin and the drum surface for the heat flux, a surface adhesion heat transfer coefficient is to be included in this equation written between the liquid solid interface temperature T_F and the average temperature of copper drum T_{Cu} . Extending the one dimensional heat flux equation right upto spray water may not be valid since steady state fully developed heat flow may be unlikely in view of the very short residence time. From the modified flux equation, simulation of the casting operation for thin strip thicknesses can be carried out.

7.2 MICROSCOPIC MODEL

- 1) By using the unsteady state energy equation for the drum and the path of a particular cylindrical element of the drum traced during the course of motion for any R.P.M., a more realistic formulation of the model is possible. This is illustrated in Fig. 7.1., and explained below :

Energy Equation :

$$\rho_{Cu} C_{pCu} \frac{\partial T_{Cu}}{\partial \tau} = k_{Cu} \left[\frac{1}{r} \frac{\partial}{\partial r} \left(r \frac{\partial T_{Cu}}{\partial r} \right) \right] \quad (7.1)$$

$$(R_d - t_{Cu} < r < R_d)$$

$$(0 < \tau < n \cdot \Delta \tau)$$

For any value of ω (R.P.M.), the residence time of the drum cylindrical element is defined in each of the 'n' number of steps.

$$\text{i.e., } \Delta T = \frac{\Delta \beta}{n} \text{ seconds} \quad (7.2)$$

When the drum enters the heat supply zone to the 1st element ($0 < \tau < 1 \cdot \Delta \tau$), the following are the boundary conditions :

$$\text{At } \tau = 0, \quad T_{Cu} = T_{Cuin}, \quad R_d - t_{Cu} < r < R_d \quad (7.3)$$

$$\text{At } 0 < \tau < 1 \cdot \Delta \tau, \quad r = R_d, \quad k_{Cu} \frac{\partial T_{Cu}}{\partial r} = \frac{R_d \cdot \Delta \beta \cdot k_S (T_F - T_{Cu})}{\ln \left[\frac{R_d + t_1}{R_d} \right]} \quad (7.4)$$

$$r = R_d - t_{Cu}, \quad k_{Cu} \frac{\partial T_{Cu}}{\partial r} = (R_d - t_{Cu}) \Delta \beta h_{CuW} (T_{Cu} - T_W) \quad (7.5)$$

From this the temperature at the end of $1 \cdot \Delta \tau$ seconds across the wall thickness of the drum can be calculated using the finite difference technique. Next between $1 \cdot \Delta \tau$ and $2 \cdot \Delta \tau$ secs., the drum element corresponds to the 2nd step position in which the drum is in contact with the solid skin of thickness t_2 . In this step the boundary conditions are :

at $\tau = 1 \cdot \Delta \tau$, $T_{Cu} = T_{Cu}$'s of the previous calculations,

$$\text{and at } r = R_d - t_{Cu}, \quad k_{Cu} \frac{\partial T_{Cu}}{\partial r} = \frac{R_d \cdot \Delta \beta \cdot k_S (T_F - T_{Cu})}{\ln \left[\frac{R_d + t_2}{R_d} \right]} \quad (7.6)$$

at $r = R_d - t_{Cu}$, equation (7.5) is valid.

From this the temperature at the end of $2.\Delta t$ secs. across the thickness of drum wall can be found using again the finite difference technique. The procedure is repeated upto the position β_2 and the temperature as well as the conductive heat in each element evaluated. At β_2 , the temperature along the thickness of strip in the 'j' no. of layers is to be calculated for quantifying the bulk heat.

Final Heat Balance

For casting any strip thickness from a caster of particular geometry, at a definite cooling rate from a melt of known temperature, there exists only one particular R.P.M. . Therefore to arrive at this R.P.M. for a particular strip thickness, the procedure to map the drum and strip temperature is to be started from the lower value of R.P.M. (say 0.1 R.P.M.) and the final enthalpy balance between the the liquid metal arriving into the system and the heat going out of the system is to be tested. If this test is satisfied, then the R.P.M. and the temperatures are the actual values existing at that condition. If the test fails, then the R.P.M. is to be incremented by a small value and the test repeated again. Using this technique a sufficiently good description of the casting process based entirely on energy and mass balance is possible.

Conventional
process route

Near-net-shape
Casting techniques

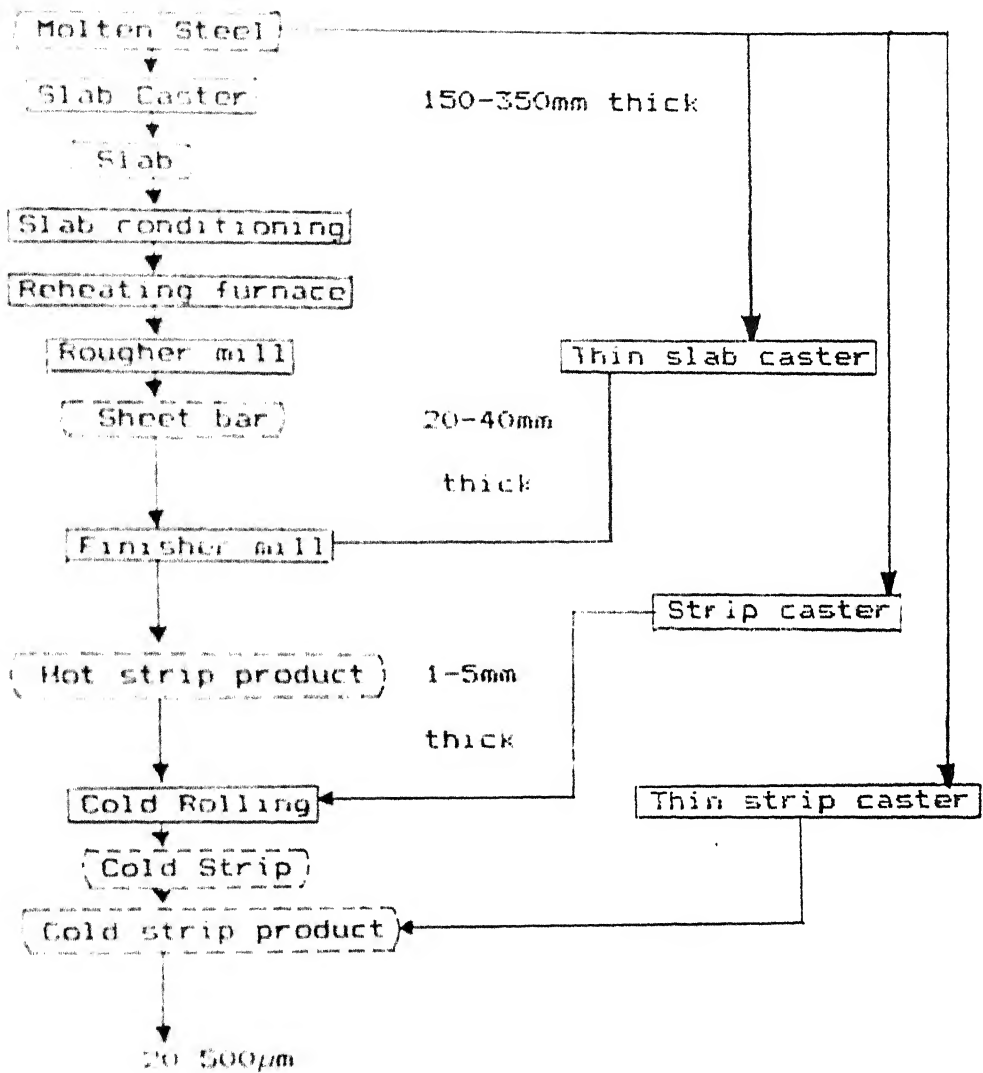


Fig. 1.1 Process routes for producing flat Rolled Products³

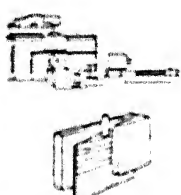




Process	Manufacturer/ operator	Technical data	Product
Stationary mould 	SMS Buschhütten	Thickn.: 40–60 mm Width: 1600 mm v_0 : 6 m/min 750,000 t/a	Thin slab Usual hot strip grades
	SMS/Nucor Corp. Crawfordsville (II 1989)		
Stationary mould 	MDH/MRW Huckingen	Thickn.: 40–70 mm Width: 1600 mm v_0 : 6 m/min	Thin slab Usual hot strip grades
Stationary mould 	Danieli Udine	Thi.: 28–50 mm Wi.: 1600–1750 mm v_0 : 6 m/min	Thin slab Strip
	Danieli Feng Lung Steel Factory Taiwan	Thickness: 75 mm Width: 1220 mm	Thin slab
Stationary mould in horizontal line HCC 	MDH/Bosch- gotthardshutte Siegen	Thickn.: 40–120 mm Width: 450 mm v_0 : 4 m/min 100,000 t/a	Thin slab All steel grades
Mould car 	British Steel Corp. Teesside Labs	Thickness: 75 mm Width: 500 mm v_0 : 10–20 m/min	Thin slab Plain carbon steel

Fig. 2.1

Stationary Mould Casters


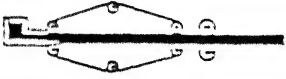
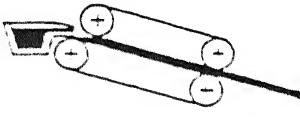

2 travelling belt moulds vertical 	Nippon Steel Corp	Thickness: 50-80 mm Width: 600 mm v_c : 4 m/min	Thin slab
2 travelling belt moulds horizontal  KCC = Kawasaki Horizontal Continuous Caster	Kawasaki Steel Corp Chiba Research Centre	Thickness: 10-30 mm Width: 100-150 mm v_c : 0.7-12.5 m/min	Strip Low-carbon steels Si-steels Stainless steels
2 travelling belt moulds inclined  Hazelett	Hazelett/ Sumitomo MI- Sumitomo HI Kashima	Thickness: 40 mm Width: 600-1300 mm v_c : 2-8 m/min 600,000 t/a (1300 mm)	Thin slab Al-killed steels Stainless steels
	Hazelett/ Nucor Corp. Darlington, S.C.	Thickness: 25-38 mm Width: 1300 mm v_c : 1.5-8 m/min 500,000 t/a (1300 mm)	Strip Carbon steels
	Hazelett/ Krupp Industrietechnik Bochum	Thickness: 70 mm Width: 180 mm abandoned	Thin slab
	Hazelett/ Bethlehem Steel + US Steel Universal, Pa	Thickness: 12-25 mm Width: 1830 mm interrupted/abandoned	Strip
2 travelling belt moulds horizontal 	Kobe Steel Nippon Kokan	no details known	

Fig. 2.2 Twin Belt Thin Slab Caster⁴

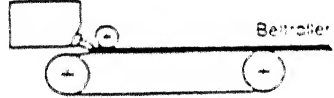
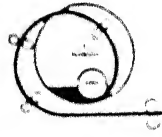
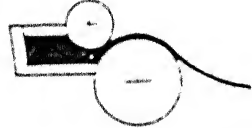
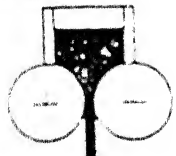
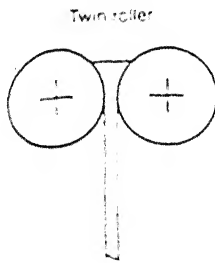
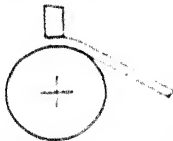
Process	Manufacturer/ operator	Technical data	Product
1 travelling casting belt and 1 roller  DeSC-Process Demag Strip Casting	MDH/MSA Belo Horizonte (1988)	Thickness: 5-10 mm Width: 900 mm v_c : 25-50 m/min 750,000 t/a	Strip All steel grades
Inside-The-Ring 	Jones + Laughlin (now LTV Steel) Pittsburgh (1967-1975)	Thickness: 5 mm Width: 380 mm v_c : 7.5 m/min	Strip
Two rollers and roller 	Kobe Steel Amagasaki	Thickness: 1-2 mm Width: 260 mm	Thin strip Stainless steels
	Nippon Metal	Thickness: 1-4 mm Width: 315/650 mm	Thin strip Stainless steels
	Krupp Stahl AG	Thickness: 1-4 mm Width: 150 mm	Thin strip Stainless steels
	Nippon Yakin	Thickness: 6 mm Width: 150 mm	Strip Stainless steels
Two rollers and roller 	Ishihara Hi/ Nippon Kokan	Thickness: 2-6 mm Width: 400 mm v_c : 25 m/min	Strip Thin strip Carbon steels Stainless steels
	Yachi Zosen Corp	Thickness: 5-10 mm Width: 300 mm	Strip

Fig. 2.3 Moving Belt with 1 or 2 Rollers⁴



Twin roller

Single roller



Yoshin Steel + Mitachi Corp	Thickness Width	< 5 mm 200 mm	Thin strip Stainless steels
Kawasaki Steel Corp	Thickness Width	0.5 mm 100 mm	Thin strip St-steels
Armco + Inland Steel + Weirton Steel + Bethlehem Steel	Thickness Width	< 5 mm 300 mm	Thin strip
Clecm/Isid	Thickness Width	2-10 mm 200 + 850 mm	Strip Thin strip Stainless steels
DEC/British Steel Corp	Thickness Width	3 mm 400 mm	Thin strip Stainless steels
CSM	Thickness Width	300 mm	Thin strip Unalloyed steels
Vöest-Alpine	Thickness Width	2-8 mm	Strip Thin strip
Thyssen Guillo Funke - IGF Aachen	Thickness Width	0.1-2 mm 150 mm	Thin strip St-steels
API für Eisenforschung Düsseldorf	Thickness Width	1 mm 100 mm	Thin strip St-steels
Armco + Westinghouse Middletown	Thickness Width	0.8-3 mm 75 mm	Thin strip
Allegheny Ludlum	Thickness Width	1-2 mm 300 mm	Thin strip Stainless steels

Fig. 2.4

Single and Twin Roll Caster⁴

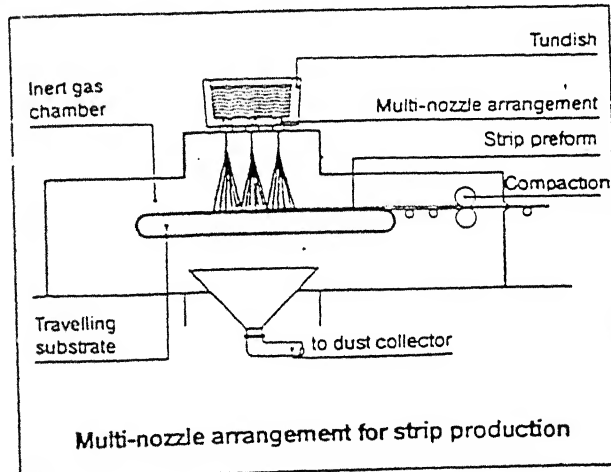
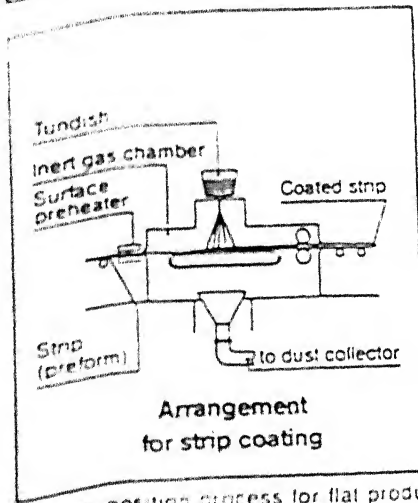
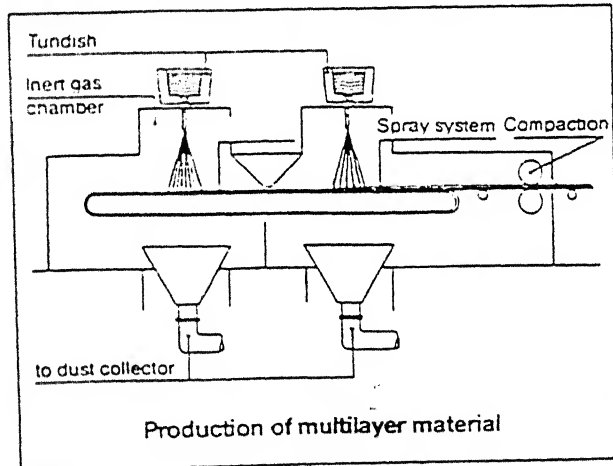
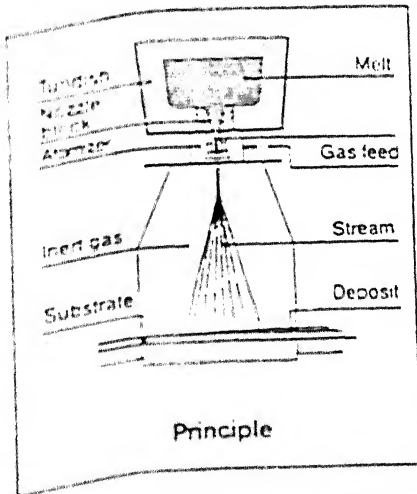


Fig. 2.6 Heat Transfer Coefficient Data

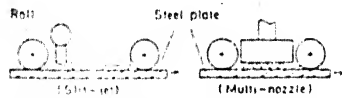


Fig. 1 Schematic diagram of model cooling devices

Table 1. Specifications of model cooling devices

Cooling method	Slit-jet	Multi-mist jet	Multi-spray
Design pressure	3.0 kg/cm ²	1.2	1.2
Amount of water	2.8 m ³ /min-piece	1.8 m ³ /min-piece	4.8
Nozzle pitch	—	50 x 40 mm	40 x 30
Number of nozzles	1 piece	114	184
Impinged water flux	4000 l/m ² min	—	—

① Cooling length of Slit-jet = 1.0 mm

Table 2. Experimental conditions

Water temperature	55 ~ 150 mm
Impinged water flux	0, 200 ~ 325 mm
Impinged water flux	1800 ~ 7000 l/m ² min
Water temperature	23 ± 4.5 °C
Specimen	265 x 265 x 31 mm (SUS 310S)

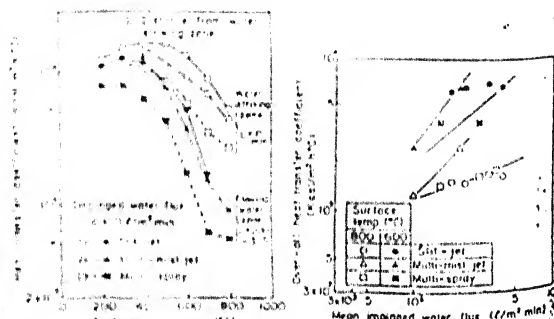
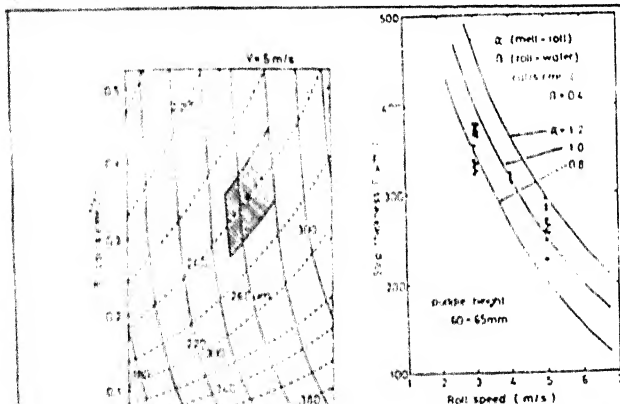


Fig. 2 Influence of the distance from water striking point on the heat transfer coefficient

Investigation of Heat Transfer Characteristics in Various Rapid Cooling Methods on a Hot surface



Dependence of heat transfer coefficient on roll surface temp. and strip thickness.

Calculation of Heat Transfer Coefficient during Rapid Solidification in a Double Roller Method

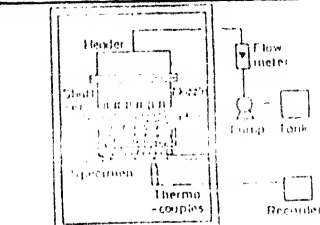


Fig. 1. Experimental apparatus

Table 1. Experimental conditions.

Nozzle	Full cone
Density	1.67 ~ 2.33 pieces/m ²
Arrangement	Triangular
Spray distance D	50 ~ 150 mm
Water thickness h	0 ~ 50 mm
Impinged water flux W	1000 ~ 7000 l/m ² min
Specimen	265 x 265 x 31 mm (SUS 310S)
Water temperature	2 ~ 10 °C

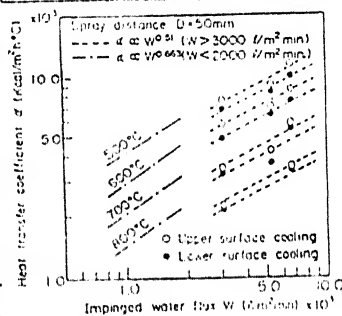


Fig. 2. Effect of impinged water flux.

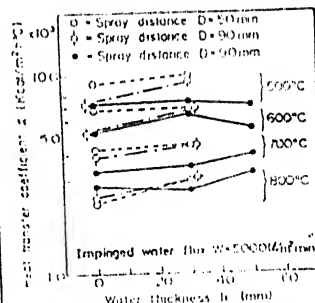
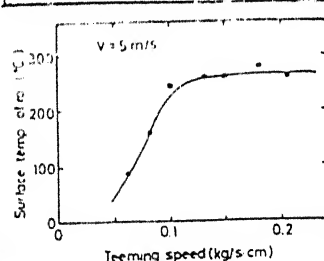


Fig. 3. Effect of water thickness.

Characteristics of Heat Transfer of Multi-Water Spray Nozzle



Surface temperature of roll.

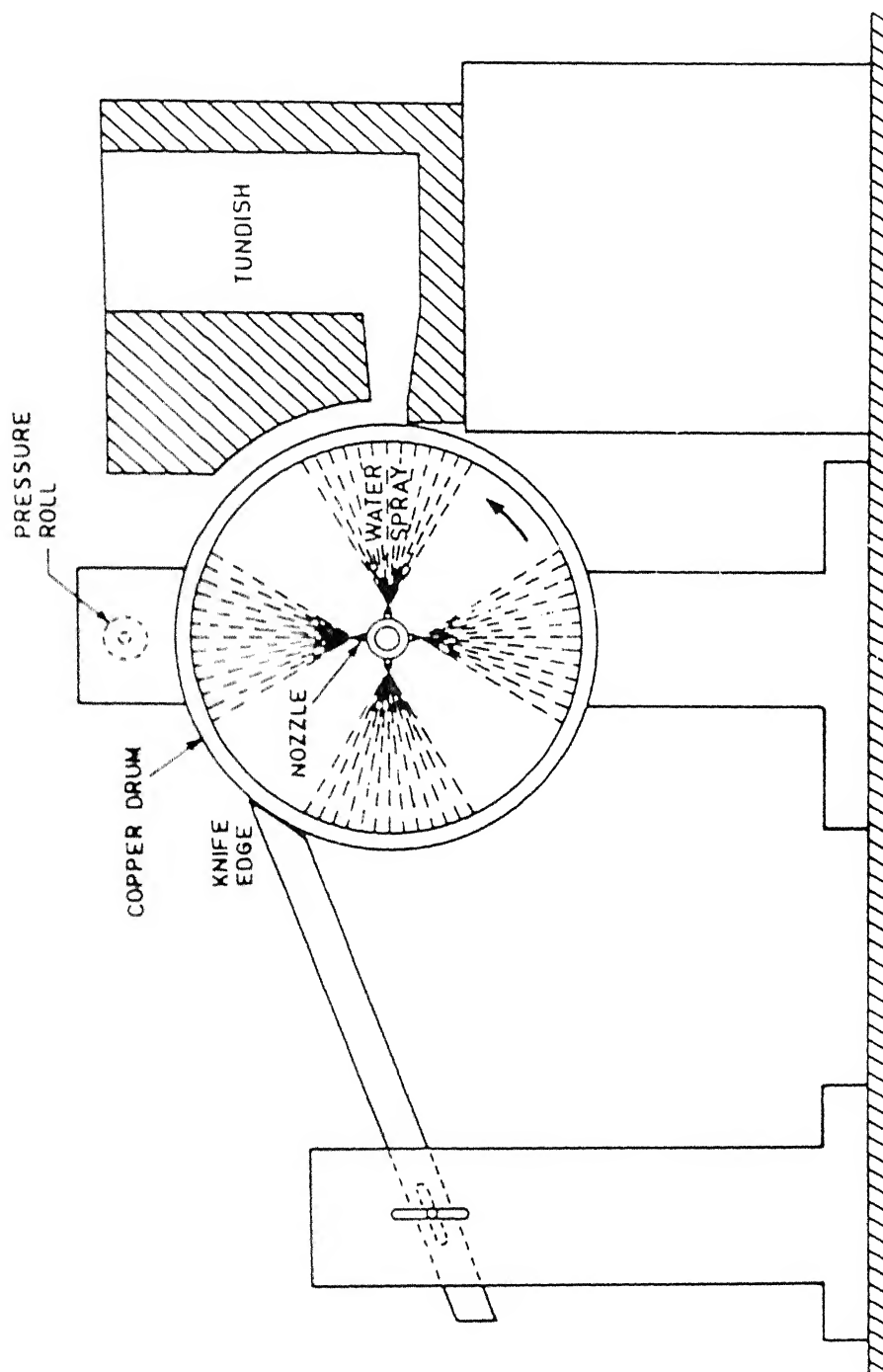


Fig. 3.1 - Schematic sketch of the Single Roll (Drum) Horizontal Strip Caster

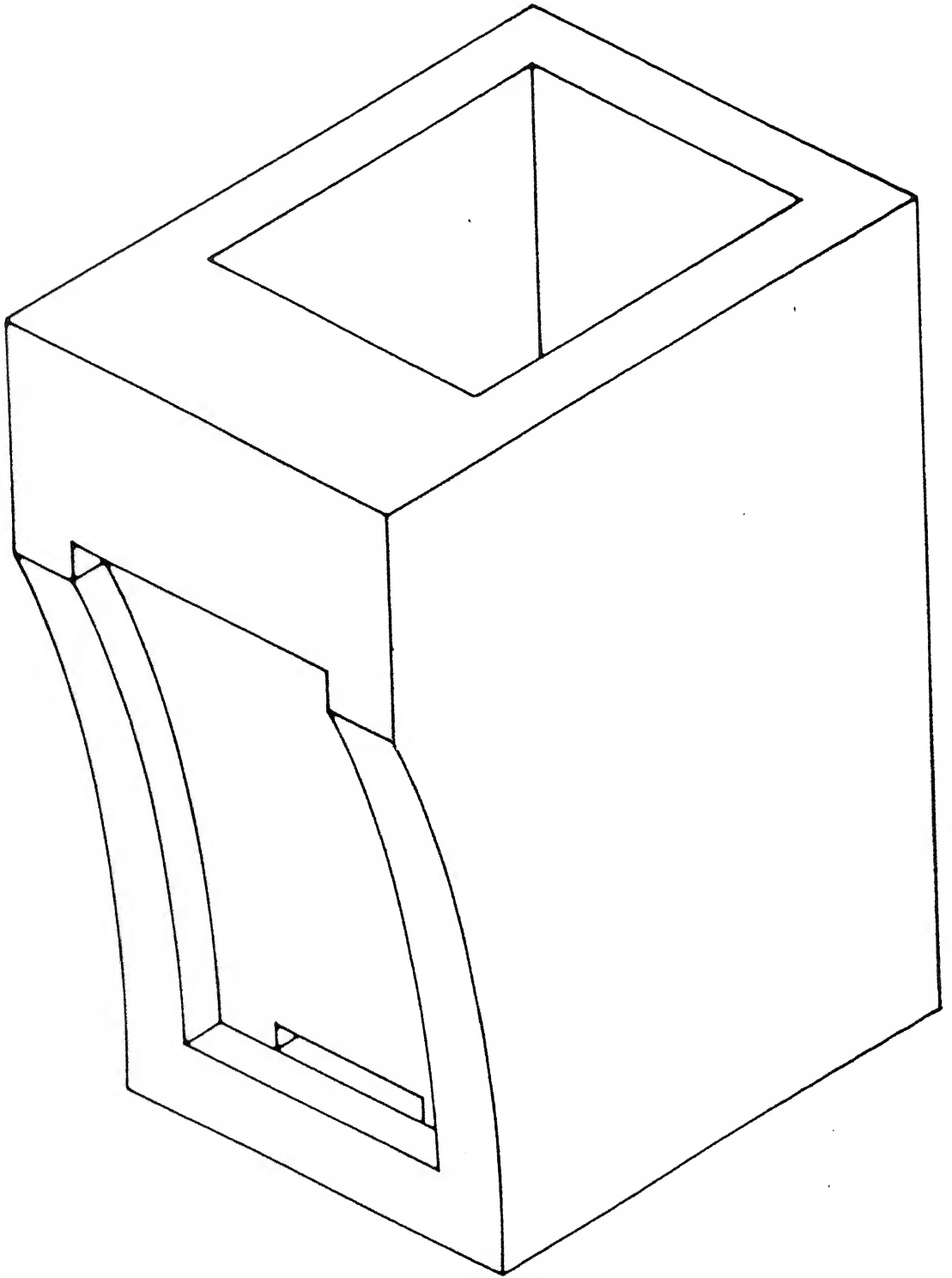


Fig. 3.2 Schematic sketch of the Tundish

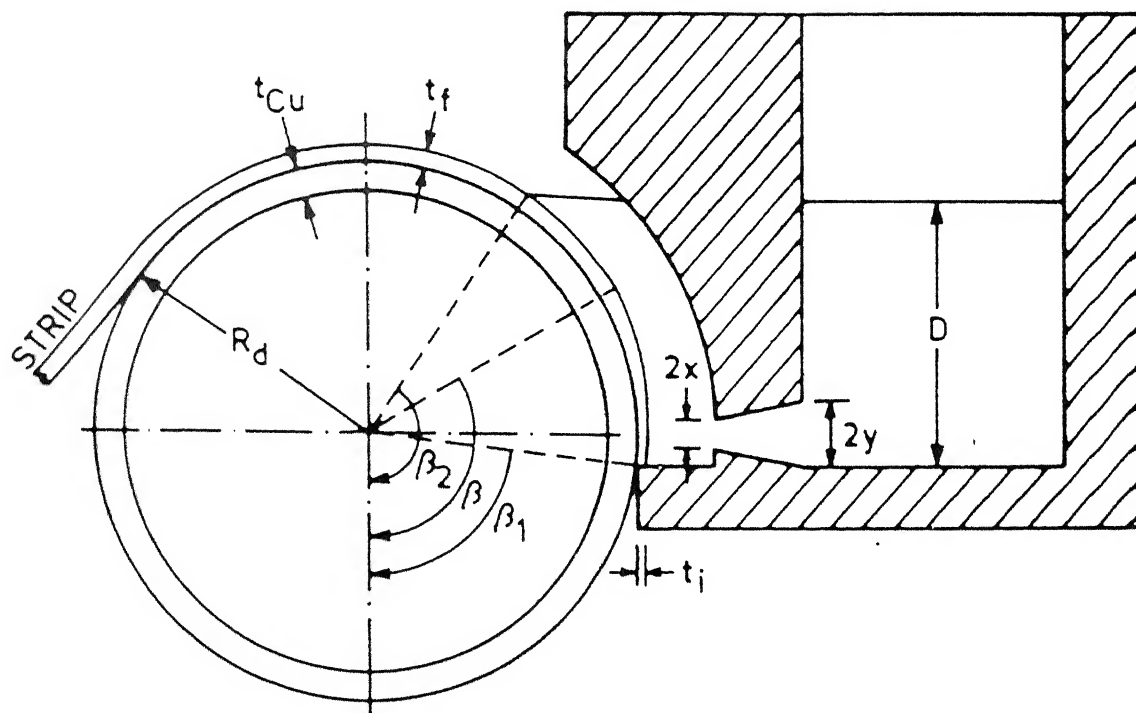


Fig. 3.3 Schematic sketch of the Physical Phenomenon

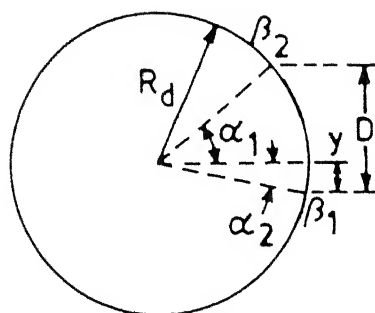


Fig. 4.1 Sketch to establish Angular Relationships

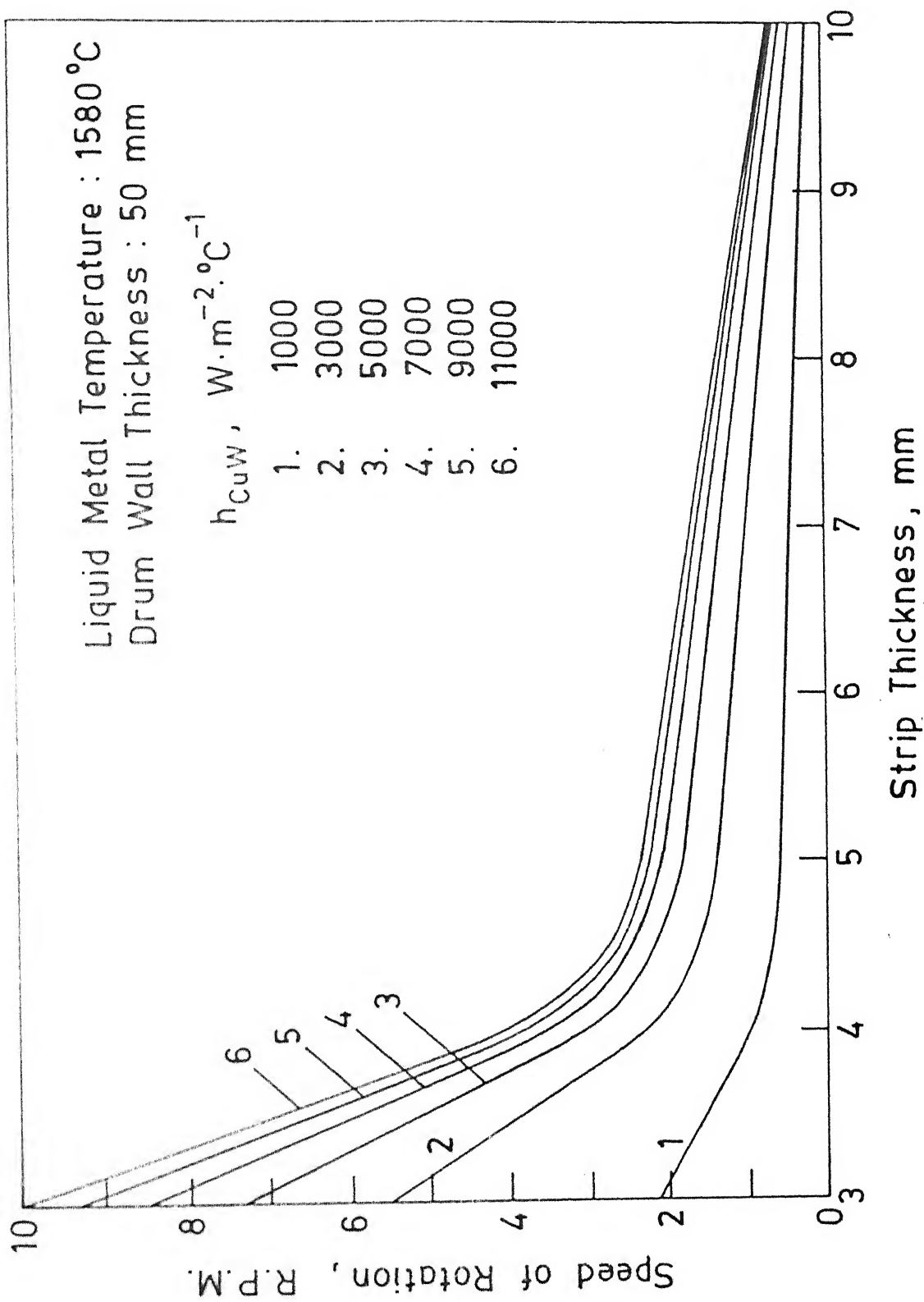


Fig. 4.2 Effect of the Speed of Rotation (R.P.M.) on the Strip Thickness at different cooling conditions

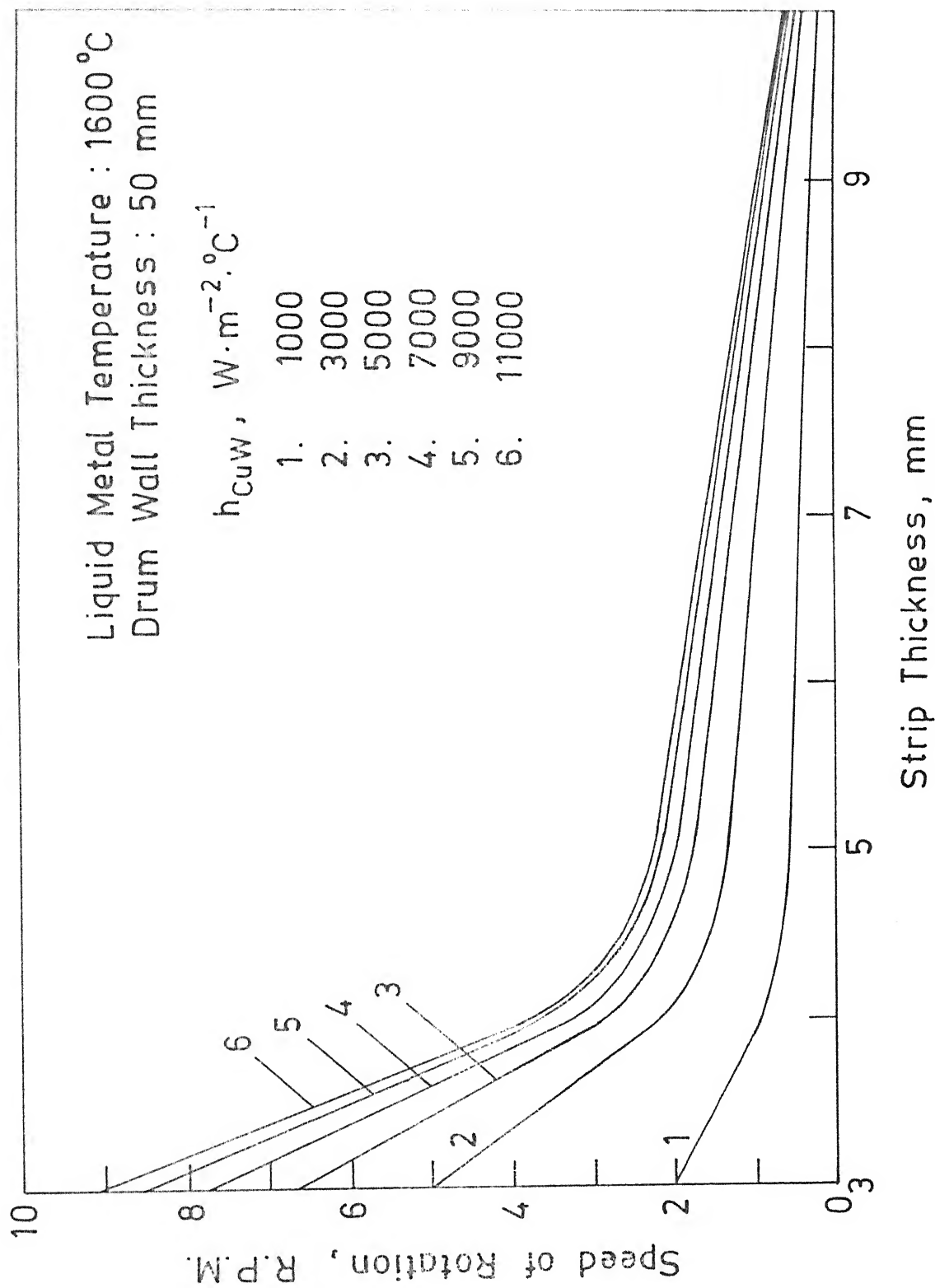


Fig. 4.3 Effect of the Speed of Rotation (R.P.M.) on the Strip Thickness at different cooling conditions

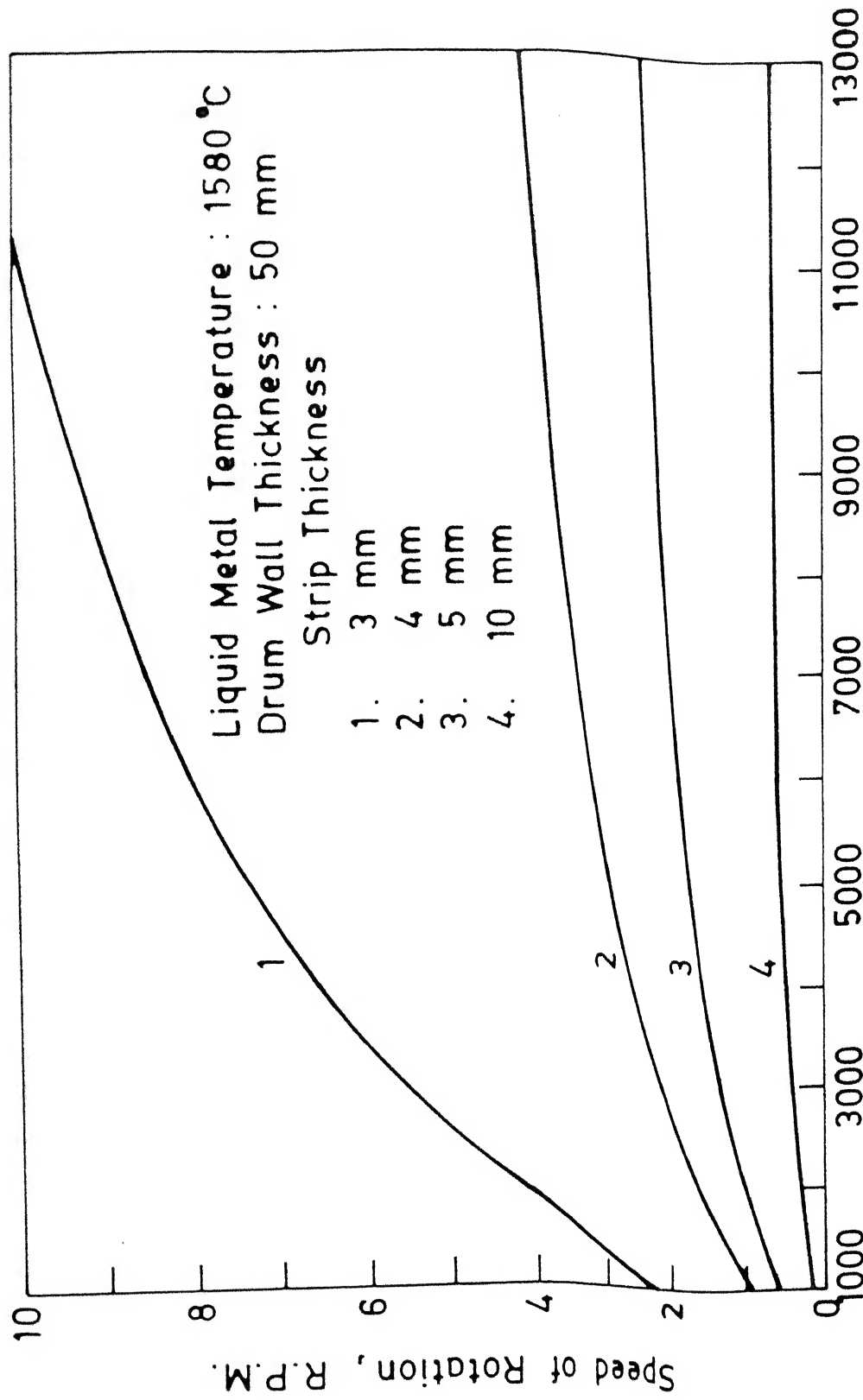


Fig. 4.4 Effect of the Cooling conditions at the inner surface of Drum on R.P.M.

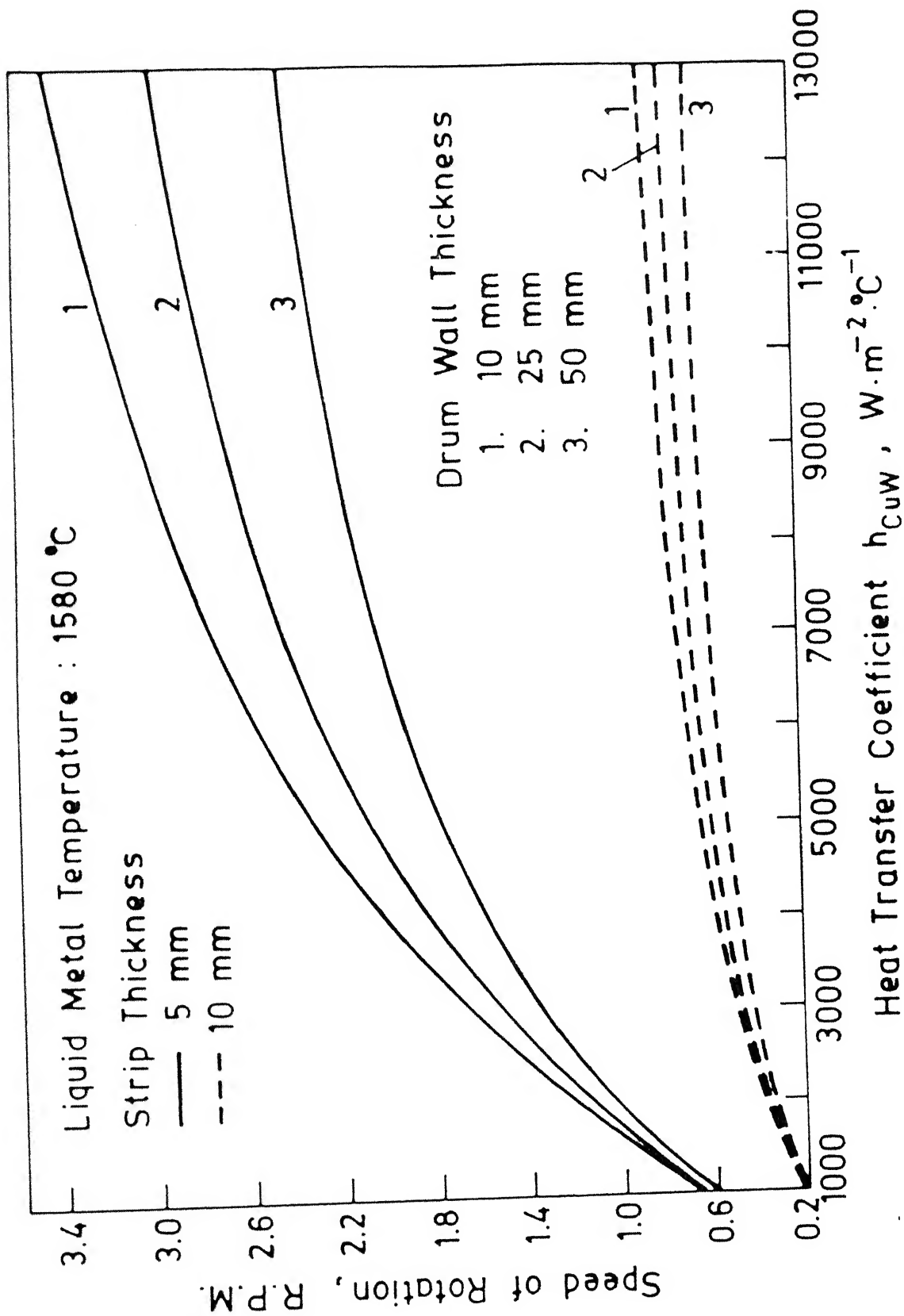


Fig. 4.6 Effect of the Thickness of Copper Drum Wall on R.P.M.

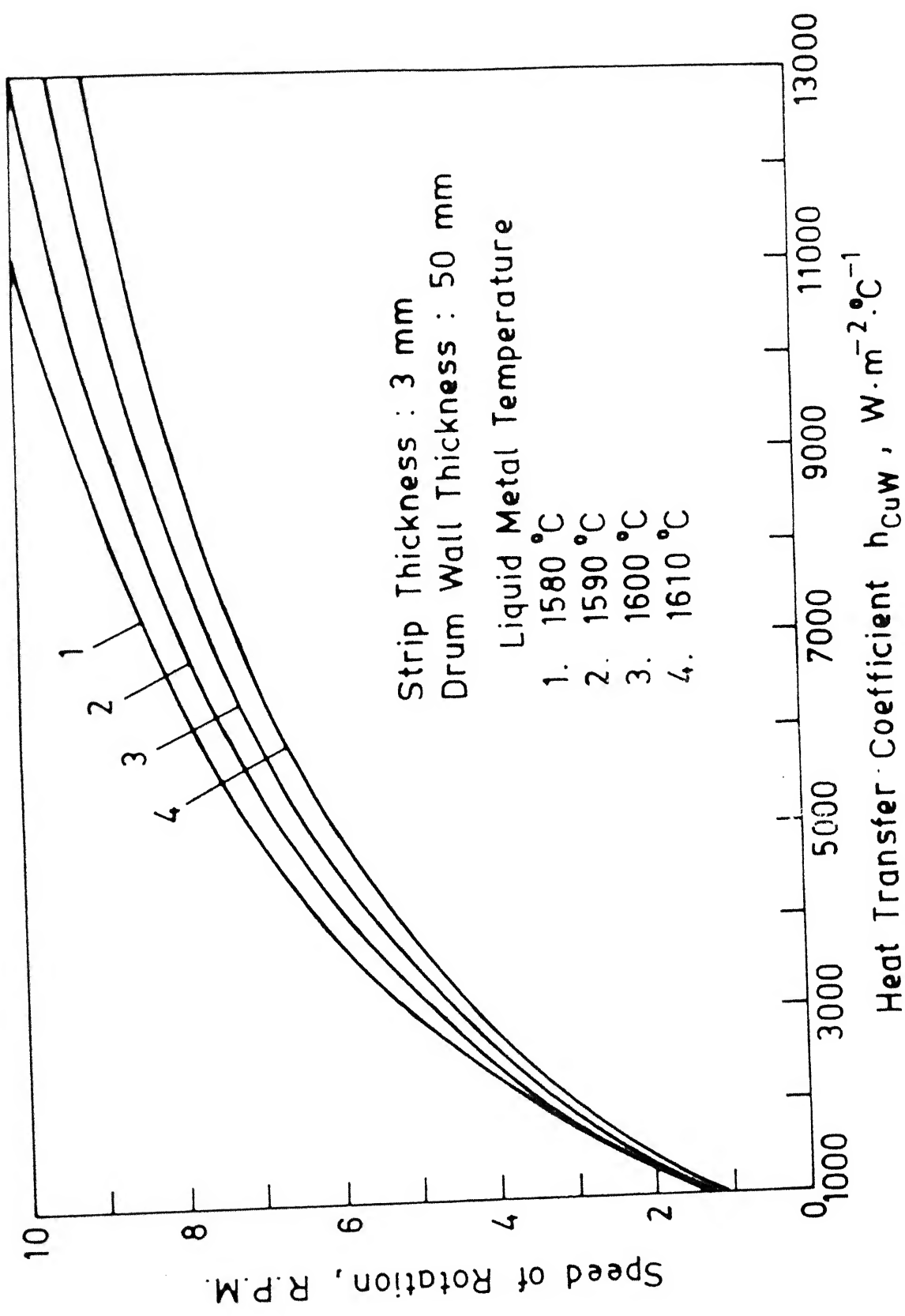


Fig. 4.7 Effect of the Superheat of Melt on R.P.M.

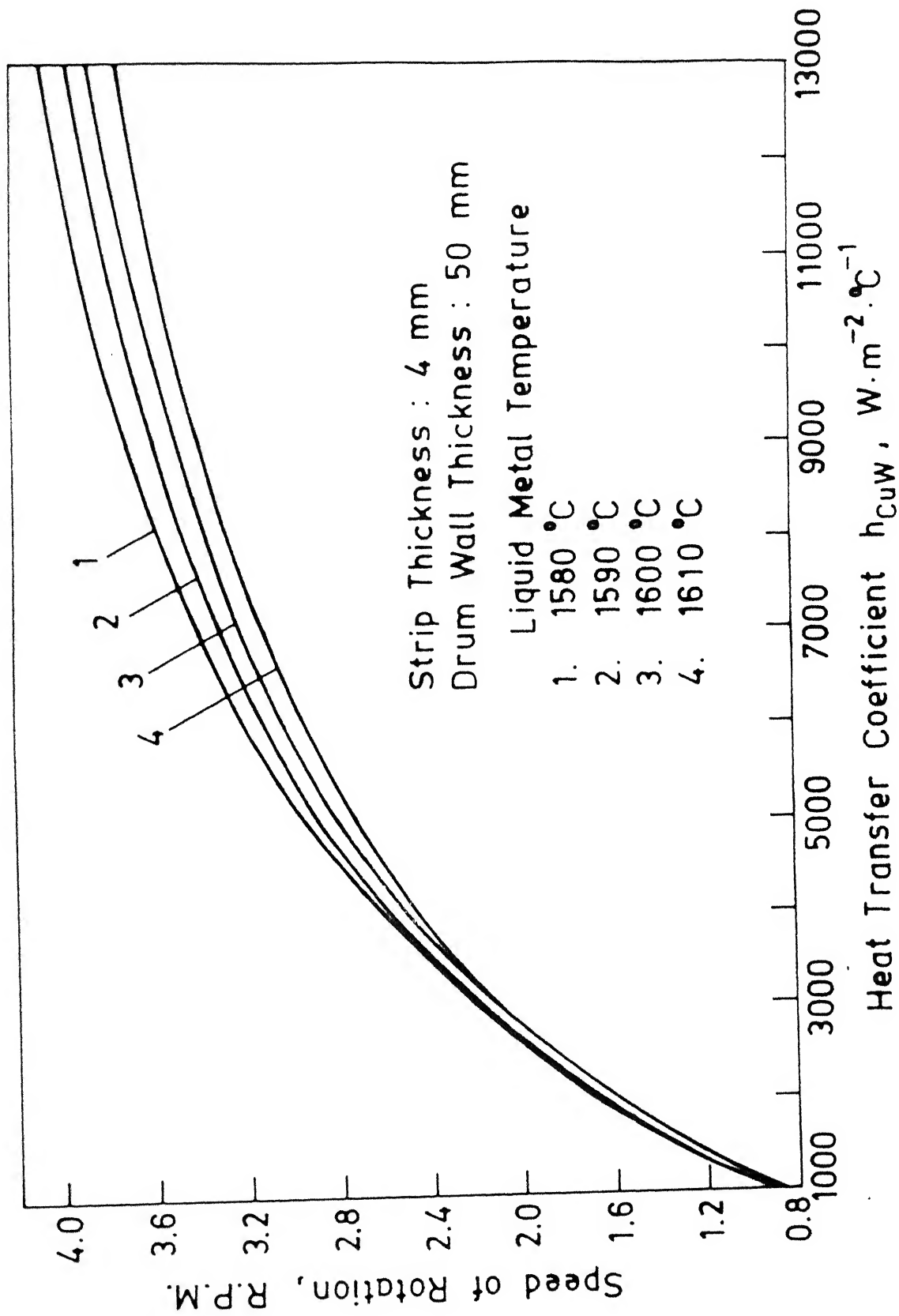


Fig. 4.8 Effect of the Superheat of Melt on R. P. M.

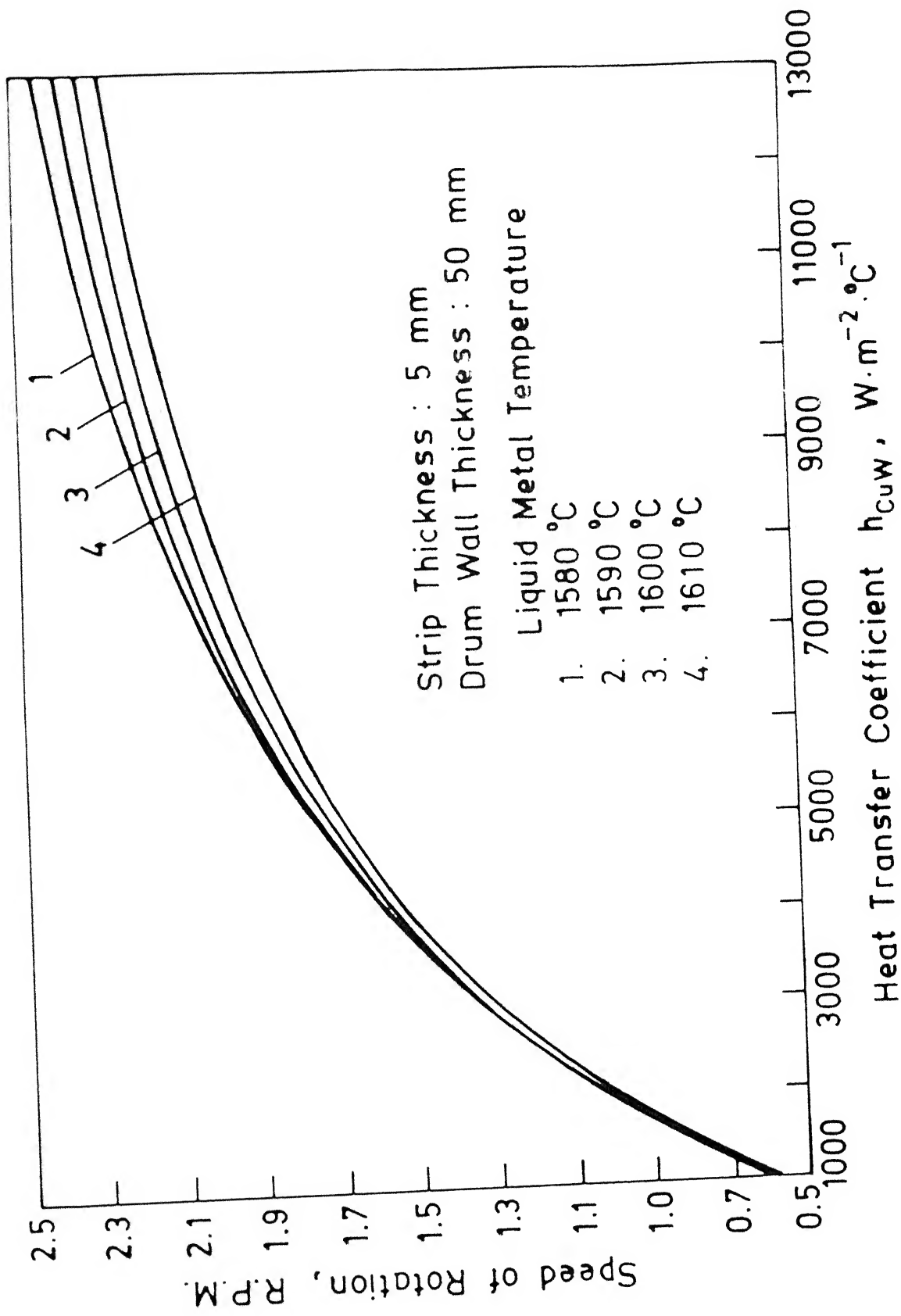


Fig. 4.9 Effect of the Superheat of Melt on R.P.M.

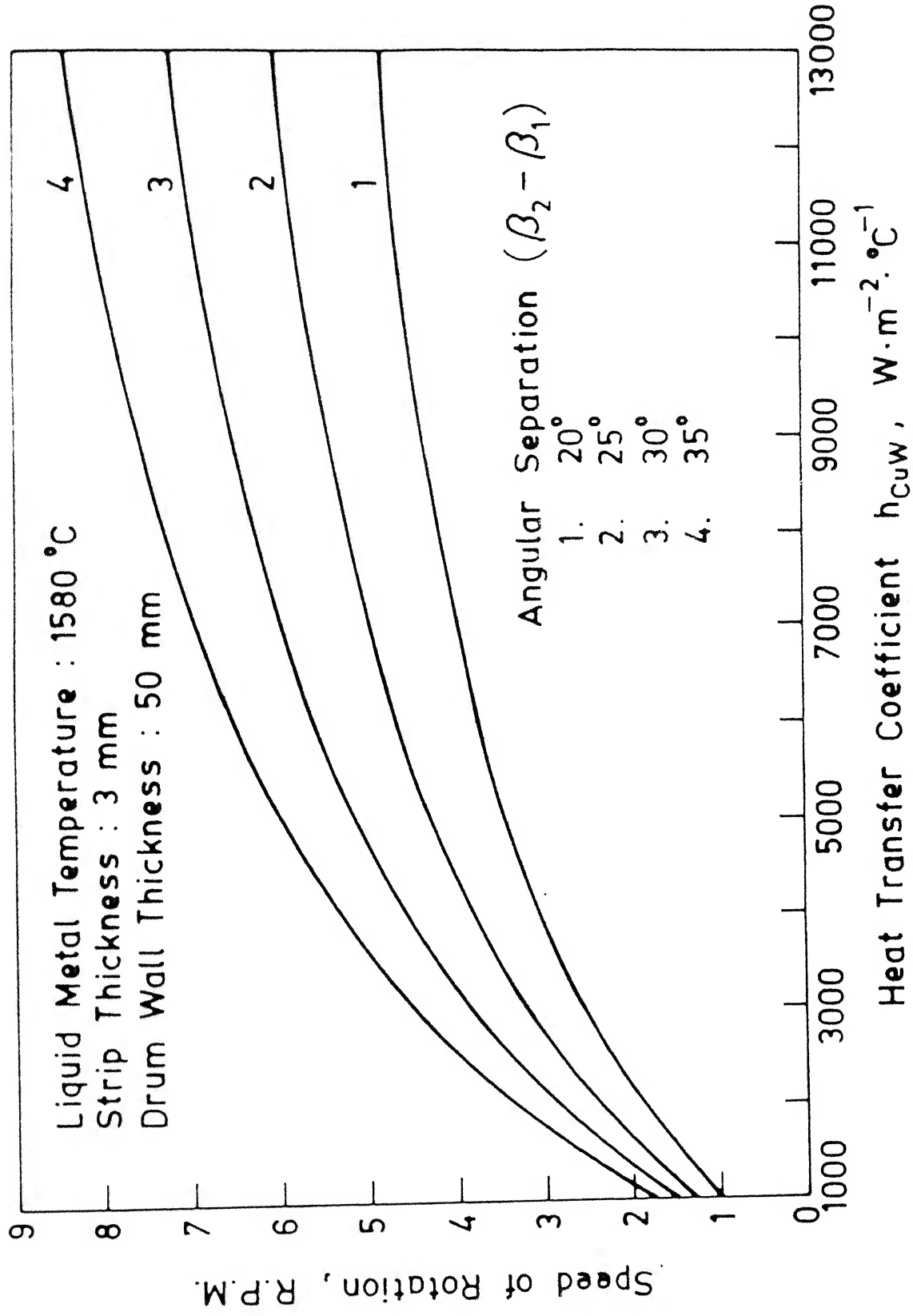


Fig. 4.10 Effect of the Metal Head on R.P.M. for casting
a particular Strip Thickness

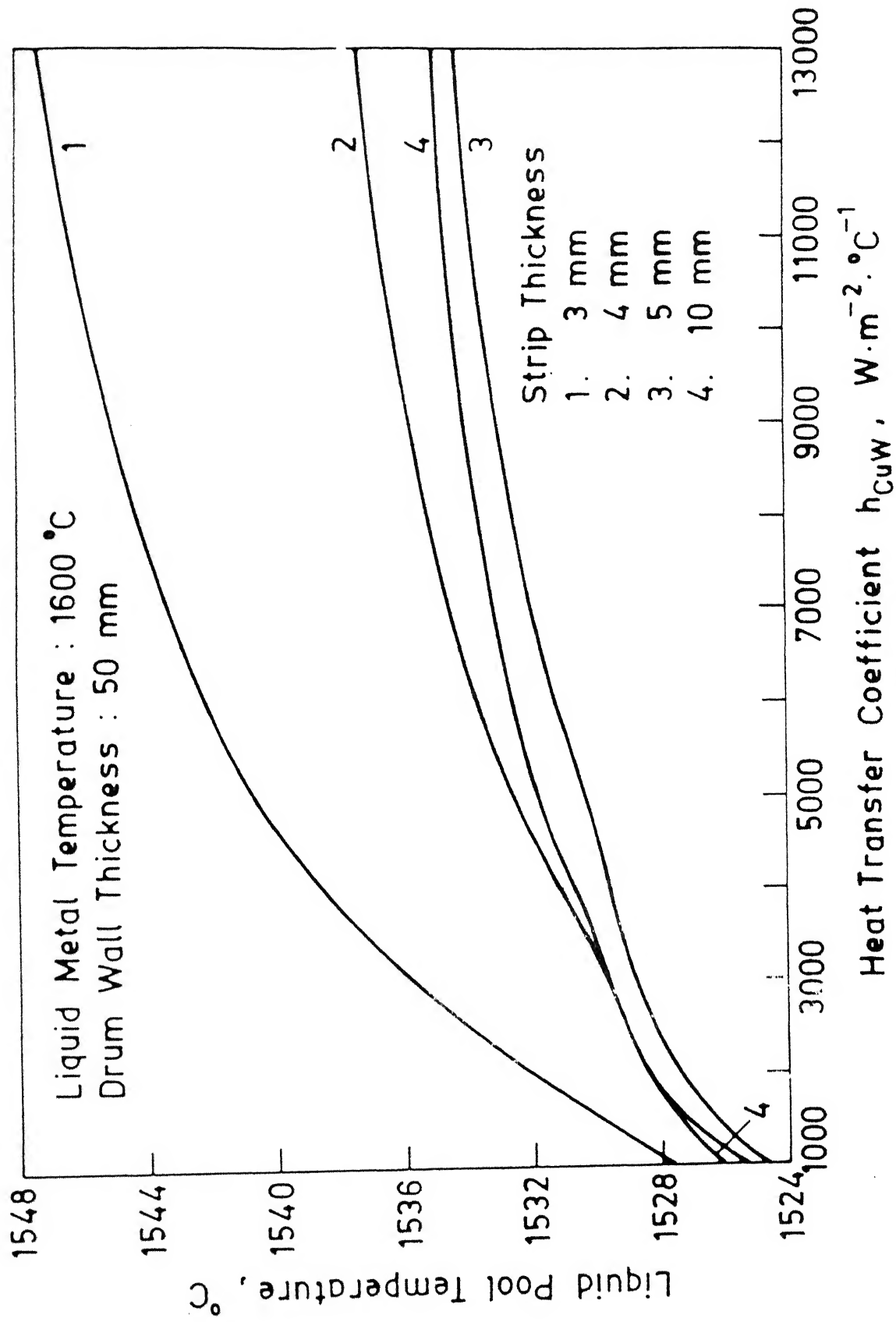


Fig. 4.11 Effect on Liquid Pool Temperature under different Cooling conditions

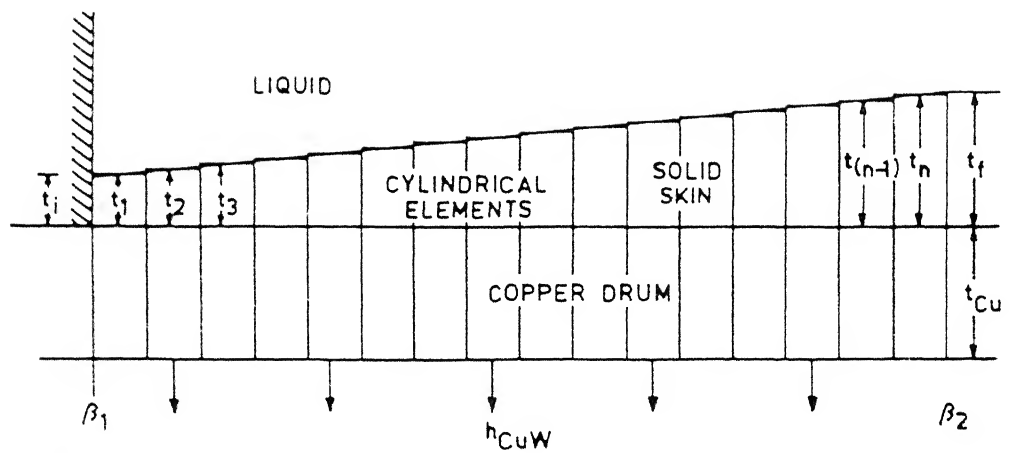


Fig. 5.2 Schematic sketch of the Growth of Solid Skin on Copper Drum

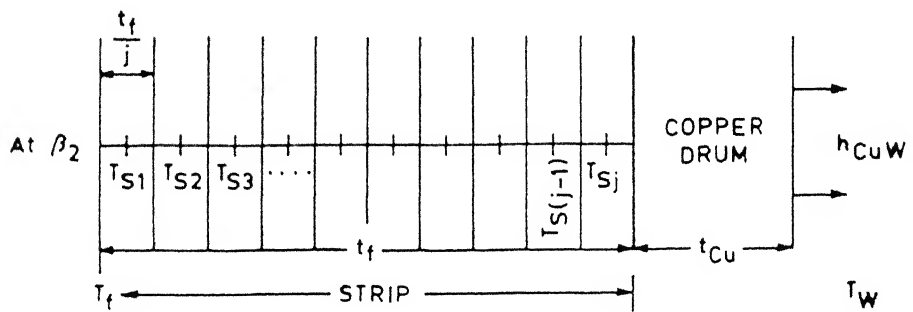


Fig. 5.3 Schematic sketch of the Thermal Composite Layers of Strip at B for evaluating the Bulk Heat

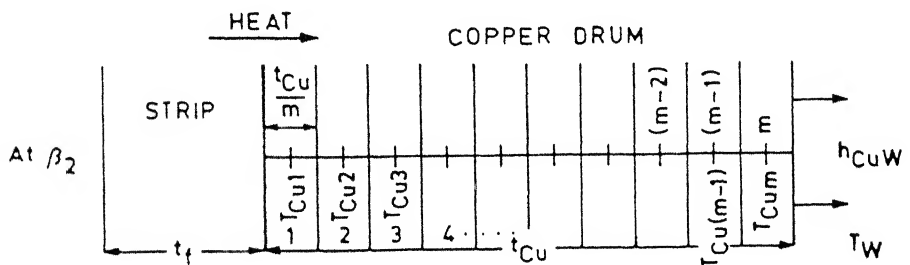


Fig. 5.4 Schematic sketch of the Thermal Composite Layers of the Wall of Copper Drum at B for evaluating the Bulk Heat

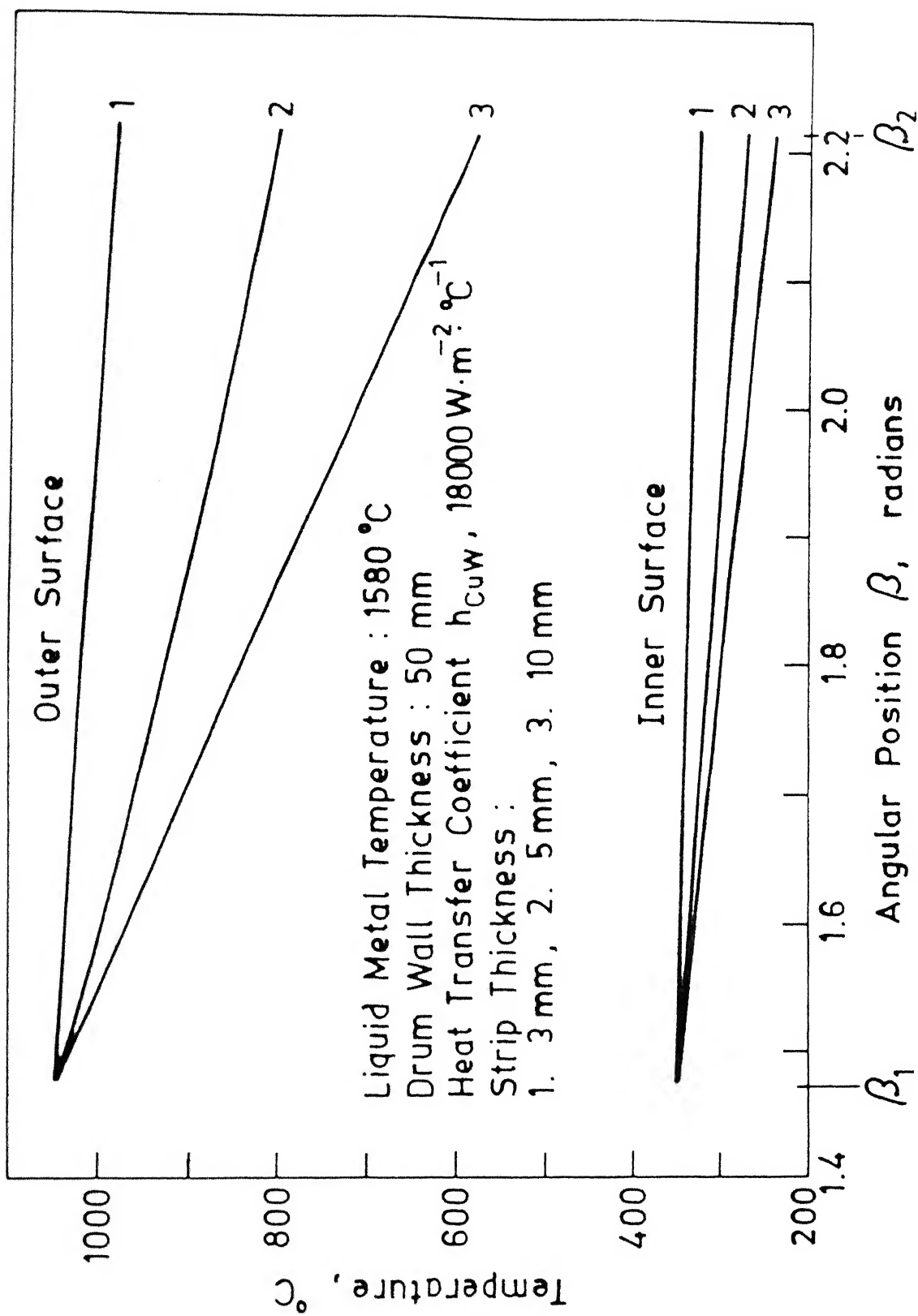


Fig. 5.5 Effect of Casting different Strip Thicknesses on the Surface Temperature of Copper Drum

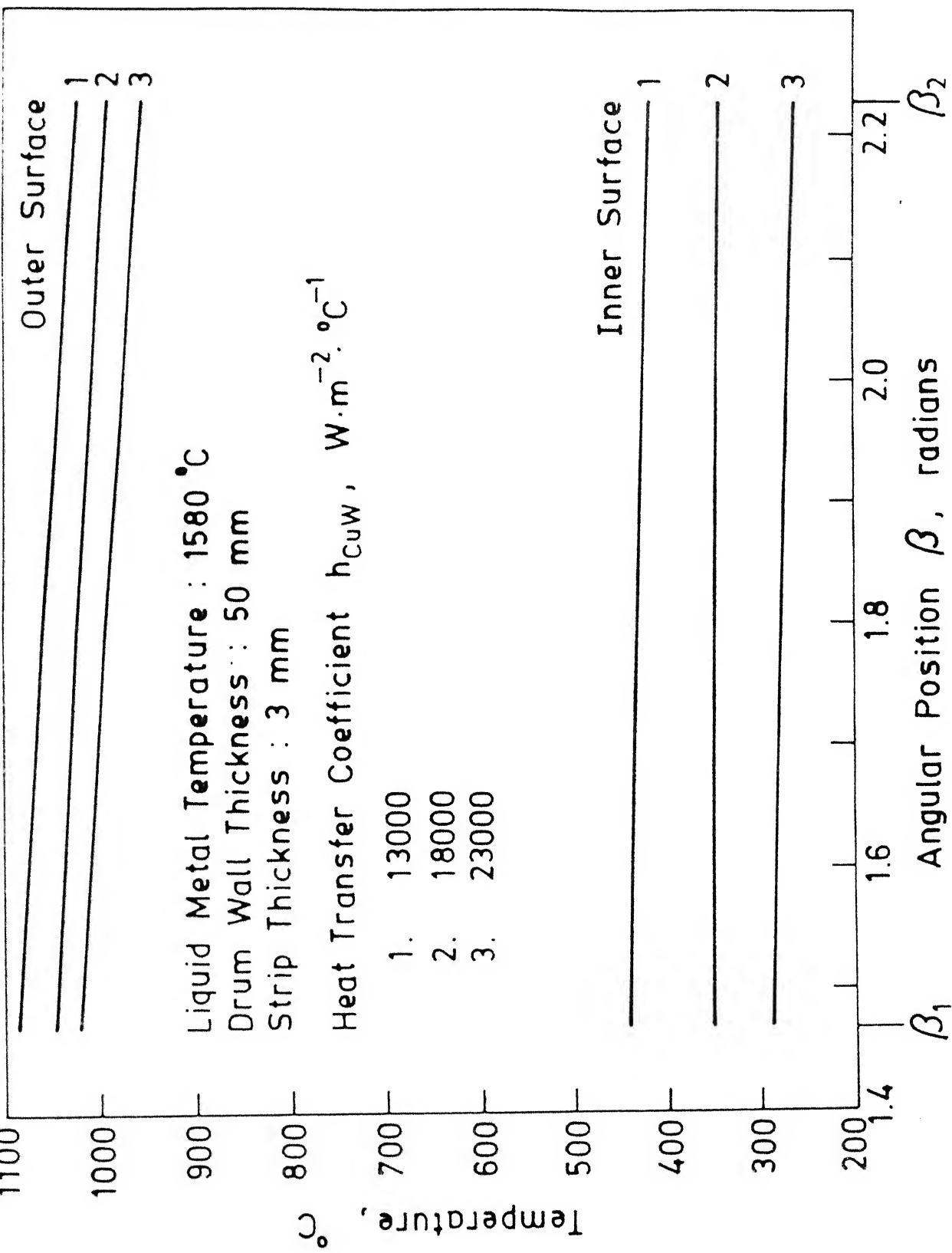


Fig. 5.6 Effect of Cooling condition on the Surface Temperature of Copper Drum

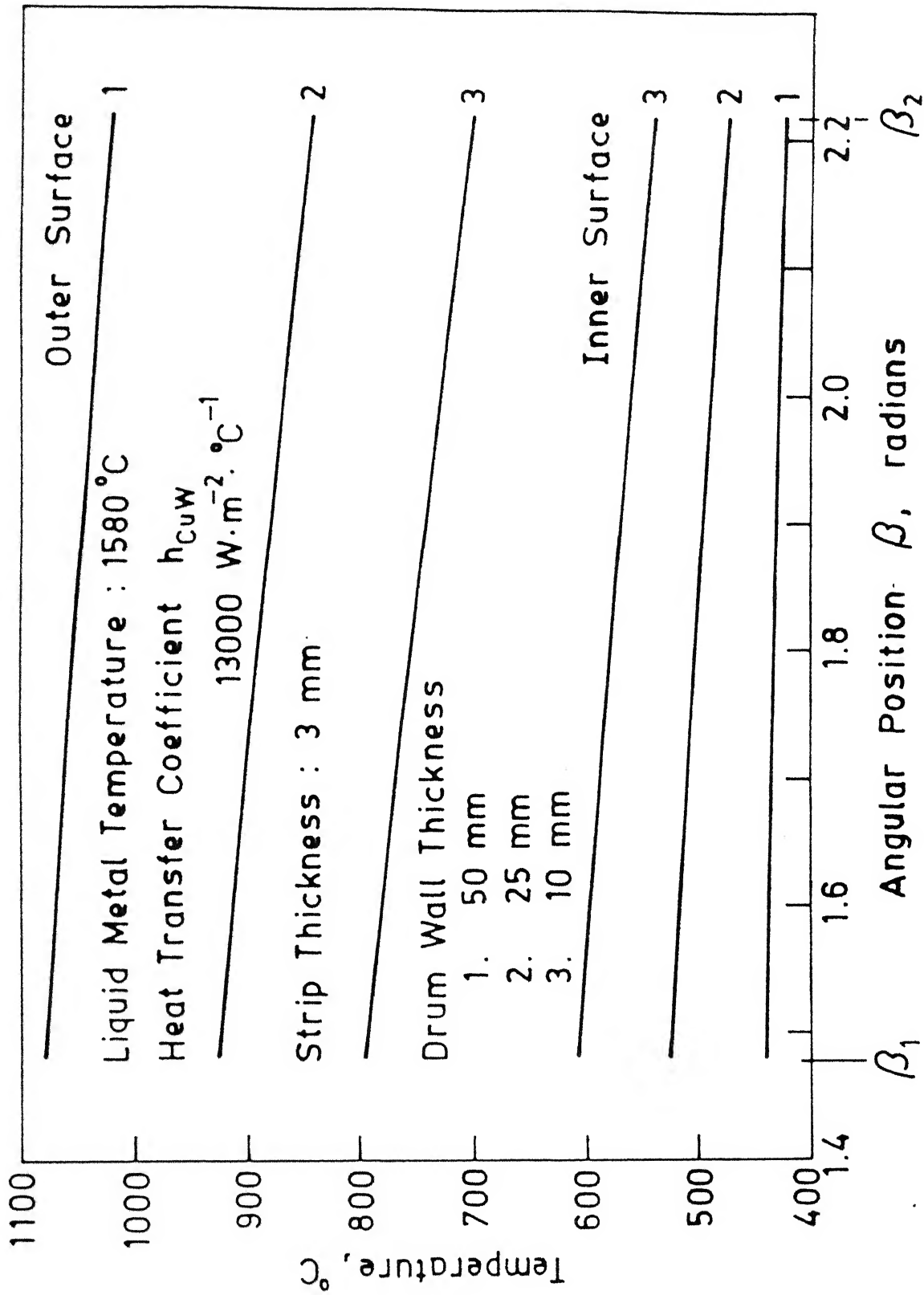


Fig. 5.7 Effect of Drum Wall Thickness on its Surface Temperature

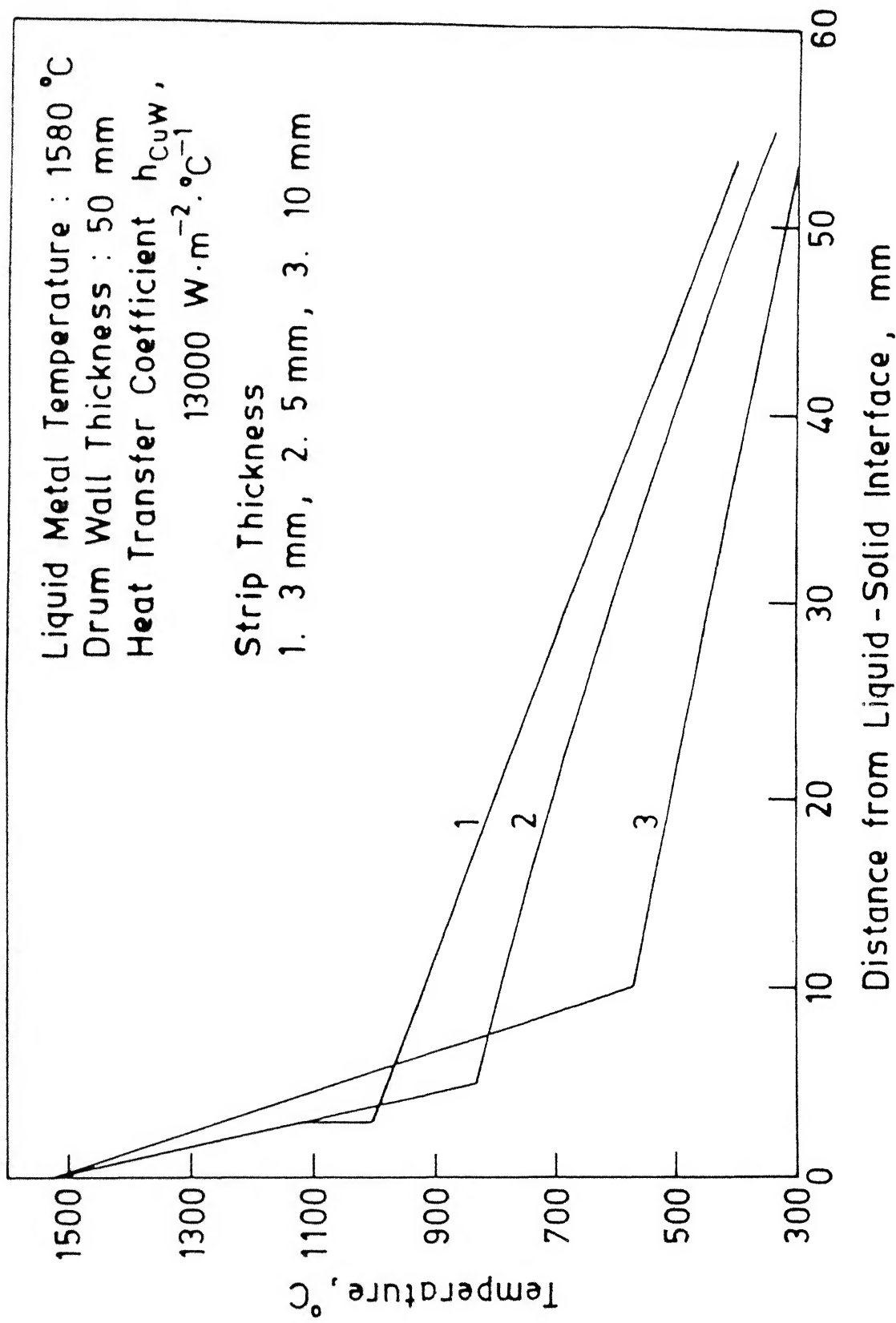


Fig. 5.8 Effect of Casting different Strip Thicknesses on the Cross sectional Temperature of Strip and Drum at exit (β_2)

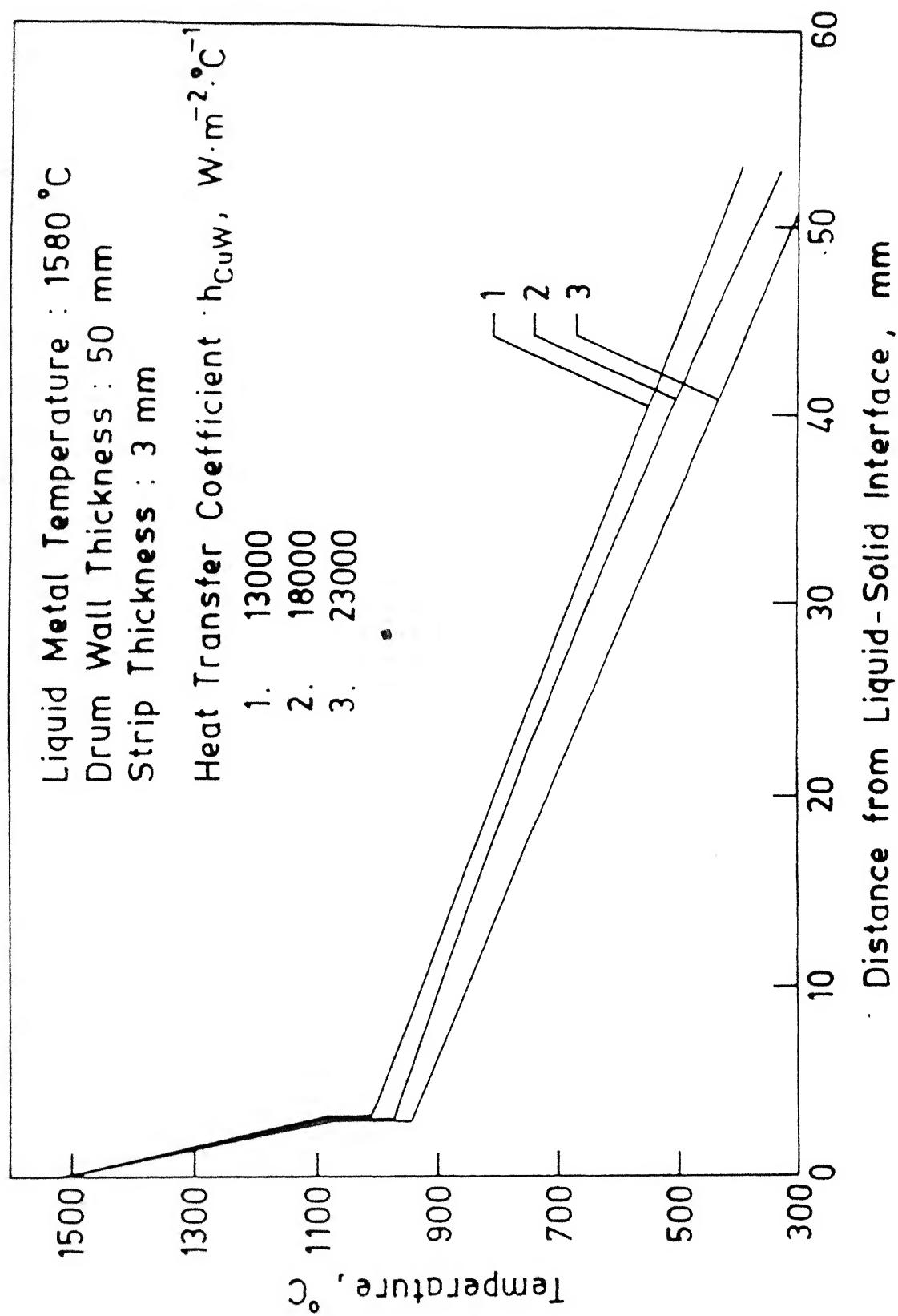


Fig. 5.9 Effect of cooling condition on the Cross sectional Temperature of Strip and Drum at exit (β_2)

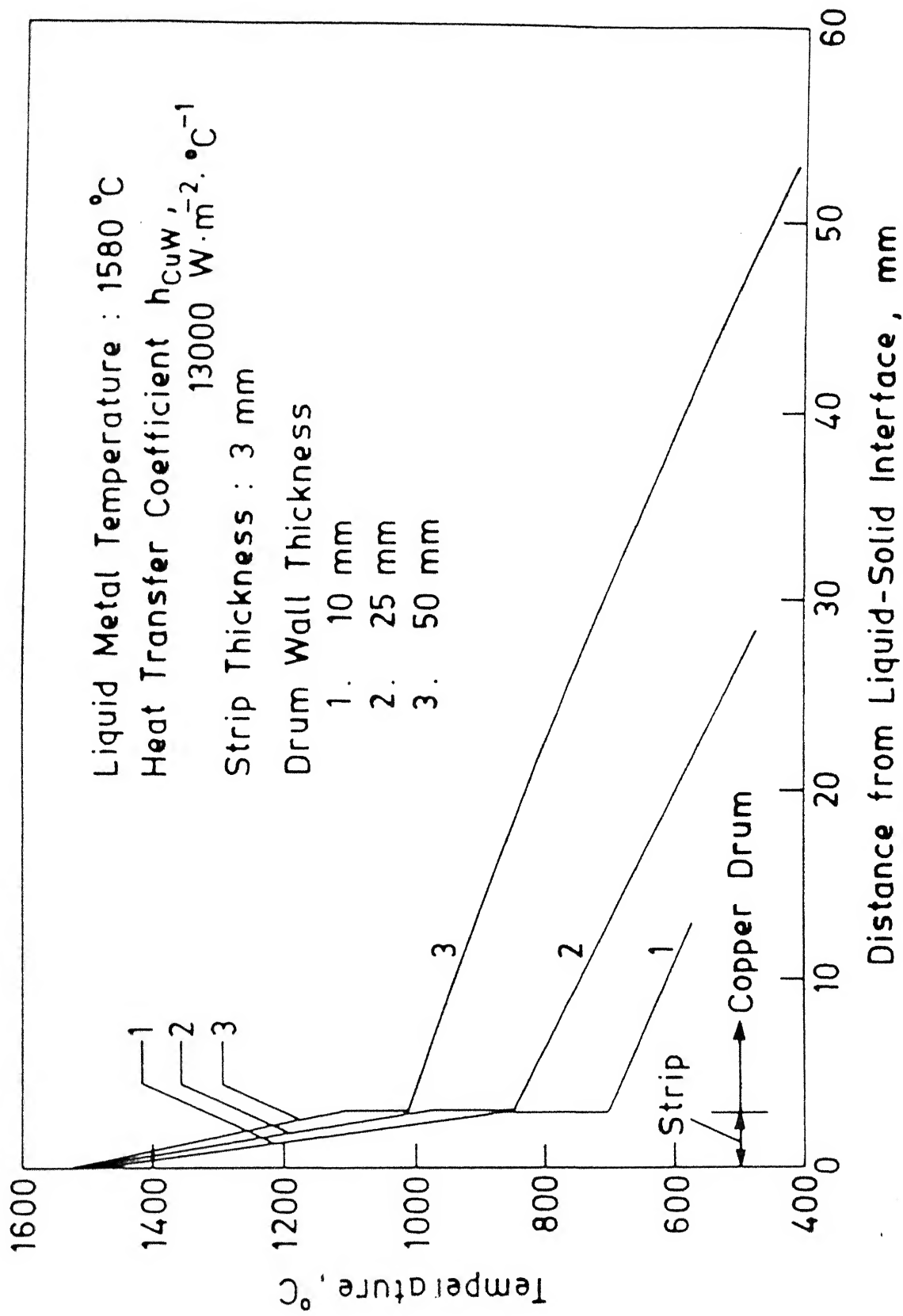


Fig. 5.10 Effect of Drum Wall Thickness on the Cross sectional Temperature of Strip and Drum at exit (β_2)

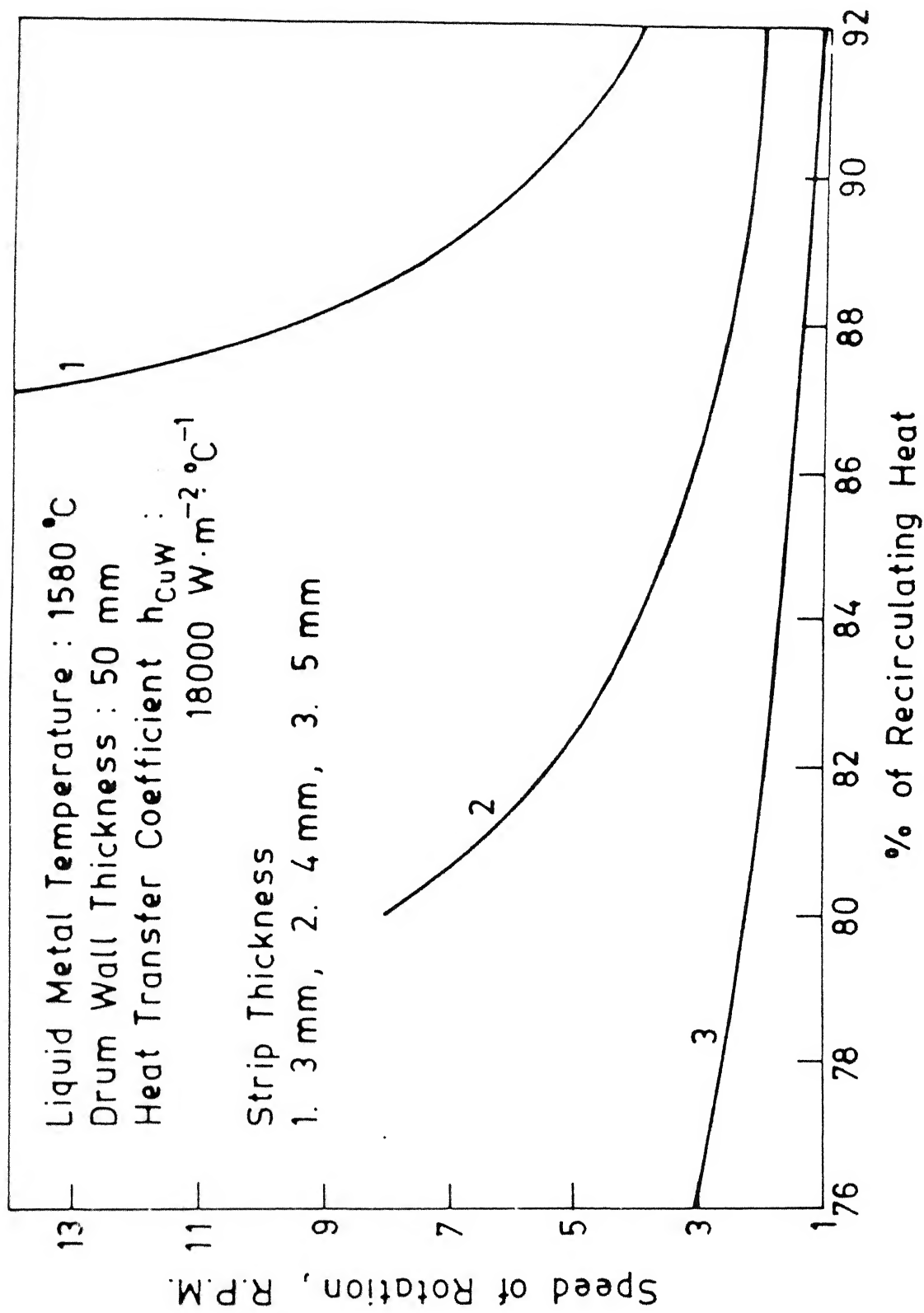


Fig. 5.11 Recirculation Heat associated with R.P.M.

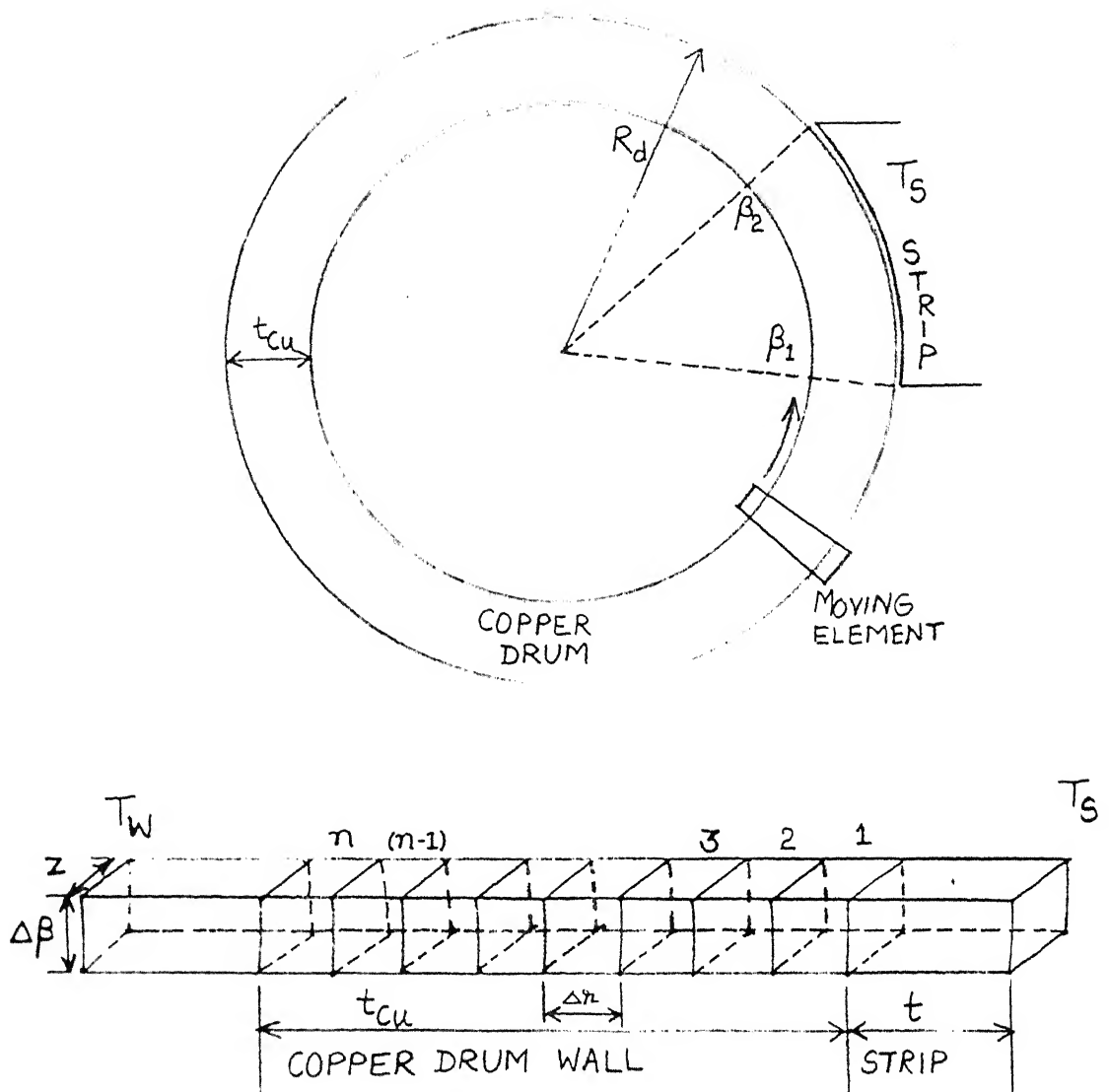


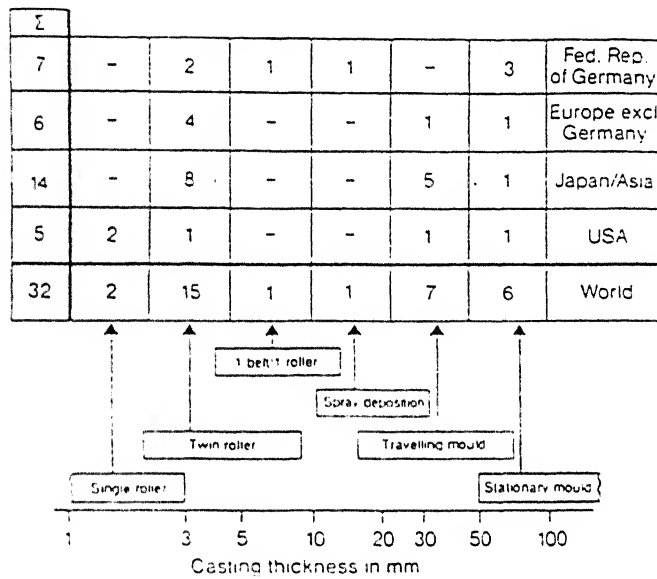
Fig. 7.1 Schematic sketch of Model based on Unsteady State Heat Transfer

Table 1.1

Comparison of the energy required to make carbon steel
strip/sheet by the three processes²

Process	kWh/ton produced	kWh/ton shipped	% material loss
Ingot casting	1760	2394	27
Continuous casting (conventional)	1442	1933	25
Direct strip casting	721	750	4

Table 2.1



World-wide activities in the field of near-net-shape Casting

Table 3.1

Specifications of Water Spray Nozzle

Make : FULLJET, 1/2 " dia

Capacity in gallons per minute
(g.p.m.) at different pressures

Pressure in p.s.i.	Capacity of Water gallons/minute
3	1.4
5	1.8
7	2.1
10	2.5
15	3.0
20	3.5
30	4.2
40	4.8
60	5.8
80	6.7
100	7.4
150	8.9

Solid Spray angle

Pressure in p.s.i.	Solid spray angle
7	64°
20	67°
80	61°

TABLE 4.1

LIQUID METAL TEMPERATURE = 1580 C

 $h_{PF} = 41068.6 \text{ W/Sq. m. C}$ $h_{CuW} = 1000 \text{ W/Sq. m. C}$

R. P. M.	POOL TEMP. DEG. C	FUNCTION FOR POOL TEMP.
0.200	1517.5	0.000869808
0.300	1518.5	0.000786530
0.400	1519.4	0.000711079
0.500	1520.2	0.000642296
0.600	1520.9	0.000579250
0.700	1521.6	0.000521152
0.800	1522.2	0.000467381
0.900	1522.7	0.000417428
1.000	1523.2	0.000370854
1.100	1523.7	0.000327293
1.200	1524.1	0.000286426
1.300	1524.5	0.000247990
1.400	1524.8	0.000211756
1.500	1525.2	0.000177516
1.600	1525.5	0.000145099
1.700	1525.8	0.000114352
1.800	1526.0	0.000085134
1.900	1526.3	0.000057322
2.000	1526.5	0.000030817
2.100	1526.8	0.000005517
2.200	1527.0	-0.000018670
2.300	1527.2	-0.000041813
2.400	1527.4	0.000063989
2.500	1527.5	-0.000085259
2.600	1527.7	-0.000105677
2.700	1527.9	-0.000125299
2.800	1528.0	-0.000144177
2.900	1528.2	-0.000162358
3.000	1528.3	-0.000179872
3.100	1528.5	-0.000196761
3.200	1528.6	-0.000213064
3.300	1528.7	-0.000228810
3.400	1528.8	-0.000244023
3.500	1529.0	-0.000258741
3.600	1529.1	-0.000272975
3.700	1529.2	-0.000286771
3.800	1529.3	-0.000300130
3.900	1529.4	-0.000313082

TABLE 4.2

LIQUID METAL TEMPERATURE = 1580 C

 $h_{PF} = 41068.6 \text{ W/Sq.m. C}$ $h_{CuW} = 1000 \text{ W/Sq.m. C}$

R. P. M.	POOL TEMP. DEG. C	FUNCTION FOR POOL TEMP.
2.110	1526.8	0.000003046
2.120	1526.8	0.000000590
2.130	1526.8	-0.000001856
2.140	1526.8	-0.000004289
2.150	1526.9	-0.000006715
2.160	1526.9	-0.000009129
2.170	1526.9	-0.000011528
2.180	1526.9	-0.000013918
2.190	1527.0	-0.000016302
2.200	1527.0	-0.000018673

Table 4.3

LIST OF CONSTANTS USED IN SIMULATION

$$\begin{aligned}
 \beta_1 &= 1.466^{\circ}\text{C}, 1.658^{\circ}\text{C} \\
 \beta_2 &= 2.007^{\circ}\text{C}, 2.182^{\circ}\text{C}, 2.217^{\circ}\text{C} \\
 R_d &= 0.25\text{m} \\
 t_{\text{Cu}} &= 10, 25, 50\text{mm} \\
 t_i &= 0.0024\text{m} \\
 t_f &= 0.003-0.010\text{m} \\
 \delta &= 0.020\text{m}
 \end{aligned}$$

$$\begin{aligned}
 T_L &= 1530^{\circ}\text{C} \\
 T_S &= 1500^{\circ}\text{C} \\
 T_F &= 0.5(T_L + T_S) = 1515^{\circ}\text{C} \\
 T_W &= 25^{\circ}\text{C} \\
 T_a &= 28^{\circ}\text{C} \\
 T_l &= 1580-1610^{\circ}\text{C}
 \end{aligned}$$

Copper Bulk Heat in = 75-90 % Copper Bulk Heat out

$$\begin{aligned}
 k_{\text{Cu}} &= 380.16 \text{ W/m} \cdot ^{\circ}\text{C} \\
 k_S &= 24 \text{ W/m} \cdot ^{\circ}\text{C} \\
 h_{\text{PF}}^{11} &= 15000-40000 \text{ W/m}^2 \cdot ^{\circ}\text{C} \\
 h_{\text{CuW}} &= 1000-13000, 18000, 23000 \text{ W/m}^2 \cdot ^{\circ}\text{C} \\
 c_{\text{ps}} &= 690 \text{ J/kg} \cdot ^{\circ}\text{C} \\
 c_{\text{pl}} &= 866 \text{ J/kg} \cdot ^{\circ}\text{C} \\
 L &= 272142 \text{ J/kg}
 \end{aligned}$$

$$\begin{aligned}
 \rho_{\text{Cu}} &= 8950 \text{ kg/m}^3 \\
 \rho_S &= 7311 \text{ kg/m}^3
 \end{aligned}$$

$$l = \frac{t_f}{0.00005}, \quad t_f \text{ in m.} \quad m = \frac{t_{\text{Cu}}}{0.00025}, \quad t_{\text{Cu}} \text{ in m.}$$

$$n = R_d \cdot (\beta_2 - \beta_1) / 0.00025, \quad R_d \text{ in m.}$$

APPENDIX - 1

Integration of the Heat Balance Equation at the melt-solid interface

$$k_S \frac{\partial T}{\partial R} = \frac{k_S (T_F - T_W)}{\ln \left[\frac{R_d + t}{R_d} \right] + \frac{k_S}{k_{Cu}} \ln \left[\frac{R_d}{R_d - t_{Cu}} \right] + \frac{k_S}{R_d h_{CuW}}} \quad (A-1)$$

$$\frac{dt}{d\beta} = \frac{\frac{k_S (T_F - T_W)}{\ln \left[\frac{R_d + t}{R_d} \right] + \frac{k_S}{k_{Cu}} \ln \left[\frac{R_d}{R_d - t_{Cu}} \right] + \frac{k_S}{R_d h_{CuW}}} - h_{PF} (T_P - T_F)}{\rho_S \cdot \omega \cdot [H(T_P) - H_S(T_F)]} \quad (A-2)$$

$$\frac{dt}{d\beta} = \frac{\frac{k_S (T_F - T_W)}{\ln \left[\frac{R_d + t}{R_d} \right] + \frac{k_S}{k_{Cu}} \ln \left[\frac{R_d}{R_d - t_{Cu}} \right] + \frac{k_S}{R_d h_{CuW}}}}{\rho_S \cdot \omega \cdot [H(T_P) - H_S(T_F)]}$$

$$= \frac{h_{PF} (T_P - T_F)}{\rho_S \cdot \omega \cdot [H(T_P) - H_S(T_F)]} \quad (A-3)$$

$$\text{Let } \frac{k_S (T_F - T_W)}{\rho_S \cdot \omega \cdot [H(T_P) - H_S(T_F)]} = a_1 \quad (A-4)$$

$$\frac{h_{PF} (T_P - T_F)}{\rho_S \cdot \omega \cdot [H(T_P) - H_S(T_F)]} = a_2 \quad (A-5)$$

and

$$\frac{k_s}{k_{Cu}} \ln \left[\frac{R_d}{R_d - t_{Cu}} \right] + \frac{k_s}{R_d h_{CuW}} = a_4 \quad (A-6)$$

$$\frac{dt}{d\beta} = \frac{(a_1 - a_4 a_2) - a_2 \ln \left[\frac{R_d + t}{R_d} \right]}{a_4 + \ln \left[\frac{R_d + t}{R_d} \right]} \quad (A-7)$$

$$\left[\frac{a_4 + \ln \left[\frac{R_d + t}{R_d} \right]}{(a_1 - a_4 a_2) - a_2 \ln \left[\frac{R_d + t}{R_d} \right]} \right] dt = d\beta \quad (A-8)$$

$$- \frac{1}{a_2} \left[\frac{a_4 + \ln \left[\frac{R_d + t}{R_d} \right]}{\left[a_4 - \frac{a_1}{a_2} \right] + \ln \left[\frac{R_d + t}{R_d} \right]} \right] dt = d\beta \quad (A-9)$$

Integrating,

$$\frac{1}{a_2} \left[\frac{a_4 + \ln \left[\frac{R_d + t}{R_d} \right]}{\left[a_4 - \frac{a_1}{a_2} \right] + \ln \left[\frac{R_d + t}{R_d} \right]} \right] dt = \int_{\beta_1}^{\beta_2} d\beta \quad (A-10)$$

$$= \frac{1}{a_2} \int_{t_1}^{t_f} \left[1 + \frac{a_1}{a_2 \left[\left[a_4 - \frac{a_1}{a_2} \right] + \ln \left[\frac{R_d + t}{R_d} \right] \right]} \right] dt = \beta_2 - \beta_1 \quad (A-11)$$

$$= \frac{(t_f - t_1)}{a_2} - \frac{a_1}{a_2^2} \int_{t_1}^{t_f} \left[\frac{1}{\left[a_4 - \frac{a_1}{a_2} \right] + \ln \left[\frac{R_d + t}{R_d} \right]} \right] dt = \beta_2 - \beta_1 \quad (A-12)$$

$$\int \left[\frac{1}{\left[a_4 - \frac{a_1}{a_2} \right] + \ln \left[\frac{R_d + t}{R_d} \right]} \right] dt = \quad (A-13)$$

$$\text{Let } \left[a_4 - \frac{a_1}{a_2} \right] + \ln \left[\frac{R_d + t}{R_d} \right] = u \quad (A-14)$$

$$\implies \frac{R_d + t}{R_d} = e^{u - \left[a_4 - \frac{a_1}{a_2} \right]} \quad (A-15)$$

Differentiating equation (A-15)

$$\frac{R_d}{R_d + t} \cdot \frac{1}{R_d} dt = du \quad (A-16)$$

$$u = \left(a_1 - \frac{a_1}{a_2} \right) \quad (A-17)$$

$$dt = (R_d + t) du - R_d e$$

Equation (A-13) becomes,

$$\int \frac{R_d e^{u - \left(a_1 - \frac{a_1}{a_2} \right)}}{u} du = R_d e^{- \left(a_1 - \frac{a_1}{a_2} \right)} \int \frac{e^u}{u} du \quad (A-18)$$

or

$$\int \frac{e^u}{u} = \int \frac{1}{u} \left(1 + u + \frac{u^2}{2!} + \frac{u^3}{3!} + \dots + \frac{u^{n-1}}{(n-1)!} \right) \quad (A-19)$$

$$\int \frac{e^u}{u} = \int \left(\frac{1}{u} + 1 + \frac{u}{2!} + \frac{u^2}{3!} + \dots + \frac{u^{n-2}}{(n-1)!} \right) du \quad (A-20)$$

$$= \ln u + u + \frac{u}{2 \cdot 2!} + \frac{u^2}{3 \cdot 3!} + \dots + \frac{u^{n-1}}{(n-1) \cdot (n-1)!} \quad (A-21)$$

This series is diverging and no approximation can be made.

BIBLIOGRAPHY

- 1 Anon : 'Direct strip casting by Nippon Metal Industry', Continuous Casting supplement of Steel Times Int., 1987(3), p12
- 2 Pimputkar S M , Carbonara R S, Rayment J J, McCall J L, Clauer A H 'Comparison of the single and double roller processes for casting low carbon steel', Rapidly quenched metals; Steeb S., Warlimont (Eds.), Elsevier Pub.,1985, p95-100
- 3 Mehrotra S P, Koria S C (Eds.), 'Short term course on Continuous casting of steel', IIT-Bangur, July 1989
- 4 Reichelt W , Werner K 'Near-net-shape casting of flat products', Met Plant & Tech., 1988, p18-25
- 5 Cygler M, Wolf M 'Continuous strip and thin slab casting of steel-An overview', Iron Making Steelmaking, 1986(8), p27-33
- 6 Jaffrey D, Dover I, Hamilton I 'Recent developments in continuous casting technology : An overview', Metals Forum, 1984(2), p67-78
- 7 Birat J P 'Manufacture of flat products for 21st century' Ironmaking Steelmaking, 1987, Vol.14(2), p84-92

- 8 Stanek V , Szekeley J 'Mathematical model of a closed mold (Watts) horizontal continuous casting process', Met. Trans. 1976, Vol.7B, p619-630
- 9 Miyazawa K , Szekeley J 'A math. model of the splat cooling process using the twin roll technique', Met Trans., 1981, 12A, p1047-1057
- 10 Clyne T W 'The use of heat flow modelling to explore solidification phenomena', Met. Trans., 1982, 13B, p471-477
- 11 Stanek V , Szekeley J 'A math. model of a drum and ring horizontal strip casting process', Met. Trans., 1983, 14B, p487-493,
- 12 Clyne T W 'Numerical treatment of rapid solidification', Met. Trans., 1984, 15B, p369-381
- 13 Gutierrez, Szekeley J 'A math. model of the planar flow melt spinning process', Met. Trans., 1986, 17B, p695-703
- 14 Yu H 'A fluid mechanics model of the planar flow melt spinning process under low reynolds no. conditions' Met. Trans., 1987, 18B, p557-563
- 15 Stanley A B, Daniel K A 'A simple fluid mechanical model for planar flow melt spinning casting process' Met. Trans., 1988, 19B, p571-579

- 16 Takeshita K , Shingu P H 'An analysis of the heat transfer problem with phase transformation during rapid quenching' Trans. Japan Inst. of Metals, 1983, Vol.24(3), p293-300
- 17 Takeshita K, Shingu P H 'An analysis of the ribbon formation process by the single roller rapid solidification technique', ibid p529-536
- 18 Granasy L 'An analysis of the ribbon formation on the single roller rapid solidification technique' Trans. Japan Inst. of Metals, 1986, Vol.27(1), p51-60
- 19 Takeshita K , Shingu P H 'An analysis of melt puddle formation in the single roller chill block casting', ibid p141-148
- 20 Takeshita K, Shingu P H 'Thermal contact during the cooling by the single roller chill block casting' ibid p454-462
- 21 Miyazawa K , Ohashi T, Kasama A, Kajioka H 'Theoretical analysis of twin roll rapid solidification process with taking account of supercooling phenomenon of melt', Trans. ISIJ, 1986, Vol.26, p-B258

- 22 Elmio K., Masao Y., Shibuya K., Miyake S., Ozawa M., Kan T.
'Estimation of heat transfer coefficient during rapid solidification in a double roller method', Trans. ISIJ, Vol.27, 1987
- 23 Ohnishi A., Takashima H., Hariki M. 'Characterstics of heat transfer of multi water spray nozzle' ibid p B-299
- 24 Hariki M., Takashima H., Donishi A. 'Investigation of heat transfer characterstics in various rapid cooling methods on a hot surface' Trans ISIJ, 1988, Vol.28, p B-62